A Beginner's Guide to ICP-MS

Part I

ROBERT THOMAS

Amazingly, 18 years after the commercialization of inductively coupled plasma mass spectrometry (ICP-MS), less than 4000 systems have been installed worldwide. If you compare this number with another rapid multielement technique, inductively coupled plasma optical emission spectrometry (ICP-OES), first commercialized in 1974, the difference is quite significant. In 1992, 18 years after ICP-OES was introduced, more than 9000 units had been sold, and if you compare it with the same time period that ICP-MS has been available, the difference is even more dramatic. From 1983 to the present day, more than 17,000 ICP-OES systems have been installed — more than four times the number of ICP-MS systems. If the comparison is made with all atomic spectroscopy instrumentation (ICP-MS, ICP-OES, graphite furnace atomic absorption [GFAA] and flame atomic absorption [FAA]), the annual turnover for ICP-MS is less than 7% of the total atomic spectroscopy market — 400 units compared to approximately 6000 atomic spectroscopy systems. It's even more surprising when you consider that ICP-MS offers so much more than the other techniques, including two of its most attractive features — the rapid multielement capabilities of ICP-OES, combined with the superb detection limits of GFAA.

ICP-MS — ROUTINE OR RESEARCH?

Clearly, one of the reasons is price — an ICP-MS system typically costs twice as much as an ICP-OES system and three times more than a GFAA system. But in a competitive world, the "street price" of an ICP-MS system is much closer to a top-of-the-line ICP-OES system fitted with sampling accessories or a GFAA system that has all the bells and whistles on it. So if ICP-MS is not significantly more expensive than ICP-OES and GFAA, why hasn't it been more widely accepted by the analytical community? I firmly believe that the major reason why ICP-MS has not gained the popularity of the other trace element techniques is that it is still considered a complicated research technique, requiring a very skilled person to operate it. Manufacturers of ICP-MS equipment are constantly striving to make the systems easier to operate, the software easier to use, and the hardware easier to maintain, but even after 18 years it is still not perceived as a mature, routine tool like flame AA or ICP-OES. This might be partially true because of the relative complexity of the instrumentation; however, in my opinion, the dominant reason for this misconception is that there has not been good literature available explaining the basic principles and benefits of ICP-MS in a way that is compelling and easy to understand for someone with very little knowledge of the technique. Some excellent textbooks (1, 2) and numerous journal papers (3–5) are available that describe the fundamentals, but they tend to be far too heavy for a novice reader. There is no question in my mind that the technique needs to be presented in a more user-friendly way to make routine analytical laboratories more comfortable with it. Unfortunately, the publishers of the "for Dummies" series of books have not yet found a mass (excuse the pun) market for writing one on ICP-MS. So until that time, we will be presenting a number of short tutorials on the technique, as a follow-up to the poster that was included in the February 2001 issue of *Spectroscopy*.

During the next few months, we will be discussing the following topics in greater depth:

- principles of ion formation
- sample introduction
- plasma torch/radio frequency generator
- interface region
- ion focusing
- mass separation
- ion detection
- sampling accessories
- applications.

We hope that by the end of this series, we will have demystified ICP-MS, made it

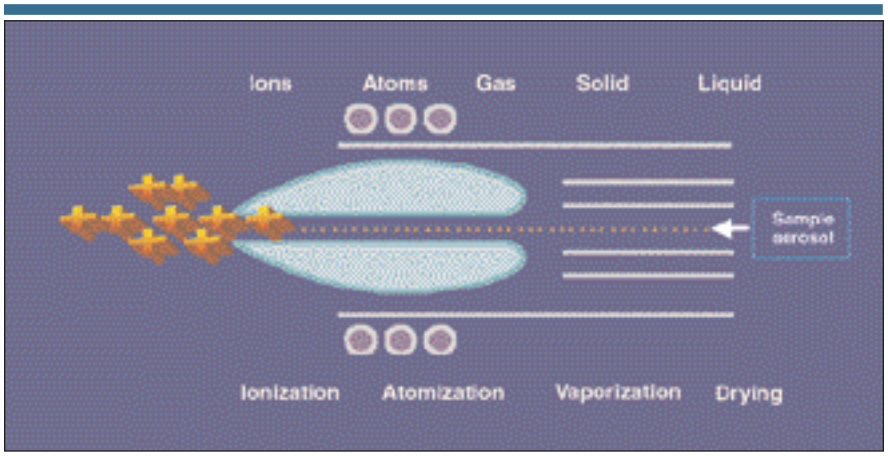

Figure 1. Generation of positively charged ions in the plasma.

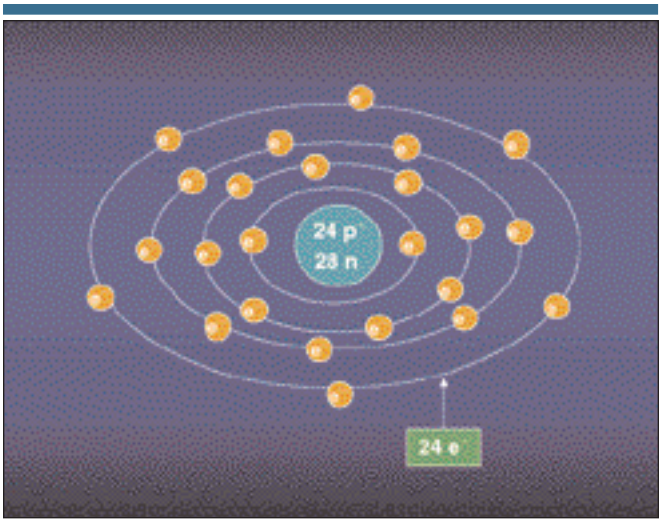

Figure 2. Simplified schematic of a chromium ground-state atom (Cr^0).

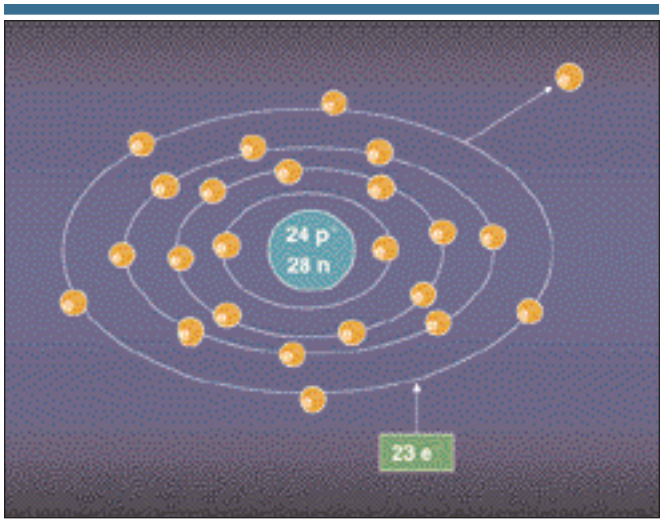

Figure 3. Conversion of a chromium ground-state atom (Cr^0) to an ion (Cr^+).

a little more compelling to purchase, and ultimately opened up its potential as a routine tool to the vast majority of the trace element community that has not yet realized the full benefits of its capabilities.

GENERATION OF IONS IN THE PLASMA

We'll start this series off with a brief description of the fundamental principle used in ICP-MS — the use of a high-temperature plasma discharge to generate positively charged ions. The sample, typically in liquid form, is pumped into the sample introduction system, which is made up of a spray chamber and nebulizer. It emerges as an aerosol and eventually finds its way — by way of a sample injector — into the base of the plasma. As it travels through the different heating zones of the plasma torch it is dried, vaporized, atomized, and ionized. During this time, the sample is transformed from a liquid aerosol to solid particles, then into a gas. When it finally arrives at the analytical zone of the plasma, at approximately 6000–7000 K, it exists as excited atoms and ions, representing the elemental composition of the sample.

The excitation of the outer electron of a ground-state atom, to produce wavelength-specific photons of light, is the fundamental basis of atomic emission. However, there is also enough energy in the plasma to remove an electron from its orbital to generate an ion. It is the generation, transportation, and detection of significant numbers of these positively charged ions that give ICP-MS its characteristic ultratrace detection capabilities.

It is also important to mention that, although ICP-MS is predominantly used for the detection of positive ions, negative ions (such as halogens) are also produced in the plasma. However, because the extraction and transportation of negative ions is different from that of positive ions, most commercial instruments are not designed to measure them. The process of the generation of positively charged ions in the plasma is shown conceptually in greater detail in Figure 1.

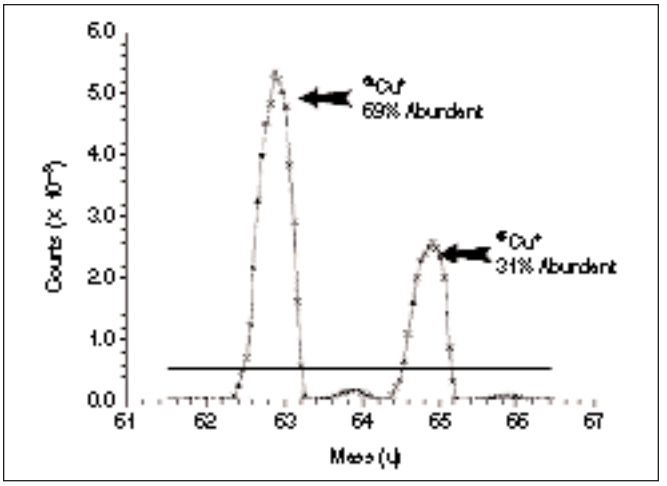

Figure 4. Mass spectra of the two copper isotopes — $^{63}Cu^{+}$ and $^{65}Cu^{+}$.

Table I. Breakdown of the atomic structure of copper isotopes.

	^{63}Cu	^{65}Cu
Number of protons (p^+)	29	29
Number of electrons (e^-)	29	29
Number of neutrons (n)	34	36
Atomic mass ($p^+ + n$)	63	65
Atomic number (p^+)	29	29
Natural abundance	69.17%	30.83%
Nominal atomic weight	63.55*	

* Calculated using the formulae $0.6917n + 0.3083n + p^+$ (referenced to the atomic weight of carbon)

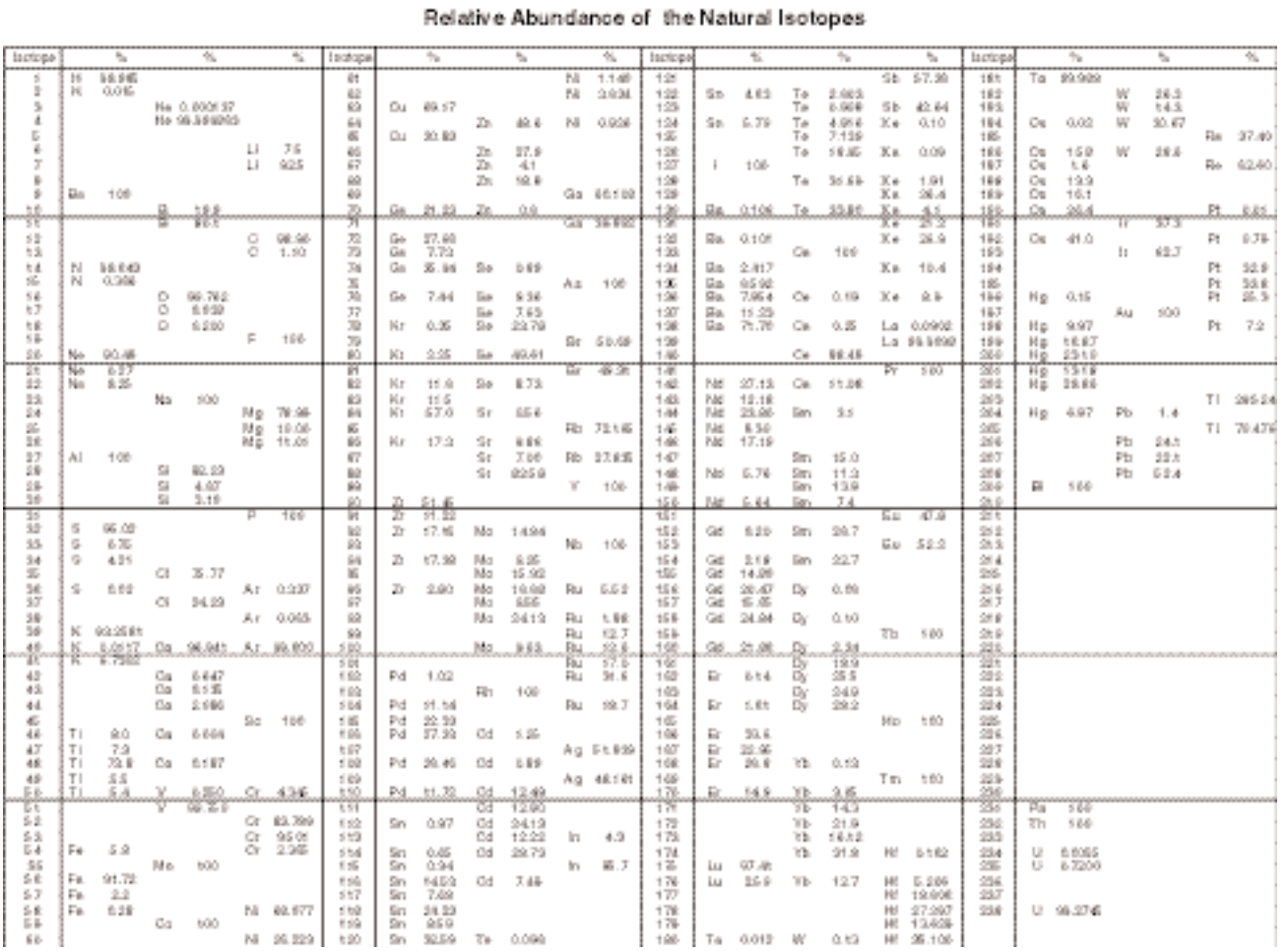

Figure 5. Relative abundance of the naturally occurring isotopes of all the elements (6). Reproduced with the permission of PerkinElmer Instruments (Norwalk, CT).

ION FORMATION

Figures 2 and 3 show the actual process of conversion of a neutral ground-state atom to a positively charged ion. Figure 2 shows a very simplistic view of the chromium atom Cr^0, consisting of a nucleus with 24 protons (p^+) and 28 neutrons (n), surrounded by 24 orbiting electrons (e^-) (It must be emphasized that this is not meant to be an accurate representation of the electrons' shells and subshells, but simply a conceptual explanation for the purpose of clarity). From this we can say that the atomic number of chromium is 24 (number of protons), and its atomic mass is 52 (number of protons + neutrons).

If energy is then applied to the chromium ground-state atom in the form of heat from a plasma discharge, one of the orbiting electrons will be stripped off the outer shell. This will result in only 23 electrons left orbiting the nucleus. Because the atom has lost a negative charge (e^-) but still has 24 protons (p^+) in the nucleus, it is converted into an ion with a net positive charge. It still has an atomic mass of 52 and an atomic number of 24, but is now a positively charged ion and not a neutral ground-state atom. This process is shown in Figure 3.

NATURAL ISOTOPES

This is a very basic look at the process, because most elements occur in more than one form (isotope). In fact, chromium has four naturally occurring isotopes, which means that the chromium atom exists in four different forms, all with the same atomic number of 24 (number of protons), but with different atomic masses (numbers of neutrons).

To make this a little easier to understand, let's take a closer look at an element like copper, which has only two different isotopes — one with an atomic mass of 63 (^{63}Cu) and the other with an atomic mass of 65 (^{65}Cu). They both have the same number of protons and electrons, but differ in the number of neutrons in the nucleus. The natural abundances of ^{63}Cu and ^{65}Cu are 69.1% and 30.9%, respectively, which gives copper a nominal atomic mass of 63.55 — the value you see for copper in atomic weight reference tables. Details of the atomic structure of the two copper isotopes are shown in Table I.

When a sample containing naturally occurring copper is introduced into the plasma, two different ions of copper, $^{63}Cu^+$ and $^{65}Cu^+$, are produced, which generate different mass spectra — one at mass 63 and another at mass 65. This can be seen in Figure 4, which is an actual ICP-MS spectral scan of a sample containing copper. It shows a peak for the $^{63}Cu^+$ ion on the left, which is 69.17% abundant, and a peak for $^{65}Cu^+$ at 30.83% abundance, on the right. You can also see small peaks for two Zn isotopes at mass 64 (^{64}Zn) and mass 66 (^{66}Zn) (Zn has a total of five isotopes at masses 64, 66, 67, 68, and 70). In fact, most elements have at least two or three isotopes and many elements, including zinc and lead, have four or more isotopes. Figure 5 is a chart that shows the relative abundance of the naturally occurring isotopes of all the elements.

During the next few months, we will systematically take you on a journey through the hardware of an ICP mass spectrometer, explaining how each major component works, and finishing the series with an overview of how the technique is being used to solve real-world application problems. Our goal is to present both the basic principles and benefits of the technique in a way that is clear, concise, and very easy to understand. We hope that by the end of the series, you and your managers will be in a better position to realize the enormous benefits that ICP-MS can bring to your laboratory.

REFERENCES

(1) A. Montasser, *Inductively Coupled Plasma Mass Spectrometry* (Wiley-VCH, Berlin, 1998).

(2) F. Adams, R. Gijbels, and R. Van Grieken, *Inorganic Mass Spectrometry* (John Wiley and Sons, New York, 1988.).

(3) R.S. Houk, V.A. Fassel, and H.J. Svec, *Dynamic Mass Spectrom.* **6**, 234 (1981).

(4) A.R. Date and A.L. Gray, *Analyst* **106**, 1255 (1981).

(5) D.J. Douglas and J.B. French, *Anal. Chem.* **53**, 37 (1982).

(6) *Isotopic Composition of the Elements: Pure Applied Chemistry* **63**(7), 991–1002 (1991).

Robert Thomas *is the principal of his own freelance writing and scientific consulting company, Scientific Solutions, based in Gaithersburg, MD. He can be contacted by email at thomasrj@bellatlantic.net or via his web site at www.scientificsolutions1.com.*◆

A Beginner's Guide to ICP-MS

Part II: The Sample-Introduction System

ROBERT THOMAS

Part II of Robert Thomas' series on inductively coupled plasma mass spectrometry looks at one of the most critical areas of the instrument — the sample introduction system. He discusses the fundamental principles of converting a liquid into a fine-droplet aerosol suitable for ionization in the plasma, and provides an overview of the different types of commercially available nebulizers and spray chambers.

The majority of inductively coupled plasma mass spectrometry (ICP-MS) applications involve the analysis of liquid samples. Even though spectroscopists adapted the technique over the years to handle solids, it was developed in the early 1980s primarily to analyze solutions. There are many ways of introducing a liquid into an ICP mass spectrometer, but they all basically achieve the same result — they generate a fine aerosol of the sample so it can be efficiently ionized in the plasma discharge. The sample-introduction area has been called the Achilles heel of ICP-MS because it is considered the weakest component of the instrument, with only 1–2% of the sample finding its way into the plasma (1). Although there has recently been much improvement in this area, the fundamental design of an ICP-MS sample introduction system has not dramatically changed since the technique was first introduced in 1983.

Before discussing the mechanics of aerosol generation in greater detail, let us look at the basic components of a sample introduction system. Figure 1 shows the proximity of the sample introduction area relative to the rest of the ICP mass spectrometer, while Figure 2 represents the individual components.

The mechanism of introducing a liquid sample into analytical plasma can be considered as two separate events — aerosol generation using a nebulizer and droplet selection by way of a spray chamber. Sharp carried out a thorough investigation of both processes (2).

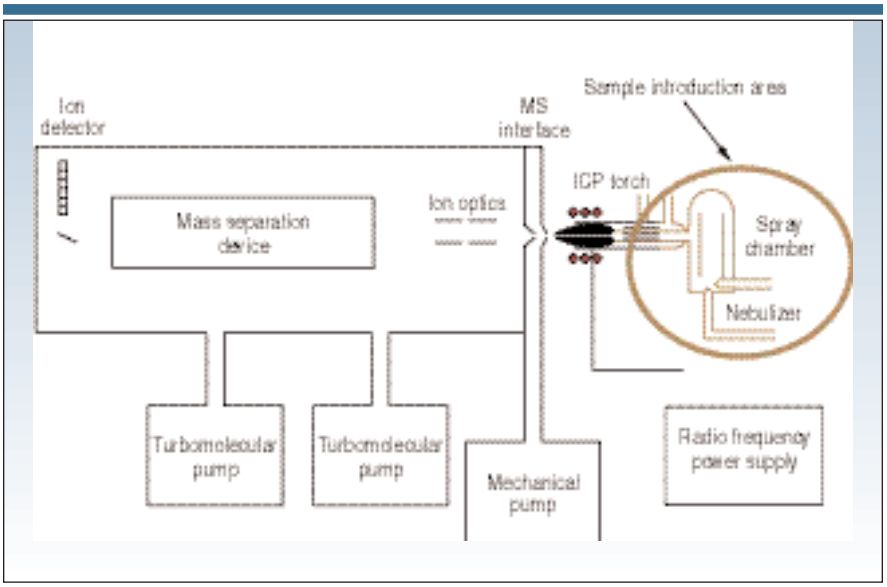

Figure 1. ICP-MS system diagram showing the location of the sample introduction area.

AEROSOL GENERATION

As mentioned previously, the main function of the sample introduction system is to generate a fine aerosol of the sample. It achieves this purpose with a nebulizer and a spray chamber. The sample is normally pumped at ~1 mL/min via a peristaltic pump into the nebulizer. A peristaltic pump is a small pump with lots of minirollers that rotate at the same speed. The constant motion and pressure of the rollers on the pump tubing feed the sample to the nebulizer. The benefit of a peristaltic pump is that it ensures a constant flow of liquid, irrespective of differences in viscosity between samples, standards, and blanks. After the sample enters the nebulizer, the liquid is broken up into a fine aerosol by the pneumatic action of gas flow (~1 L/min) smashing the liquid into tiny droplets, which is very similar to the spray mechanism of a can of deodorant. Although pumping the sample is the most common approach to introducing it, some pneumatic nebulizers, such as the concentric design, don't need a pump because they rely on the natural venturi effect of the positive pressure of the nebulizer gas to suck the sample through the tubing. Solution nebulization is conceptually represented in Figure 3, which shows aerosol generation using a nebulizer with a crossflow design.

DROPLET SELECTION

Because the plasma discharge is inefficient at dissociating large droplets, the spray chamber's function is primarily to allow only the small droplets to enter the plasma. Its secondary purpose is to smooth out pulses that occur during the nebulization process, due mainly to the peristaltic pump. Several ways exist to en-

sure only the small droplets get through, but the most common way is to use a double-pass spray chamber where the aerosol emerges from the nebulizer and is directed into a central tube running the whole length of the chamber. The droplets travel the length of this tube, where the large droplets (greater than ~10 µm in diameter) fall out by gravity and exit through the drain tube at the end of the spray chamber. The fine droplets (~5–10 µm in diameter) then pass between the outer wall and the central tube, where they eventually emerge from the spray chamber and are transported into the sample injector of the plasma torch (3). Although many different designs are available, the spray chamber's main function is to allow only the smallest droplets into the plasma for dissociation, atomization, and finally ionization of the sample's elemental components. Figure 4 presents a simplified schematic of this process.

Let us now look at the different nebulizer and spray chamber designs that are most commonly used in ICP-MS. This article cannot cover every type available because a huge market has developed over the past few years for application-specific customized sample introduction components. This market created an industry of small OEM (original equipment manufacturers) companies that manufacture parts for instrument companies as well as selling directly to ICP-MS users.

NEBULIZERS

By far the most common design used for ICP-MS is the pneumatic nebulizer, which uses mechanical forces of a gas flow (normally argon at a pressure of 20–30 psi) to generate the sample aerosol. The most popular designs of pneumatic nebulizers include concentric, microconcentric, microflow, and crossflow. They are usually made from glass, but other nebulizer materials, such as various kinds of polymers, are becoming more popular, particularly for highly corrosive samples and specialized applications. I want to emphasize at this point that nebulizers designed for use with ICP-optical emission spectroscopy (OES) are not recommended for ICP-MS. This fact results from a limitation in total dissolved solids (TDS) that can be put into the ICP-MS interface area. Because the orifice sizes of the sampler and skimmer cones used in ICP-MS are so small (~0.6–1.2 mm), the concentration of matrix components must generally be kept below 0.2%

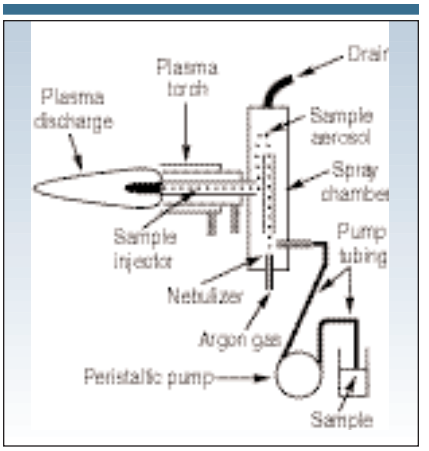

Figure 2. Diagram of the ICP-MS sample introduction area.

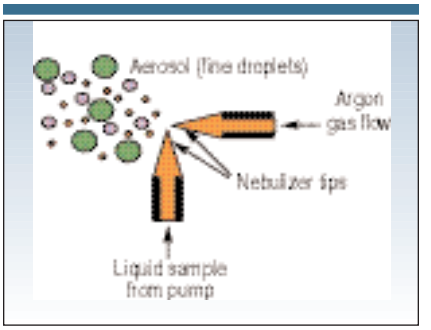

Figure 3. Conceptual representation of aerosol generation with an ICP-MS nebulizer.

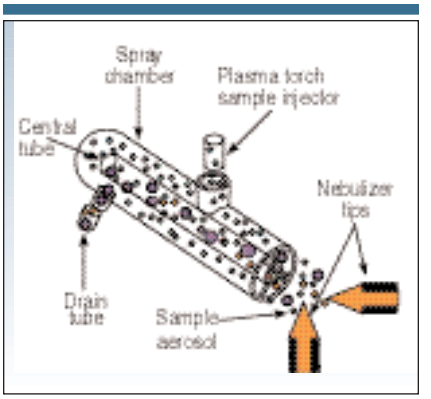

Figure 4. Simplified representation of the separation of large and fine droplets in the spray chamber.

(4). Therefore, general-purpose ICP-OES nebulizers that are designed to aspirate 1–2% dissolved solids, or high-solids nebulizers such as the Babbington, V-groove, or cone-spray nebulizers, which are designed to handle as much as 20% dissolved solids, are not ideal for use with ICP-MS. The most common of the pneumatic nebulizers used in commercial ICP mass spectrometers are the concentric and crossflow designs. The concentric design is more suitable for clean samples, while the crossflow is generally more tolerant to samples containing higher levels of solids or particulate matter.

Concentric design. In the concentric nebulizer, the solution is introduced through a capillary tube to a low-pressure region created by a gas flowing rapidly past the end of the capillary. The low pressure and high-speed gas combine to break up the solution into an aerosol, which forms at the open end of the nebulizer tip. Figure 5 illustrates the concentric design.

Concentric pneumatic nebulizers can provide excellent sensitivity and stability, particularly with clean solutions. However, the small orifices can be plagued by blockage problems, especially if large numbers of heavy matrix samples are aspirated.

Crossflow design. For samples that contain a heavier matrix or small amounts of undissolved matter, the crossflow design is probably the best option. With this design the argon gas is directed at right angles to the tip of a capillary tube, in contrast to the concentric design, where the gas flow is parallel to the capillary. The solution is either drawn up through the capillary tube via the pressure created by the high-speed gas flow or, as is most common with crossflow nebulizers, forced through the tube with a peristaltic pump. In either case, contact between the high-speed gas and the liquid stream causes the liquid to break up into an aerosol. Crossflow nebulizers are generally not as efficient as concentric nebulizers at creating the very small droplets needed for ICP-MS analyses. However, the larger diameter liquid capillary and longer distance between liquid and gas injectors reduce clogging problems. Many analysts feel that the small penalty paid in analytical sensitivity and precision when compared with concentric nebulizers is compensated by the fact that the crossflow design is far more rugged for routine use. Figure 6 shows a cross section of a crossflow nebulizer.

Microflow design. A new breed of nebulizers is being developed for ICP-MS called microflow nebulizers, which are designed to operate at much lower sample flows. While conventional nebulizers have a sample uptake rate of about 1 mL/min, microflow nebulizers typically run at less than 0.1 mL/min. They are based on the concentric principle, but

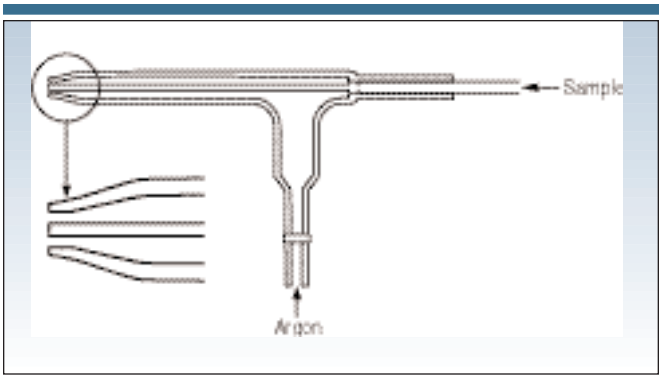

Figure 5. Diagram of a typical concentric nebulizer.

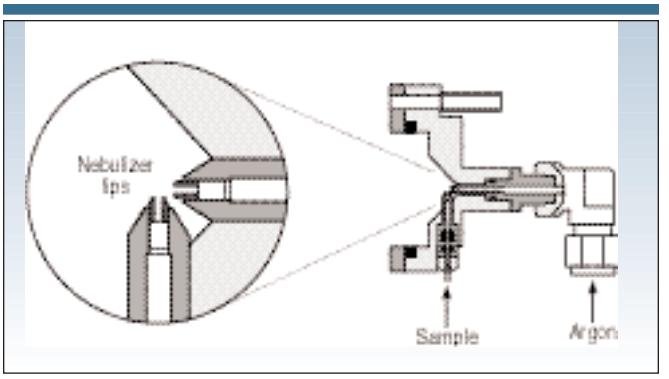

Figure 6. Schematic of a crossflow nebulizer.

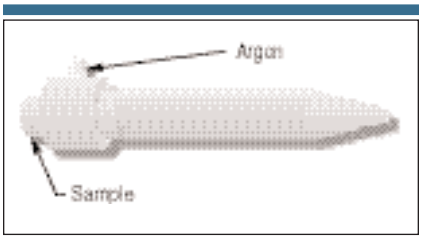

Figure 7. A typical concentric microflow nebulizer. Printed with permission from Elemental Scientific (Omaha, NE).

they usually operate at higher gas pressure to accommodate the lower sample flow rates. The extremely low uptake rate makes them ideal for applications with limited sample volume or where the sample or analyte is prone to sample introduction memory effects. These nebulizers and their components are typically constructed from polymer materials such as polytetrafluoroethylene (PTFE), perfluoroalkoxy (PFA), or polyvinylidene fluoride (PVDF). In fact, their excellent corrosion resistance means that they have naturally low blank levels. This characteristic, together with their ability to handle small sample volumes such as vapor-phase decomposition (VPD) applications, makes them an ideal choice for semiconductor labs that are carrying out ultra-trace element analysis (5). A typical microflow nebulizer made from PFA is shown in Figure 7.

SPRAY CHAMBERS

Let us now turn our attention to spray chambers. Basically two designs are used in commercial ICP-MS instrumentation — double pass and cyclonic spray chambers. The double pass is by far the most common, with the cyclonic type gaining in popularity. Another type of spray chamber based on the impact bead design (first developed for flame AA and then adapted for ICP-OES) was tried on the early ICP-MS systems with limited success, but is not generally used today. As mentioned earlier, the function of the spray chamber is to reject the larger aerosol droplets and also to smooth out pulses produced by the peristaltic pump. In addition, some ICP-MS spray chambers are externally cooled (typically to 2–5 °C) for thermal stability of the sample and to minimize the amount of solvent going into the plasma. This can have a number of beneficial effects, depending on the application, but the main benefits are reduction of oxide species and the ability to aspirate volatile organic solvents.

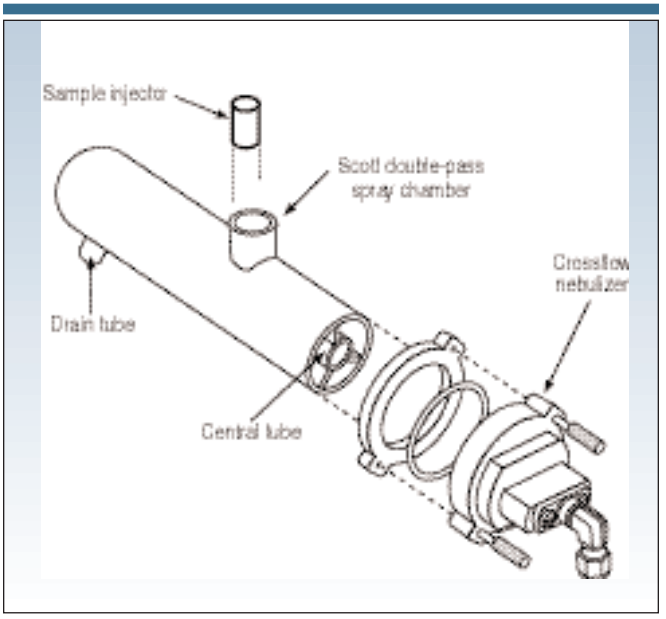

Figure 8. Schematic of a Scott double-pass spray chamber (shown with crossflow nebulizer). Printed with permission of PerkinElmer Instruments (Norwalk, CT).

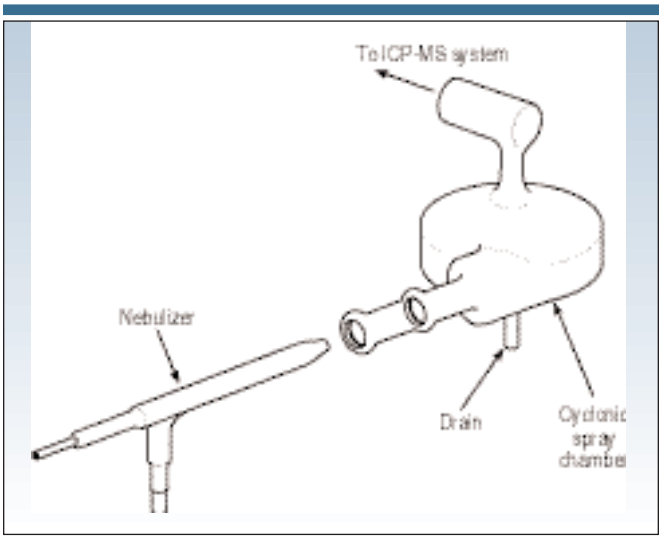

Figure 9. Schematic of a cyclonic spray chamber (shown with concentric nebulizer).

Double pass. By far the most common design of double-pass spray chamber is the Scott design, which selects the small droplets by directing the aerosol into a central tube. The larger droplets emerge from the tube and, by gravity, exit the spray chamber via a drain tube. The liquid in the drain tube is kept at positive pressure (usually by way of a loop), which forces the small droplets back between the outer wall and the central tube, where they emerge from the spray chamber into the sample injector of the plasma torch. Scott double-pass spray chambers come in a variety of shapes, sizes, and materials, but are generally considered the most rugged design for routine use. Figure 8 shows a Scott spray chamber made of a polysulfide-type material, coupled to a crossflow nebulizer.

Cyclonic spray chamber. The cyclonic spray chamber operates by centrifugal force. Droplets are discriminated according to their size by means of a vortex produced by the tangential flow of the sample aerosol and argon gas inside the chamber. Smaller droplets are carried with the gas stream into the ICP-MS, while the larger droplets impinge on the walls and fall out through the drain. It is generally accepted that a cyclonic spray chamber has a higher sampling efficiency, which, for clean samples, translates into higher sensitivity and lower detection limits. However, the droplet size distribution appears to be different from a double-pass design, and for certain types of samples, can give slightly inferior precision. An excellent evaluation of the capabilities of a cyclonic spray chamber was made by Beres and co-workers (6). Figure 9 shows a cyclonic spray chamber connected to a concentric nebulizer.

Many other nonstandard sample introduction devices are available that are not described in this particular tutorial, such as ultrasonic nebulization, membrane desolvation, flow injection, direct injection, electrothermal vaporization, and laser ablation. However, they are becoming more and more important, particularly as ICP-MS users are demanding higher performance and more flexibility. For that reason, they will be addressed in a separate tutorial at the end of this series.

REFERENCES

(1) R. A. Browner and A.W. Boorn, *Anal. Chem.* **56**, 786–798A (1984).
(2) B.L. Sharp, *Analytical Atomic Spectrometry* **3**, 613 (1980).
(3) L.C. Bates and J.W. Olesik, *Journal of Analytical Atomic Spectrometry* **5**(3), 239 (1990).
(4) R.S. Houk, *Anal. Chem.* **56**, 97A (1986).
(5) E. Debrah, S. A. Beres, T.J. Gluodennis, R.J. Thomas, and E.R. Denoyer, *Atomic Spectroscopy*, 197–202 (September 1995).
(6) S. A. Beres, P. H. Bruckner, and E.R. Denoyer, *Atomic Spectroscopy*, 96–99 (March/April 1994).

Robert Thomas *is the principal of his own freelance writing and scientific marketing consulting company, Scientific Solutions, based in Gaithersburg, MD. He specializes in trace element analysis and can be contacted by e-mail at thomasrj@bellatlantic.net or via his web site at www.scientificsolutions1.com.* ◆

"News Spectrum" continued from page 13

TRAINING COURSES

Thermo Nicolet (Madison, WI) is offering a free Spring 2001 Spectroscopic Solutions Seminar Series. The seminars will cover basic FT-IR spectroscopy, microspectroscopy, dispersive Raman microscopy, Raman spectroscopy, and specialized sampling techniques. This year's schedule includes the following seminars:

May 22 at the Syracuse Sheraton, Syracuse, NY; May 24 at the Wyndham Westborough Hotel, Westborough, MA; May 24 at the Marriott Oak Brook, Oak Brook, IL; June 5 at the East Lansing Marriott, East Lansing, MI; June 5 at the Embassy Suites, Overland Park, KS; June 7 at the Sheraton Indianapolis, Indianapolis, IN; June 12 at the Delta Meadowvale Conference Center, Mississauga, Ontario, Canada; June 12 at the Embassy Suites, Brookfield, WI; July 10 at the Coast Terrace Inn, Edmonton, Alberta, Canada; and July 26 at the Ala Moana Hotel, Honolulu, HI.

For more information, contact Thermo Nicolet, (800) 201-8132 fax: (608) 273-5046, e-mail: nicinfo@thermonicolet.com, web site: www.thermonicolet.com. ◆

A Beginner's Guide to ICP-MS

Part III: The Plasma Source

ROBERT THOMAS

Part III of Robert Thomas' series on inductively coupled plasma–mass spectroscopy (ICP-MS) looks at the area where the ions are generated — the plasma discharge. He gives a brief historical perspective of some of the common analytical plasmas used over the years and discusses the components that are used to create the ICP. He finishes by explaining the fundamental principles of formation of a plasma discharge and how it is used to convert the sample aerosol into a stream of positively charged ions.

Inductively coupled plasmas are by far the most common type of plasma sources used in today's commercial ICP–optical emission spectrometry (OES) and ICP-MS instrumentation. However, it wasn't always that way. In the early days, when researchers were attempting to find the ideal plasma source to use for spectrometric studies, it was unclear which approach would prove to be the most successful. In addition to ICPs, some of the other novel plasma sources developed were direct current plasmas (DCP) and microwave-induced plasmas (MIP). A DCP is formed when a gas (usually argon) is introduced into a high current flowing between two or three electrodes. Ionization of the gas produces an inverted Y-shaped plasma. Unfortunately, early DCP instrumentation was prone to interference effects and also had some usability and reliability problems. For these reasons, the technique never became widely accepted by the analytical community (1). However, its one major benefit was that it could aspirate high levels of dissolved or suspended solids, because there was no restrictive sample injector for the solid material to block. This feature alone made it attractive for some laboratories, and once the initial limitations of DCPs were better understood, the technique became more accepted. In fact, for those who want a DCP excitation source coupled with an optical emission instrument today, an Echelle-based grating using a solid-state detector is commercially available (2).

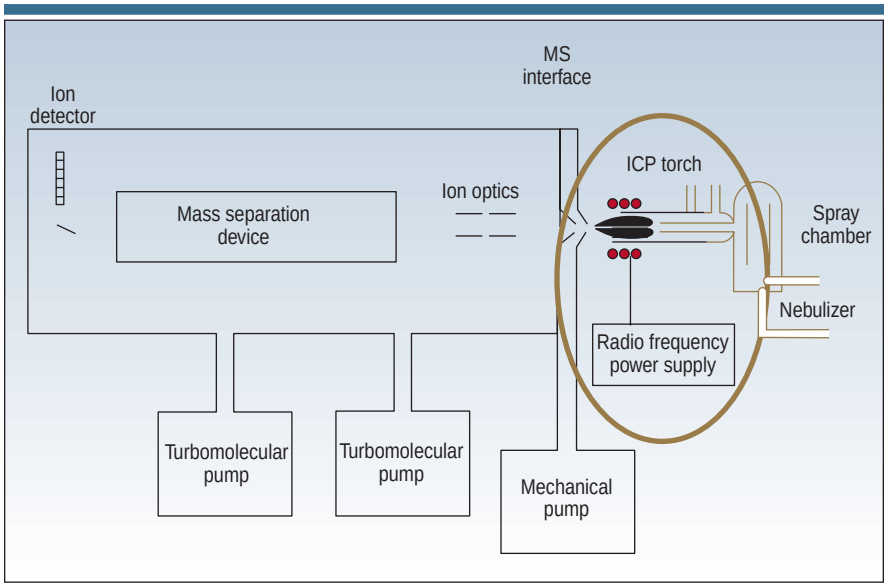

Figure 1. Schematic of an ICP-MS system showing the location of the plasma torch and radio frequency (RF) power supply.

Limitations in the DCP approach led to the development of electrodeless plasma, of which the MIP was the simplest form. In this system, microwave energy (typically 100–200 W) is supplied to the plasma gas from an excitation cavity around a glass or quartz tube. The plasma discharge in the form of a ring is generated inside the tube. Unfortunately, even though the discharge achieves a very high power density, the high excitation temperatures exist only along a central filament. The bulk of the MIP never gets hotter than 2000–3000 K, which means it is prone to very severe matrix effects. In addition, they are easily extinguished during aspiration of liquid samples. For these reasons, they have had limited success as an emission source, because they are not considered robust enough for the analysis of real-world, solution-based samples. However, they have gained acceptance as an ion source for mass spectrometry (3) and also as emission-based detectors for gas chromatography.

Because of the limitations of the DCP and MIP approaches, ICPs became the dominant focus of research for both optical emission and mass spectrometric studies. As early as 1964, Greenfield and co-workers reported that an atmospheric-pressure ICP coupled with OES could be used for elemental analysis (4). Although crude by today's standards, the system showed the enormous possibilities of the ICP as an excitation source and most definitely opened the door in the early 1980s to the even more exciting potential of using the ICP to generate ions (5).

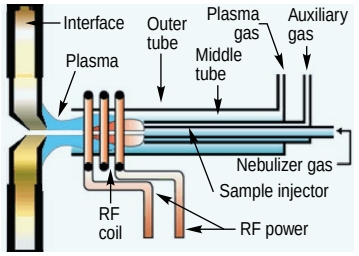

Figure 2. Detailed view of a plasma torch and RF coil relative to the ICP-MS interface.

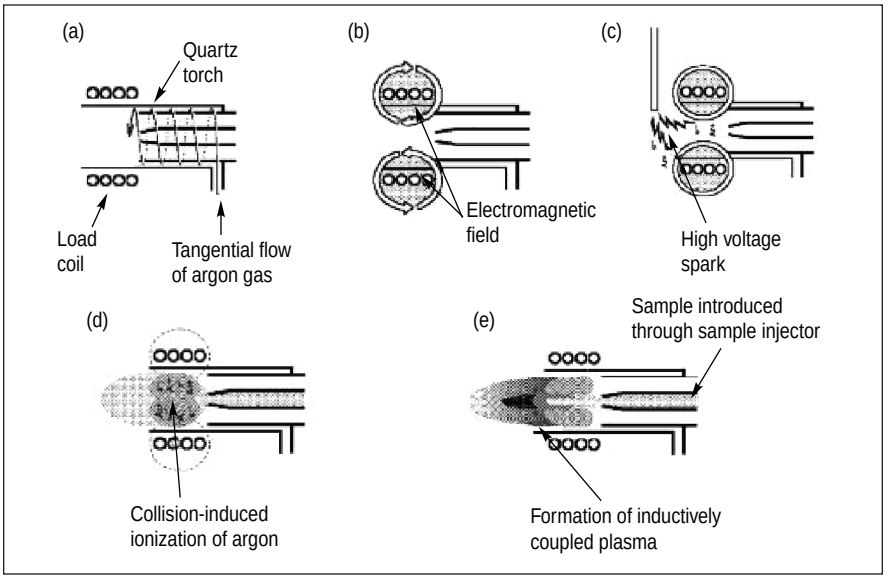

Figure 3. (right) Schematic of an ICP torch and load coil showing how the inductively coupled plasma is formed. (a) A tangential flow of argon gas is passed between the outer and middle tube of the quartz torch. (b) RF power is applied to the load coil, producing an intense electromagnetic field. (c) A high-voltage spark produces free electrons. (d) Free electrons are accelerated by the RF field, causing collisions and ionization of the argon gas. (e) The ICP is formed at the open end of the quartz torch. The sample is introduced into the plasma via the sample injector.

THE PLASMA TORCH

Before we take a look at the fundamental principles behind the creation of an inductively coupled plasma used in ICP-MS, let us take a look at the basic components that are used to generate the source: a plasma torch, a radio frequency (RF) coil, and RF power supply. Figure 1 shows their proximity to the rest of the instrument; Figure 2 is a more detailed view of the plasma torch and RF coil relative to the MS interface.

The plasma torch consists of three concentric tubes, which are usually made from quartz. In Figure 2, these are shown as the outer tube, middle tube, and sample injector. The torch can either be one-piece with all three tubes connected, or it can be a demountable design in which the tubes and the sample injector are separate. The gas (usually argon) used to form the plasma (plasma gas) is passed between the outer and middle tubes at a flow rate of ~12–17 L/min. A second gas flow, the auxiliary gas, passes between the middle tube and the sample injector at ~1 L/min and is used to change the position of the base of the plasma relative to the tube and the injector. A third gas flow, the nebulizer gas, also flowing at ~1 L/min carries the sample, in the form of a fine-droplet aerosol, from the sample introduction system (for details, see Part II of this series: *Spectroscopy* **16**[5], 56–60 [2001]) and physically punches a channel through the center of the plasma. The sample injector is often made from materials other than quartz, such as alumina, platinum, and sapphire, if highly corrosive materials need to be analyzed. It is worth mentioning that although argon is the most suitable gas to use for all three flows, there are analytical benefits in using other gas mixtures, especially in the nebulizer flow (6). The plasma torch

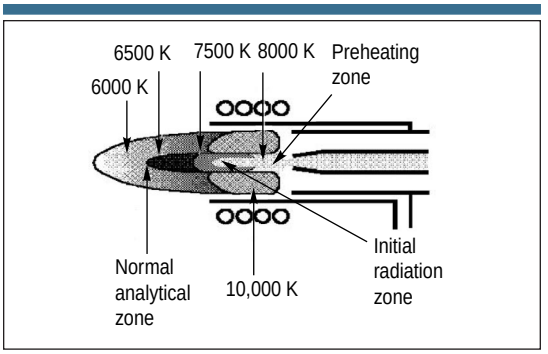

Figure 4. Different temperature zones in the plasma.

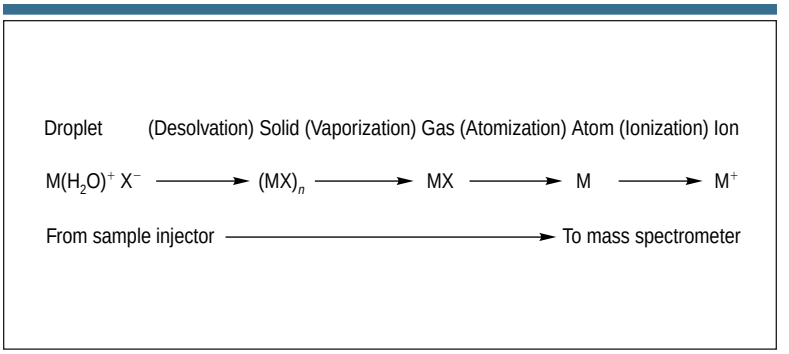

Figure 5. Mechanism of conversion of a droplet to a positive ion in the ICP.

is mounted horizontally and positioned centrally in the RF coil, approximately 10–20 mm from the interface. It must be emphasized that the coil used in an ICP-MS plasma is slightly different from the one used in ICP-OES. In all plasmas, there is a potential difference of a few hundred volts produced by capacitive coupling between the RF coil and the plasma. In an ICP mass spectrometer, this would result in a secondary discharge between the plasma and the interface cone, which could negatively affect the performance of the instrument. To compensate for this, the coil must be grounded to keep the interface region as close to zero potential as possible. I will discuss the full implications of this in greater detail in Part IV of this series.

FORMATION OF AN ICP DISCHARGE

Let us now discuss the mechanism of formation of the plasma discharge. First, a tangential (spiral) flow of argon gas is directed between the outer and middle tube of a quartz torch. A load coil, usually copper, surrounds the top end of the torch and is connected to a radio frequency generator. When RF power (typically 750–1500 W, depending on the sample) is applied to the load coil, an alternating current oscillates within the coil at a rate corresponding to the frequency of the generator. In most ICP generators this frequency is either 27 or 40 MHz. This RF oscillation of the current in the coil causes an intense electromagnetic field to be created in the area at the top of the torch. With argon gas flowing through the torch, a high-voltage spark is applied to the gas, which causes some electrons to be stripped from their argon atoms. These electrons, which are caught up and accelerated in the magnetic field, then collide with other argon atoms, stripping off still more electrons. This collision-induced ionization of the argon continues in a chain reaction, breaking down the gas into argon atoms, argon ions, and electrons, forming what is known as an inductively coupled plasma discharge. The ICP discharge is then sustained within the torch and load coil as RF energy is continually transferred to it through the inductive coupling process. The sample aerosol is then introduced into the plasma through a third tube called the sample injector. This whole process is conceptionally shown in Figure 3.

THE FUNCTION OF THE RF GENERATOR

Although the principles of an RF power supply have not changed since the work of Greenfield (4), the components have become significantly smaller. Some of the early generators that used nitrogen or air required 5–10 kW of power to sustain the plasma discharge — and literally took up half the room. Most of today's generators use solid-state electronic components, which means that vacuum power amplifier tubes are no longer required. This makes modern instruments significantly smaller and, because vacuum tubes were notoriously unreliable and unstable, far more suitable for routine operation.

As mentioned previously, two frequencies have typically been used for ICP RF generators: 27 and 40 MHz. These frequencies have been set aside specifically for RF applications of this kind, so they will not interfere with other communication-based frequencies. The early RF generators used 27 MHz, while the more recent designs favor 40 MHz. There appears to be no significant analytical advantage of one type over the other. However, it is worth mentioning that the 40-MHz design typically runs at lower power levels, which produces lower signal intensity and reduced background levels. Because it uses slightly lower power, this might be considered advantageous when it comes to long-term use of the generator.

The more important consideration is the coupling efficiency of the RF generator to the coil. The majority of modern solid-state RF generators are on the order of 70–75% efficient, meaning that 70–75% of the delivered power actually makes it into the plasma. This wasn't always the case, and some of the older vacuum tube–designed generators were notoriously inefficient; some of them experienced more than a 50% power loss. Another important criterion to consider is the way the matching network compensates for changes in impedance (a material's resistance to the flow of an electric current) produced by the sample's matrix components or differences in solvent volatility. In older crystal-controlled generators, this was usually done with servo-driven capacitors. They worked very well with most sample types, but because they were mechanical devices, they struggled to compensate for very rapid impedance changes produced by some samples. As a result, the plasma was easily extinguished, particularly during aspiration of volatile organic solvents.

These problems were partially overcome by the use of free-running RF generators, in which the matching network was based on electronic tuning of small changes in frequency brought about by the sample solvent or matrix components. The major benefit of this approach was that compensation for impedance changes was virtually instantaneous because there were no moving parts. This allowed for the successful analysis of many sample types that would probably have extinguished the plasma of a crystal-controlled generator.

IONIZATION OF THE SAMPLE

To better understand what happens to the sample on its journey through the plasma source, it is important to understand the different heating zones within the discharge. Figure 4 shows a cross-sectional representation of the discharge along with the approximate temperatures for different regions of the plasma.

As mentioned previously, the sample aerosol enters the injector via the spray chamber. When it exits the sample injector, it is moving at such a velocity that it physically punches a hole through the center of the plasma discharge. It then goes through a number of physical changes, starting at the preheating zone and continuing through the radiation zone before it eventually becomes a positively charged ion in the analytical zone. To explain this in a very simplistic way, let's assume that the element exists as a trace metal salt in solution. The first step that takes place is desolvation of the droplet. With the water molecules stripped away, it then becomes a very small solid particle. As the sample moves further into the plasma, the solid particle changes first into a gaseous form and then into a ground-state atom. The final process of conversion of an atom to an ion is achieved mainly by collisions of energetic argon electrons (and to a lesser extent by argon ions) with the ground-state atom (7). The ion then emerges from the plasma and is directed into the interface of the mass spectrometer (for details on the mechanisms of ion generation, please refer to Part I of this series: *Spectroscopy* **16**[4], 38–42 [2001]). This process of conversion of droplets into ions is represented in Figure 5.

The next installment of this series will focus on probably the most crucial area of an ICP mass spectrometer — the interface region — where the ions generated in the atmospheric plasma have to be sampled with consistency and electrical integrity by the mass spectrometer, which is under extremely high vacuum.

REFERENCES

(1) A.L. Gray, *Analyst* **100,** 289–299 (1975).
(2) G.N. Coleman, D.E. Miller, and R.W. Stark, *Am. Lab.* **30**(4), 33R (1998).
(3) D.J. Douglas and J.B. French, *Anal. Chem.* **53,** 37-41 (1981).
(4) S. Greenfield, I.L. Jones, and C.T. Berry, *Analyst* **89,** 713–720 (1964).
(5) R.S. Houk, V.A. Fassel, and H.J. Svec, *Dyn. Mass Spectrom.* **6,** 234 (1981).
(6) J.W. Lam and J.W. McLaren, *J. Anal. Atom. Spectom.* **5,** 419–424 (1990).
(7) T. Hasegawa and H. Haraguchi, *ICPs in Analytical Atomic Spectrometry,* A. Montaser and D.W. Golightly, Eds., 2d ed. (VCH, New York, 1992).

Robert Thomas *is the principal of his own freelance writing and scientific marketing consulting company, Scientific Solutions, based in Gaithersburg, MD. He specializes in trace-element analysis and can be contacted by e-mail at thomasrj@bellatlantic.net or via his web site at www.scientificsolutions1.com.* ◆

A Beginner's Guide to ICP-MS

Part IV: The Interface Region

ROBERT THOMAS

The interface region is probably the most critical area of the whole inductively coupled plasma mass spectrometry (ICP-MS) system. It certainly gave the early pioneers of the technique the most problems to overcome. Although we take all the benefits of ICP-MS for granted, the process of taking a liquid sample, generating an aerosol that is suitable for ionization in the plasma, and then sampling a representative number of analyte ions, transporting them through the interface, focusing them via the ion optics into the mass spectrometer, finally ending up with detection and conversion to an electronic signal, are not trivial tasks. Each part of the journey has its own unique problems to overcome but probably the most challenging is the movement of the ions from the plasma to the mass spectrometer. Let's begin by explaining how the ion-sampling process works, which will give readers an insight into the many problems faced by the early researchers.

SAMPLING THE IONS

Figure 1 shows the proximity of the interface region to the rest of the instrument. The role of the interface is to transport the ions efficiently, consistently, and with electrical integrity from the plasma, which is at atmospheric pressure (760 Torr), to the mass spectrometer analyzer region, which is at approximately 10^{-6} Torr. One first achieves this by directing the ions into the interface region. The interface consists of two metallic cones with very small orifices, which are maintained at a vacuum of ~2 Torr with a mechanical roughing pump. After the ions are generated in the plasma, they pass through the first cone, known as the sampler cone, which has an orifice diameter of 0.8–1.2 mm. From there they travel a short distance to the skimmer cone, which is generally sharper than the sampler cone and has a much smaller orifice (0.4–0.8 mm i.d.). Both cones are usually made of nickel, but they can be made of materials such as platinum that are far more tolerant to corrosive liquids. To reduce the effects of the high-temperature plasma on the cones, the interface housing is water-cooled and made from a material that dissipates heat easily, such as copper or aluminum. The ions then emerge from the skimmer cone, where they are directed through the ion optics, and finally are guided into the mass separation device. Figure 2 shows the interface region in greater detail; Figure 3 shows a close-up of the sampler and skimmer cones.

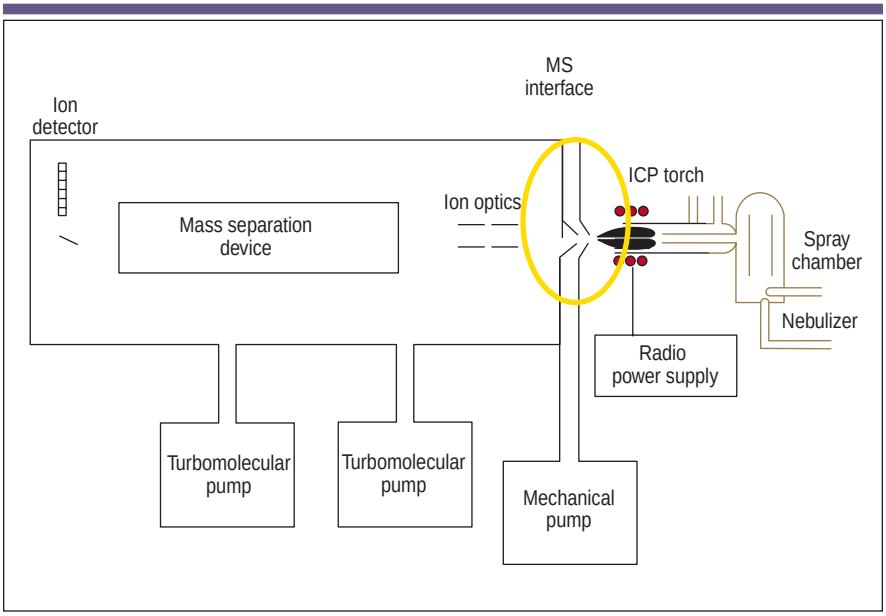

Figure 1. Schematic of an inductively coupled plasma mass spectrometry (ICP-MS) system, showing the proximity of the interface region.

CAPACITIVE COUPLING

This process sounds fairly straightforward but proved very problematic during the early development of ICP-MS because of an undesired electrostatic (capacitive) coupling between the load coil and the plasma discharge, producing a potential difference of 100–200 V. Although this potential is a physical characteristic of all inductively coupled plasma discharges, it is particularly serious in an ICP mass spectrometer because the capacitive coupling creates an electrical discharge between the plasma and the sampler cone. This discharge, commonly called the pinch effect or secondary discharge, shows itself as arcing in the region where the plasma is in contact with the sampler cone (1). This process is shown very simplistically in Figure 4.

If not taken care of, this arcing can cause all kinds of problems, including an increase in doubly charged interfering species, a wide kinetic energy spread of sampled ions, formation of ions gener-

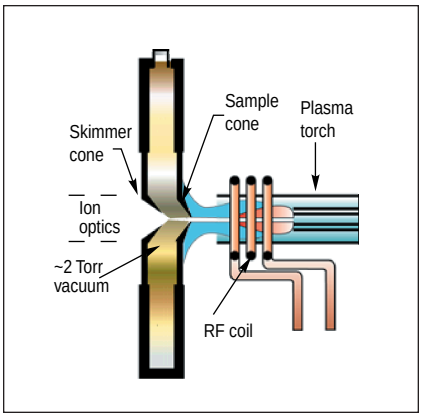

Figure 2. Detailed view of the interface region.

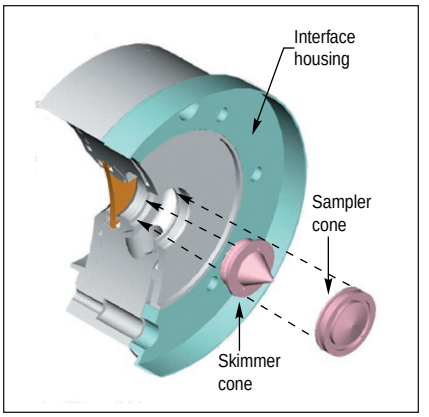

Figure 3. Close-up view of the sampler and skimmer cones. (Courtesy PerkinElmer Instruments, Norwalk, CT.)

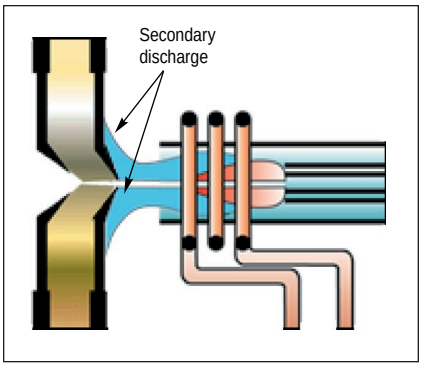

Figure 4. Interface area affected by secondary discharge.

ated from the sampler cone, and a decreased orifice lifetime. These problems were reported by many of the early researchers of the technique (2, 3). In fact, because the arcing increased with sampler cone orifice size, the source of the secondary discharge was originally thought to be the result of an electro-gasdynamic effect, which produced an increase in electron density at the orifice (4). After many experiments it was eventually realized that the secondary discharge was a result of electrostatic coupling of the load coil to the plasma. The problem was first eliminated by grounding the induction coil at the center, which had the effect of reducing the radio frequency (RF) potential to a few volts. This effect can be seen in Figure 5, taken from one of the early papers, which shows the reduction in plasma potential as the coil is grounded at different positions (turns) along its length.

Originally, the grounding was implemented by attaching a physical grounding strap from the center turn of the coil to the interface housing. In today's instrumentation the grounding is achieved in a number of different ways, depending on the design of the interface. Some of the most popular designs include balancing the oscillator inside the circuitry of the RF generator (5); positioning a grounded shield or plate between the coil and the plasma torch (6); or using two interlaced coils where the RF fields go in opposing directions (7). They all work differently but achieve a similar result of reducing or eliminating the secondary discharge.

ION KINETIC ENERGY

The impact of a secondary discharge cannot be overestimated with respect to its effect on the kinetic energy of the ions being sampled. It is well documented that the energy spread of the ions entering the mass spectrometer must be as low as possible to ensure that they can all be focused efficiently and with full electrical integrity by the ion optics and the mass separation device. When the ions emerge from the argon plasma, they will all have different kinetic energies based on their mass-to-change ratio. Their velocities should all be similar because they are controlled by rapid expansion of the bulk plasma, which will be neutral as long as it is maintained at zero potential. As the ion beam passes through the sampler cone into the skimmer cone, expansion will take place, but its composition and integrity will be maintained, assuming the plasma is neutral. This can be seen in Figure 6.

Electrodynamic forces do not play a role as the ions enter the sampler or the skimmer because the distance over which the ions exert an influence on each other (known as the *Debye length*) is small (typically 10^{-3}–10^{-4} mm) compared with the diameter of the orifice (0.5–1.0 mm) (8), as Figure 7 shows.

It is therefore clear that maintaining a neutral plasma is of paramount importance to guarantee electrical integrity of the ion beam as it passes through the interface region. If a secondary discharge is present, it changes the electrical characteristics of the plasma, which will affect the kinetic energy of the ions differently, depending on their mass. If the plasma is at zero potential, the ion energy spread is in the order of 5–10 eV. However, if a secondary discharge is present, it results in a much wider spread of ion energies entering the mass spectrometer (typically 20–40 eV), which makes ion focusing far more complicated (8).

BENEFITS OF A WELL-DESIGNED INTERFACE

The benefits of a well-designed interface are not readily obvious if simple aqueous samples are analyzed using only one set of operating conditions. However, it becomes more apparent when many different sample types are being analyzed, requiring different operating parameters. A true test of the design of the interface occurs when plasma conditions need to be changed, when the sample matrix changes, or when a dry sample aerosol is being introduced into the ICP-MS. Analytical scenarios like these have the potential to induce a secondary discharge, change the kinetic energy of the ions entering the mass spectrometer, and affect the tuning of the ion optics. It is therefore

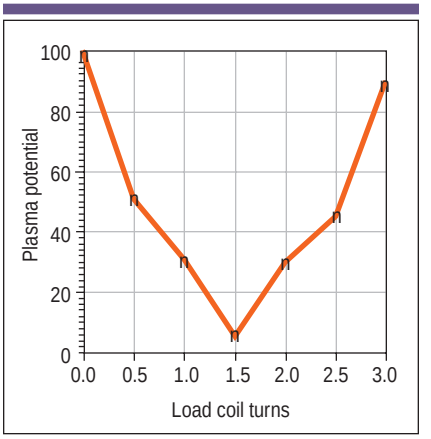

Figure 5. Reduction in plasma potential as the load coil is grounded at different positions (turns) along its length.

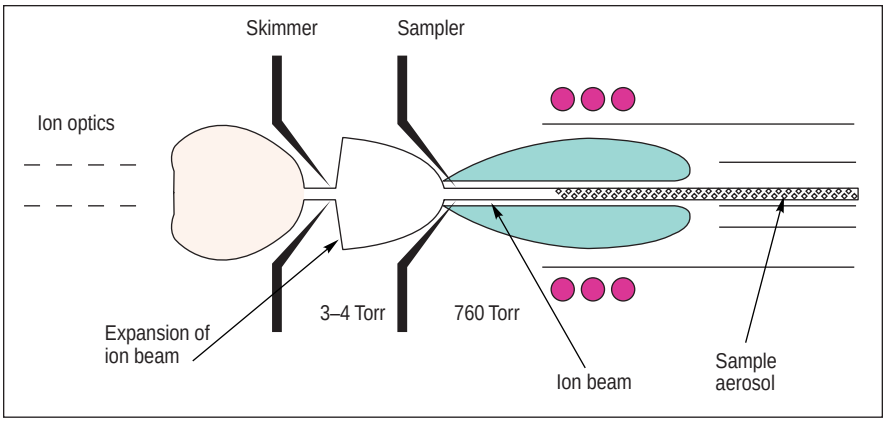

Figure 6. The composition of the ion beam is maintained, assuming a neutral plasma.

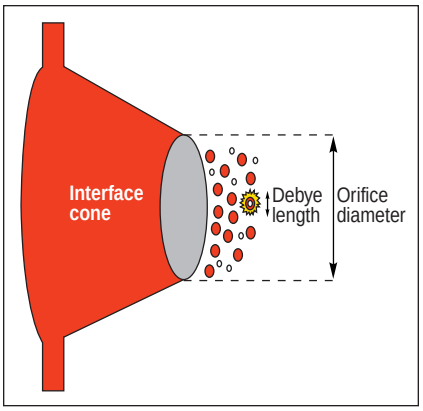

Figure 7. Electrodynamic forces do not affect the composition of the ion beam entering the sampler or the skimmer cone.

critical that the interface grounding mechanism can handle these types of real-world applications, of which typical examples include

• The use of cool-plasma conditions. It is standard practice today to use cool-plasma conditions (500–700 W power and 1.0–1.3 L/min nebulizer gas flow) to lower the plasma temperature and reduce argon-based polyatomic interferences such as $^{40}Ar^{16}O$, ^{40}Ar, and ^{38}ArH, in the determination of difficult elements like ^{56}Fe, ^{40}Ca, and ^{39}K. Such dramatic changes from normal operating conditions (1000 W, 0.8 L/min) will affect the electrical characteristics of the plasma.

• Running volatile organic solvents. Analyzing oil or organic-based samples requires a chilled spray chamber (typically −20 °C) or a membrane desolvation system to reduce the solvent loading on the plasma. In addition, higher RF power (1300–1500 W) and lower nebulizer gas flow (0.4–0.8 L/min) are required to dissociate the organic components in the sample. A reduction in the amount of solvent entering the plasma combined with higher power and lower nebulizer gas flow translate into a hotter plasma and a change in its ionization mechanism.

• Reducing oxides. The formation of oxide species can be problematic in some sample types. For example, in geochemical applications it is quite common to sacrifice sensitivity by lowering the nebulizer gas flow and increasing the RF power to reduce the formation of rare earth oxides, which can interfere spectrally with the determination of other analytes. Unfortunately these conditions have the potential to induce a secondary discharge.

• Running a "dry" plasma. Sampling accessories such as membrane desolvators, laser ablation systems, and electrothermal vaporization devices are being used more routinely to enhance the flexibility of ICP-MS. The major difference between these sampling devices and a conventional liquid sample introduction system, is that they generate a "dry" sample aerosol, which requires totally different operating conditions compared with a conventional "wet" plasma. An aerosol containing no solvent can have a dramatic effect on the ionization conditions in the plasma.

Even though most modern ICP-MS interfaces have been designed to minimize the effects of the secondary discharge, it

"Tutorial" continued on page 34

of the vendor) have been checked to ensure compliance with the regulations. The audit should be planned and should cover items such as the design and programming phases, product testing and release, documentation, and support; a report of the audit should be produced after the visit. Two published articles have covered vendor audits in more detail (3, 4).

The minimum audit is a remote vendor audit using a checklist that the vendor completes and returns to you. This is usually easy to complete, but the writer of the checklist must ensure that the questions are written in a way that can be understood by the recipient, because language and cultural issues could affect a remote checklist. Moreover, there is little way of checking the answers you receive. However, for smaller software systems — and some spectrometers fall into this category — a remote audit is a cost-effective way of getting information on how a vendor carries out its development process, so long as you know and understand its limitations.

SYSTEM SELECTION: PART TWO

If the vendor audit, price quote, instrument, and software are all acceptable, you'll be raising a capital expenditure request (or whatever it is called in your organization) and then generating a purchase order. The quote and the purchase order are a link in the validation chain; they provide a link into the next phase of the validation life cycle: qualification. The purchase order is the first stage in defining the initial configuration of the system, as we'll discover in the next article in this series.

REFERENCES

(1) R.D. McDowall, *Spectroscopy* **16**(2), 32–43 (2001).
(2) IEEE Standard 1012-1986, "Software Validation and Verification Plans," Institute of Electronic and Electrical Engineers, Piscataway, NJ, USA.
(3) R.D. McDowall, *Sci. Data Mgmt.* **2**(2), 8 (1998).
(4) R.D. McDowall, *Sci. Data Mgmt.* **2**(3), 8 (1998). ◆

"Tutorial" continued from page 34

shouldn't be taken for granted that they can all handle changes in operating conditions and matrix components with the same amount of ease. The most noticeable problems that have been reported include spectral peaks of the cone material appearing in the blank (9); erosion or discoloration of the sampling cones; widely different optimum plasma conditions for different masses (10); and increased frequency of tuning the ion optics (8). Of all these, probably the most inconvenient problem is regular optimization of the lens voltages, because slight changes in plasma conditions can produce significant changes in ion energies, which require regular retuning of the ion optics. Even though most instruments have computer-controlled ion optics, it becomes another variable that must be optimized. This isn't a major problem but might be considered an inconvenience for a high–sample throughput lab. There is no question that the plasma discharge, interface region, and ion optics all have to be designed in concert to ensure that the instrument can handle a wide range of operating conditions and sample types. The role of the ion optics will be discussed in greater detail in the next installment of this series.

REFERENCES

(1) A.L. Gray and A.R. Date, *Analyst* **108**, 1033 (1983).
(2) R.S. Houk, V.A. Fassel, and H.J. Svec, *Dynamic Mass Spectrosc.* **6**, 234 (1981).
(3) A.R. Date and A.L. Gray, *Analyst* **106**, 1255 (1981).
(4) A.L. Gray and A.R. Date, *Dynamic Mass Spectrosc.* **6**, 252 (1981).
(5) S.D. Tanner, *J. Anal. At. Spectrom.* **10**, 905 (1995).
(6) K. Sakata and K. Kawabata, *Spectrochim. Acta* **49B**, 1027 (1994).
(7) S. Georgitus, M. Plantz, poster paper presented at the Winter Conference on Plasma Spectrochemistry, FP4, Fort Lauderdale, FL (1996).
(8) D.J. Douglas and J.B. French, *Spectrochim. Acta* **41B**, 3, 197 (1986).
(9) D.J. Douglas, *Can. J. Spectrosc.* **34**, 2 (1089).
(10) J.E. Fulford and D.J. Douglas, *Appl. Spectrosc.* **40**, 7 (1986).

Robert Thomas *has more than 30 years experience in trace element analysis. He is the principal of his own freelance writing and scientific consulting company, Scientific Solutions, based in Gaithersburg, MD. He can be contacted by e-mail at thomasrj@bellatlantic.net or via his web site at www.scientificsolutions1.com.*◆

Beginner's Guide to ICP-MS

Part VI — The Mass Analyzer

ROBERT THOMAS

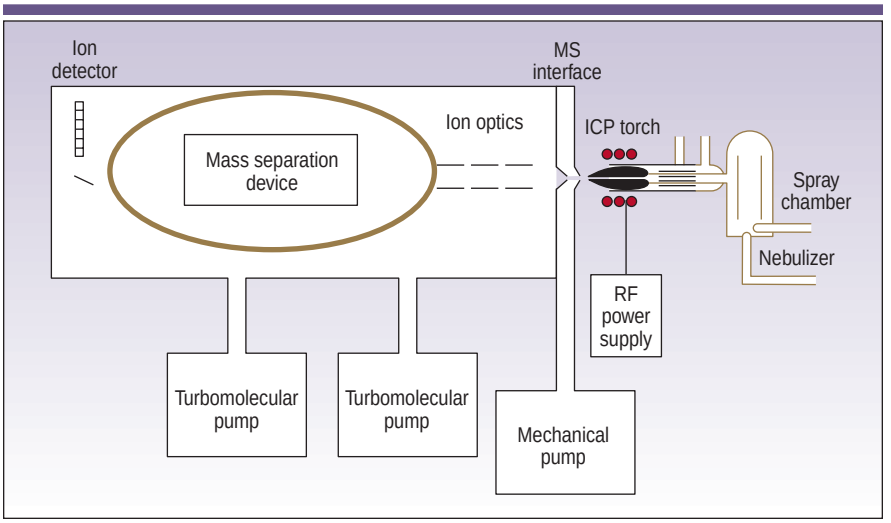

Figure 1. Schematic of an ICP-MS system showing the location of the mass separation device.

Part VI of the series on inductively coupled plasma–mass spectroscopy (ICP-MS) fundamentals deals with the heart of the system — the mass separation device. Sometimes called the mass analyzer, it is the region of the ICP mass spectrometer that separates the ions according to their mass-to-charge ratio (m/z). This selection process is achieved in a number of different ways, depending on the mass separation device, but they all have one common goal: to separate the ions of interest from all the other nonanalyte, matrix, solvent, and argon-based ions.

Although inductively coupled plasma–mass spectroscopy (ICP-MS) was commercialized in 1983, the first 10 years of its development primarily used traditional quadrupole mass filter technology to separate the ions of interest. These worked exceptionally well for most applications but proved to have limitations in determining difficult elements or dealing with more-complex sample matrices. This led to the development of alternative mass separation devices that pushed the capabilities of ICP-MS so it could be used for more challenging applications. Before we discuss these different mass spectrometers in greater detail, let's take a look at the location of the mass analyzer in relation to the ion optics and the detector. Figure 1 shows this in greater detail.

As we can see, the mass analyzer is positioned between the ion optics and the detector and is maintained at a vacuum of approximately 10^{-6} Torr with a second turbomolecular pump. Assuming the ions are emerging from the ion optics at the optimum kinetic energy (1), they are ready to be separated according to their mass-to-charge ratio by the mass analyzer. There are basically four kinds of commercially available mass analyzers: quadrupole mass filters, double focusing magnetic sector, time-of-flight, and collision–reaction cell technology. They all have their own strengths and weaknesses, which we will discuss in greater detail in the next few installments of this column. Let's first begin with the most common of the mass separation devices used in ICP-MS, the quadrupole mass filter.

QUADRUPOLE MASS FILTER TECHNOLOGY

Developed in the early 1980s, quadrupole-based systems represent approximately 90% of all ICP mass spectrometers used today. This design was the first to be commercialized; as a result, today's quadrupole ICP-MS technology is considered a very mature, routine, high-throughput, trace-element technique. A quadrupole consists of four cylindrical or hyperbolic metallic rods of the same length and diameter. They are typically made of stainless steel or molybdenum, and sometimes have a ceramic coating for corrosion resistance. Quadrupoles used in ICP-MS are typically 15–20 cm in length and about 1 cm in diameter and operate at a frequency of 2–3 MHz.

BASIC PRINCIPLES OF OPERATION

By placing a direct current (dc) field on one pair of rods and a radio frequency (rf) field on the opposite pair, ions of a selected mass are allowed to pass through the rods to the detector, while the others are ejected from the quadrupole. Figure 2 shows this in greater detail.

In this simplified example, the analyte ion (black) and four other ions (colored) have arrived at the entrance to the four rods of the quadrupole. When a particular rf-dc voltage is applied to the rods, the positive or negative bias on the rods will electrostatically steer the analyte ion of interest down the middle of the four rods to the end, where it will emerge and be converted to an electrical pulse by the detector. The other ions of different mass-to-charge ratios will pass through the spaces between the rods and be ejected

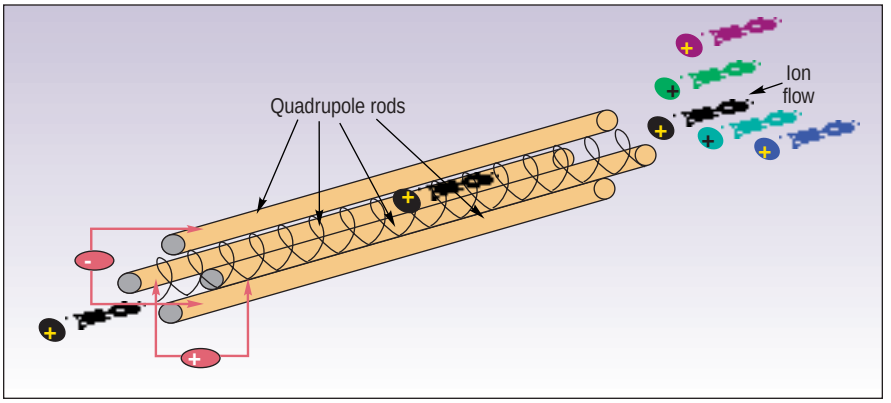

Figure 2. Schematic showing principles of a quadrupole mass filter.

from the quadrupole. This scanning process is then repeated for another analyte at a completely different mass-to-charge ratio until all the analytes in a multielement analysis have been measured. The process for the detection of one particular mass in a multielement run is represented in Figure 3. It shows a ^{63}Cu ion emerging from the quadrupole and being converted to an electrical pulse by the detector. As the rf-dc voltage of the quadrupole — corresponding to ^{63}Cu — is repeatedly scanned, the ions as electrical pulses are stored and counted by a multichannel analyzer. This multichannel data-acquisition system typically has 20 channels per mass, and as the electrical pulses are counted in each channel, a profile of the mass is built up over the 20 channels, corresponding to the spectral peak of ^{63}Cu. In a multielement run, repeated scans are made over the entire suite of analyte masses, as opposed to just one mass represented in this example.

Quadrupole scan rates are typically on the order of 2500 atomic mass units (amu) per second and can cover the entire mass range of 0–300 amu in about 0.1 s. However, real-world analysis speeds are much slower than this, and in practice 25 elements can be determined in duplicate with good precision in 1–2 min.

QUADRUPOLE PERFORMANCE CRITERIA

Two very important performance specifications of a mass analyzer govern its ability to separate an analyte peak from a spectral interference. The first is resolv-

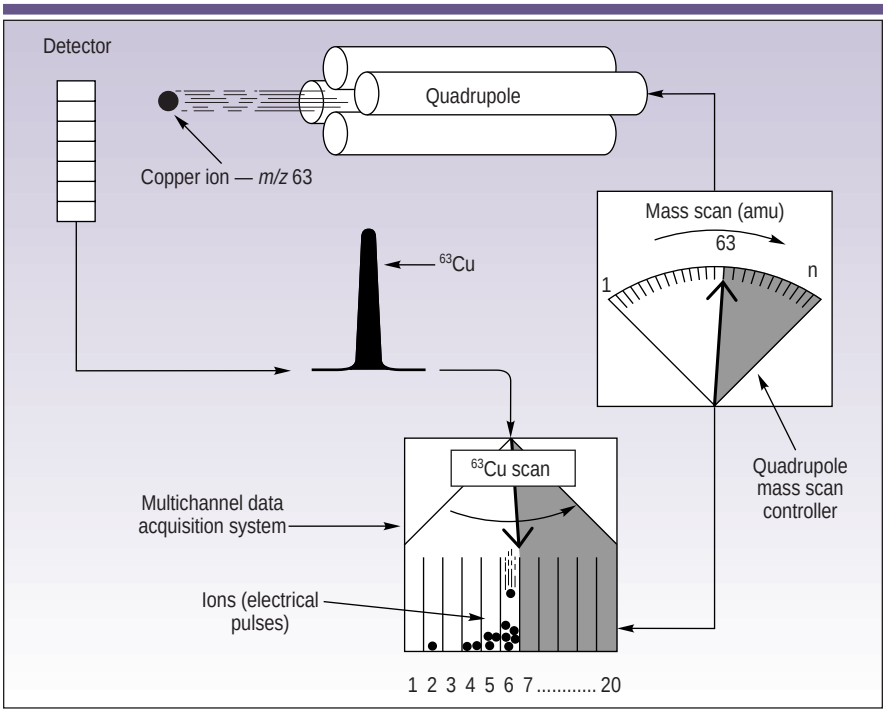

Figure 3. Profiles of different masses are built up using a multichannel data acquisition system.

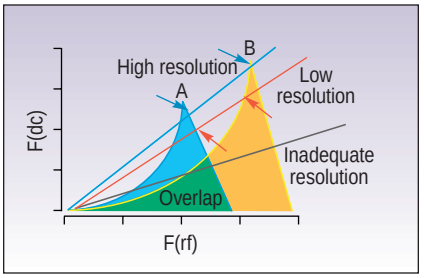

Figure 4. Simplified Mathieu stability diagram of a quadrupole mass filter, showing separation of two different masses, *A* (light blue plot) and *B* (yellow plot).

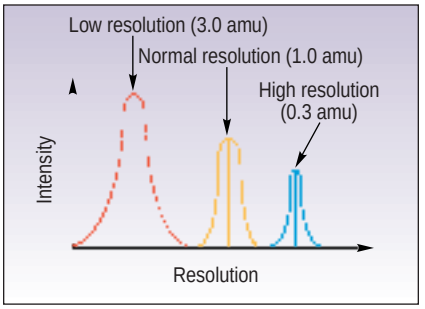

Figure 5. Sensitivity comparison of a quadrupole operated at 3.0, 1.0, and 0.3 amu resolution (measured at 10% of its peak height).

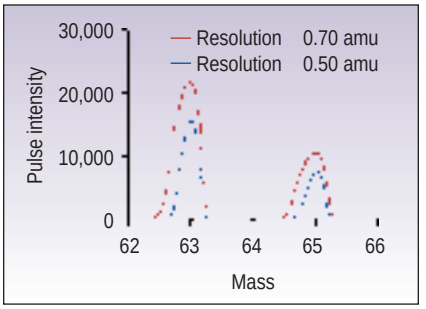

Figure 6. Sensitivity comparison of two copper isotopes, ^{63}Cu and ^{65}Cu, at resolution settings of 0.70 and 0.50 amu.

ing power (R), which in traditional mass spectrometry is represented by the following equation: $R = m/\Delta m$, where m is the nominal mass at which the peak occurs and Δm is the mass difference between two resolved peaks (2). However, for quadrupole technology, the term *resolution* is more commonly used, and is normally defined as the width of a peak at 10% of its height. The second specification is abundance sensitivity, which is the signal contribution of the tail of an adjacent peak at one mass lower and one mass higher than the analyte peak (3). Even though they are somewhat related and both define the quality of a quadrupole, the abundance sensitivity is probably the most critical. If a quadrupole has good resolution but poor abundance sensitivity, it will often prohibit the measurement of an ultratrace analyte peak next to a major interfering mass.

RESOLUTION

Let us now discuss this area in greater detail. The ability to separate different masses with a quadrupole is determined by a combination of factors including shape, diameter, and length of the rods, frequency of quadrupole power supply, operating vacuum, applied rf-dc voltages, and the motion and kinetic energy of the ions entering and exiting the quadrupole. All these factors will have a direct impact on the stability of the ions as they travel down the middle of the rods and thus the quadrupole's ability to separate ions of differing mass-to-charge ratios. This is represented in Figure 4, which shows a simplified version of the Mathieu mass stability plot of two separate masses (*A* and *B*) entering the quadrupole at the same time (4).

Any of the rf-dc conditions shown under the light blue plot will allow only mass *A* to pass through the quadrupole, while any combination of rf-dc voltages under the yellow plot will allow only mass *B* to pass through the quadrupole. If the slope of the rf-dc scan rate is steep, represented by the light blue line (high resolution), the spectral peaks will be narrow, and masses *A* and *B* will be well separated (equivalent to the distance between the two blue arrows). However, if the slope of the scan is shallow, represented by the red line (low resolution), the spectral peaks will be wide, and masses *A* and *B* will not be so well separated (equivalent to the distance between the two red arrows). On the other hand, if the slope of the scan is too shallow, represented by the gray line (inadequate resolution), the peaks will overlap each other (shown by the green area of the plot) and the masses will pass through the quadrupole without being separated. In theory, the resolution of a quadrupole mass filter can be varied between 0.3 and 3.0 amu. How-

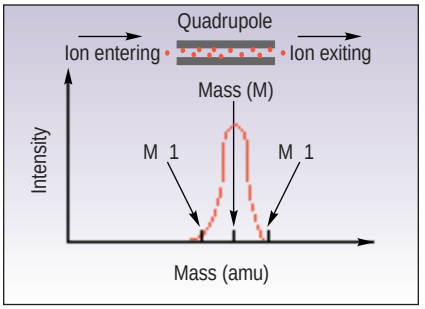

Figure 7. Ions entering the quadrupole are slowed down by the filtering process and produce peaks with a pronounced tail or shoulder at the low-mass end.

ever, improved resolution is always accompanied by a sacrifice in sensitivity, as seen in Figure 5, which shows a comparison of the same mass at a resolution of 3.0, 1.0, and 0.3 amu.

We can see that the peak height at 3.0 amu is much larger than the peak height at 0.3 amu but, as expected, it is also much wider. This would prohibit using a resolution of 3.0 amu with spectrally complex samples. Conversely, the peak width at 0.3 amu is very narrow, but the sensitivity is low. For this reason, a compromise between peak width and sensitivity usually has to be reached, depending on the application. This can clearly be seen in Figure 6, which shows a spectral overlay of two copper isotopes — ^{63}Cu and ^{65}Cu — at resolution settings of 0.70 and 0.50 amu. In practice, the quadrupole is normally operated at a resolution of 0.7–1.0 amu for most applications.

It is worth mentioning that most quadrupoles are operated in the first stability region, where resolving power is typically ~400. If the quadrupole is operated in the second or third stability regions, resolving powers of 4000 (5) and 9000 (6), respectively, have been achieved. However, improving resolution using this approach has resulted in a significant loss of signal. Although there are ways of improving sensitivity, other problems have been encountered, and as a result, to date there are no commercial instruments available based on this design.

Some instruments can vary the peak width *on-the-fly*, which means that the resolution can be changed between 3.0 and 0.3 amu for every analyte in a multielement run. For some challenging applications this can be beneficial, but in reality they are rare. So, even though quadrupoles can be operated at higher resolution (in the first stability region), until now the slight improvement has not become a practical benefit for most routine applications.

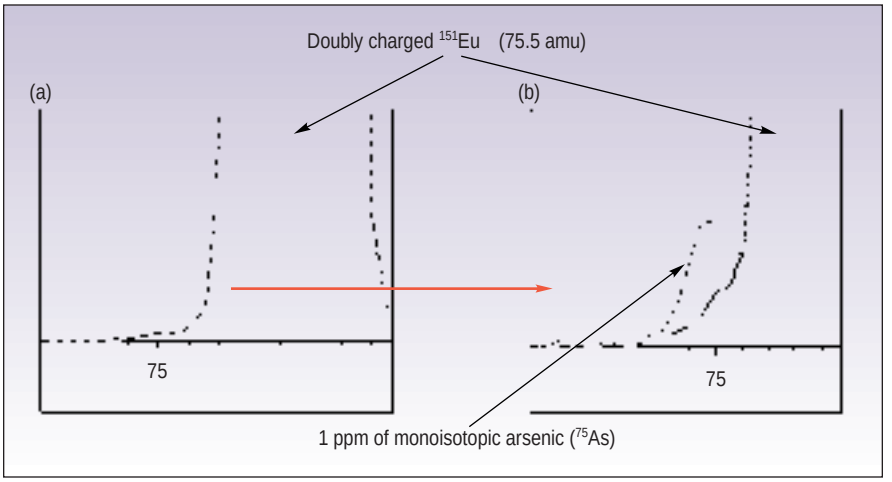

Figure 8. A low abundance sensitivity specification is critical to minimize spectral interferences, as shown by (a) a spectral scan of 50 ppm of $^{151}Eu^{++}$ at 75.5 amu and (b) an expanded view, which shows how the tail of the $^{151}Eu^{++}$ elevates the spectral background of 1 ppb of As at mass 75.

ABUNDANCE SENSITIVITY

We can see in Figure 6 that the tails of the spectral peaks drop off more rapidly at the high mass end of the peak compared with the low mass end. The overall peak shape, particularly its low mass and high mass tail, is determined by the abundance sensitivity of the quadrupole,

which is affected by a combination of factors including design of the rods, frequency of the power supply, and operating vacuum (7). Even though they are all important, probably the biggest impacts on abundance sensitivity are the motion and kinetic energy of the ions as they enter and exit the quadrupole. If one looks at the Mathieu stability plot in Figure 3, it can be seen that the stability boundaries of each mass are less defined (not so sharp) on the low mass side than they are on the high mass side (4). As a result, the characteristics of ion motion at the low mass boundary is different from the high mass boundary and is therefore reflected in poorer abundance sensitivity at the low mass side compared with the high mass side. In addition, the velocity (and therefore the kinetic energy) of the ions entering the quadrupole will affect the ion motion and, as a result, will have a direct impact on the abundance sensitivity. For that reason, factors that affect the kinetic energy of the ions, like high plasma potential and the use of lens components to accelerate the ion beam, will degrade the instrument's abundance sensitivity (8).

These are the fundamental reasons why the peak shape is not symmetrical with a quadrupole and explains why there is always a pronounced shoulder at the low mass side of the peak compared to the high mass side — as represented in Figure 7, which shows the theoretical peak shape of a nominal mass M. We can see that the shape of the peak at one mass lower (M − 1) is slightly different from the other side of the peak at one mass higher (M + 1) than the mass M. For this reason, the abundance sensitivity specification for all quadrupoles is always worse on the low mass side than on the high mass side and is typically 1×10^{-6} at M − 1 and 1×10^{-7} at M + 1. In other words, an interfering peak of 1 million counts per second (cps) at M − 1 would produce a background of 1 cps at M, while it would take an interference of 10^7 cps at M + 1 to produce a background of 1 cps at M.

BENEFITS OF GOOD ABUNDANCE SENSITIVITY

Figure 8 shows an example of the importance of abundance sensitivity. Figure 8a is a spectral scan of 50 ppm of the doubly charged europium ion — $^{151}Eu^{++}$ at 75.5 amu (a doubly charged ion is one with two positive charges, as opposed to a normal singly charged positive ion, and exhibits a *m/z* peak at half its mass). We can see that the intensity of the peak is so great that its tail overlaps the adjacent mass at 75 amu, which is the only available mass for the determination of arsenic. This is highlighted in Figure 8b, which shows an expanded view of the tail of the $^{151}Eu^{++}$, together with a scan of 1 ppb of As at mass 75. We can see very clearly that the ^{75}As signal lies on the sloping tail of the $^{151}Eu^{++}$ peak. Measurement on a sloping background like this would result in a significant degradation in the arsenic detection limit, particularly as the element is monoisotopic and no alternative mass is available. This example shows the importance of a low abundance sensitivity specification in ICP-MS.

DIFFERENT QUARDUPOLE DESIGNS

Many different designs of quadrupole are used in ICP-MS, all made from different materials with various dimensions, shapes, and physical characteristics. In addition, they are all maintained at slightly different vacuum chamber pressures and operate at different frequencies. Theory tells us that hyperbolic rods should generate a better hyperbolic (elliptical) field than cylindrical rods, resulting in higher transmission of ions at higher resolution. It also tells us that a higher operating frequency means a higher rate of oscillation — and therefore separation — of the ions as they travel down the quadrupole. Finally, it is very well accepted that a higher vacuum produces fewer collisions between gas molecules and ions, resulting in a narrower spread in kinetic energy of the ions and therefore less of a tail at the low mass side of a peak. However, given all these specification differences, in practice the performance of most modern quadrupole ICP-MS instrumentation is very similar.

So even though these differences will mainly be transparent to users, there are some subtle variations in each instrument's measurement protocol and the software's approach to peak quantitation. This is a very important area that we will discuss it in greater detail in a future column. The next part of the series will continue with describing the fundamental principles of other types of mass analyzers used in ICP-MS.

REFERENCES

(1) R. Thomas, *Spectroscopy* **16**(9), 38–44 (2001).
(2) F. Adams, R. Gijbels, and R. Van Grieken, *Inorganic Mass Spectrometry* (John Wiley and Sons, New York, 1988).
(3) A. Montasser, Ed. *Inductively Coupled Plasma Mass Spectrometry* (Wiley-VCH, Berlin, 1998).
(4) P.H. Dawson, Ed., *Quadrupole Mass Spectrometry and its Applications* (Elsevier, Amsterdam, 1976; reissued by AIP Press, Woodbury, NY, 1995).
(5) Z. Du, T.N. Olney, and D.J. Douglas, *J. Am. Soc. Mass Spectrom.* **8**, 1230–1236 (1997).
(6) P.H. Dawson and Y. Binqi, *Int. J. Mass Spectrom., Ion Proc.* **56**, 25 (1984).
(7) D. Potter, *Agilent Technologies Application Note*, 228–349 (January, 1996).
(8) E.R. Denoyer, D. Jacques, E. Debrah, and S.D. Tanner, *At. Spectrosc.* **16**(1), 1 (1995).

Robert Thomas *has more than 30 years experience in trace element analysis. He is the principal of his own freelance writing and scientific consulting company, Scientific Solutions, based in Gaithersburg, MD. He can be contacted by e-mail at thomasrj@bellatlantic.net or via his web site at www.scientificsolutions1.com.*◆

Beginner's Guide to ICP-MS

Part VII: Mass Separation Devices — Double-Focusing Magnetic-Sector Technology

ROBERT THOMAS

Although quadrupole mass analyzers represent more than 90% of all inductively coupled plasma mass spectrometry (ICP-MS) systems installed worldwide, limitations in their resolving power has led to the development of high resolution spectrometers based on the double-focusing magnetic-sector design. Part VII of this series on ICP-MS takes a detailed look at this very powerful mass separation device, which has found its niche in solving challenging application problems that require excellent detection capability, exceptional resolving power, and very high precision.

As discussed in Part VI of this series (1), a quadrupole-based ICP-MS system typically offers a resolution of 0.7–1.0 amu. This is quite adequate for most routine applications, but has proved to be inadequate for many elements that are prone to argon-, solvent-, or sample-based spectral interferences. These limitations in quadrupoles drove researchers in the direction of traditional high resolution, magnetic-sector technology to improve quantitation by resolving the analyte mass away from the spectral interference (2). These ICP-MS instruments, which were first commercialized in the late 1980s, offered resolving power as high as 10,000, compared with a quadrupole, which was approximately 300. This dramatic improvement in resolving power allowed difficult elements like Fe, K, As, V, and Cr to be determined with relative ease, even in complex sample matrices.

TRADITIONAL MAGNETIC-SECTOR INSTRUMENTS

The magnetic-sector design was first used in molecular spectroscopy for the structural analysis of complex organic compounds. Unfortunately, it was initially found to be unsuitable as a separation device for an ICP system because it required a few thousand volts of potential at the plasma interface area to accelerate the ions into the mass analyzer. For this reason, basic changes had to be made to the ion acceleration mechanism to optimize it as an ICP-MS separation device. This was a significant challenge when magnetic-sector systems were first developed in late 1980s. However, by the early 1990s, instrument designers solved this problem by moving the high-voltage components away from the plasma and interface and closer to the mass spectrometer. Today's instrumentation is based on two different approaches, commonly referred to as standard or reverse Nier-Johnson geometry. Both these designs, which use the same basic principles, consist of two analyzers — a traditional electromagnet and an electrostatic analyzer (ESA). In the standard (sometimes called forward) design, the ESA is positioned before the magnet, and in the reverse design it is positioned after the magnet. A schematic of a reverse Nier-Johnson spectrometer is shown in Figure 1.

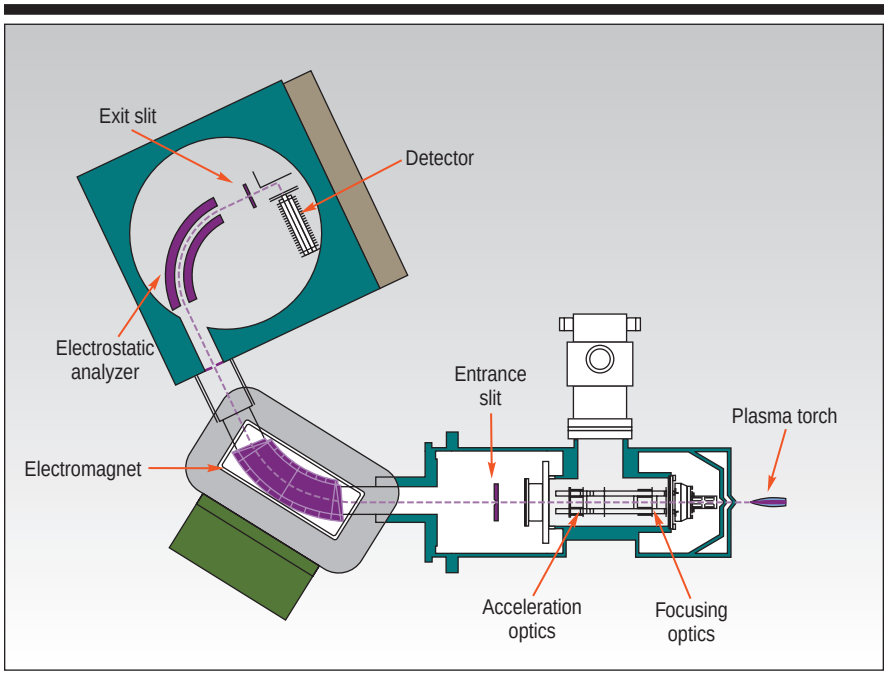

Figure 1. Schematic of a reverse Nier Johnson double-focusing magnetic-sector mass spectrometer (Courtesy of Finnigan MAT).

PRINCIPLES OF OPERATION

With this approach, ions are sampled from the plasma in a conventional manner and then accelerated in the ion optic region to a few kilovolts before they enter the mass analyzer. The magnetic field, which is dispersive with respect to ion en-

ergy and mass, then focuses all the ions with diverging angles of motion from the entrance slit. The ESA, which is only dispersive with respect to ion energy, then focuses all the ions onto the exit slit, where the detector is positioned. If the energy dispersion of the magnet and ESA are equal in magnitude but opposite in direction, they will focus both ion angles (first focusing) and ion energies (second or double focusing), when combined together. Changing the electrical field in the opposite direction during the cycle time of the magnet (in terms of the mass passing the exit slit) has the effect of freezing the mass for detection. Then as soon as a certain magnetic field strength is passed, the electric field is set to its original value and the next mass is frozen. The voltage is varied on a per-mass basis, allowing the operator to scan only the mass peaks of interest rather than the full mass range (3, 4).

Because traditional magnetic-sector technology was initially developed for the structural or qualitative identification of organic compounds, there wasn't a real necessity for rapid quantitation of spectral peaks required for trace element analysis. They functioned by scanning over a large mass range by varying the magnetic field over time with a fixed acceleration voltage. During a small window in time, which was dependant on the resolution chosen, ions of a particular mass to charge are swept past the exit slit to produce the characteristic flat top peaks. As the resolution of a magnetic-sector instrument is independent of mass, ion signals, particularly at low mass, are far apart. The result was that a large amount of time was spent scanning and settling the magnet. This was not such a major problem for qualitative analysis, but proved to be impractical for routine trace element analysis. This concept is shown in greater detail in Figure 2, which is a plot of four parameters — magnetic field strength, accelerating voltage, mass, and signal intensity — against time for four separate masses (M_1–M_4). Scanning the magnet from point A to point B, (accelerating voltage is fixed) results in a scan across the mass range, generating spectral peaks for the four different masses. It can be seen that this increased scanning and settling overhead time (often referred to as dead time) would result in valuable measurement time being lost, particularly for high sample throughput that required ultratrace detection levels.

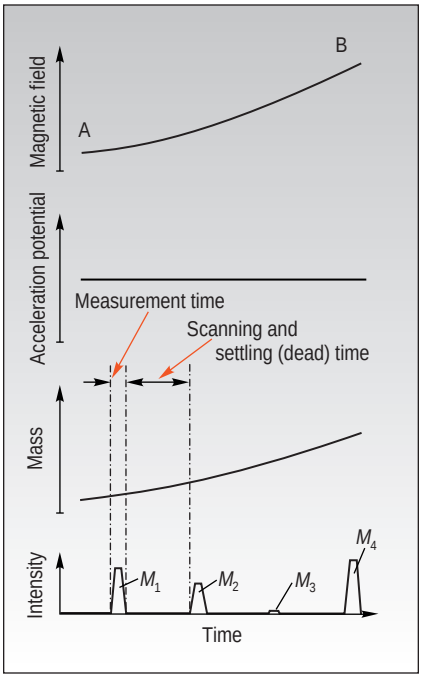

Figure 2. A plot of magnetic field strength, accelerating voltage (fixed), mass and signal intensity over time for four separate masses (M_1–M_4). Note that only the magnet is scanned, while the accelerating voltage is fixed — resulting in long scan times between the masses.

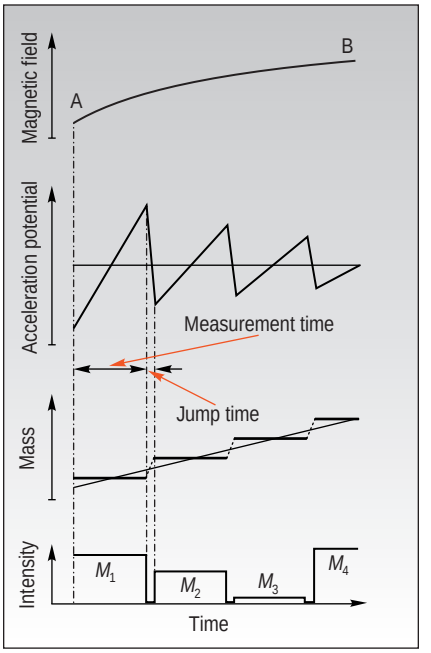

Figure 3. A plot of magnetic field strength, accelerating voltage (changed), mass and signal intensity over time for the same four masses (M_1–M_4). This time, in addition to the magnet being scanned, the accelerating voltage is also changed, resulting in rapid electric jumps between the masses.

***By** changing the electric field in the opposite direction to the field strength of the magnet during the cycle time of the magnet, it has the effect of "stopping" the mass that passes through the analyzer.*

By changing the electric field in the opposite direction to the field strength of the magnet during the cycle time of the magnet, it has the effect of "stopping" the mass that passes through the analyzer. Then, as soon as the magnetic field strength is passed, the electrical field is set to its original value and the next mass "stopped" in the same manner. The accelerating voltage, as well as its rate of change, has to be varied depending on the mass, but the benefit of this method is that only the mass peaks of interest are registered. This process is seen in Figure 3, which shows the same four masses scanned. The only difference this time is that as well as scanning the magnet from point A to point B, the accelerating voltage is also changed, resulting in a stepwise jump from one mass to the next. This means that the full mass range is covered much faster than scanning the magnet alone, because of the speed involved in electrically jumping from one mass to another (5). Once the magnet has been scanned to a particular point, an electric scan is used to cover an area of ± 10–30 % of the mass, either to measure the analyte peak or monitor other masses of interest. Peak quantitation is typically performed by taking multiple data points over a fixed mass window and integrating over a fixed period of time.

It should be pointed out that although this approach represents enormous time savings over older, single-focusing magnetic-sector technology, it is still signifi-

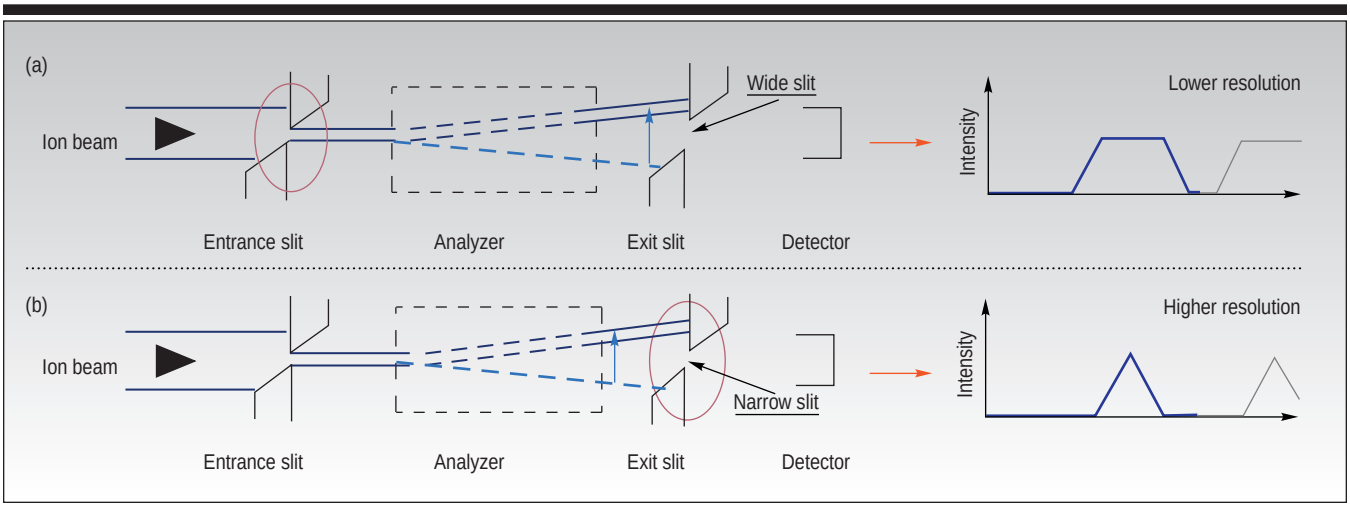

Figure 4. Resolution obtained using (a) wide and (b) narrow exit slit widths as the magnetic field is scanned. The entrance slit widths are the same in (a) and (b).

cantly slower than quadrupole-based instruments. The inherent problem lies in the fact that a quadrupole can be electronically scanned much faster than a magnet. Typical speeds for a full mass scan (0–250 amu) of a magnet are in the order of 400–500 ms compared with 100 ms for a quadrupole. In addition, it takes much longer for magnets to slow down and settle to take measurements – typically 20 ms compared to 1–2 μs for a quadrupole. So, even though in practice, the electric scan dramatically reduces the overall analysis time, modern double-focusing magnetic-sector ICP-MS systems, especially when multiple resolution settings are used, require 5–10 times as much time as quadrupole instruments. This makes them less than ideal for routine, high-throughput applications or for samples that require multielement determinations on rapid transient signals.

RESOLVING POWER

As mentioned previously, most commercial magnetic-sector ICP-MS systems offer as much as 10,000 resolving power (5% peak height/10% valley definition), which is high enough to resolve the majority of spectral interferences. It's worth emphasizing that resolving power (R), is represented by the equation: $R = m/\Delta m$, where m is the nominal mass at which the peak occurs and Δm is the mass difference between two resolved peaks (6). In a quadrupole, the resolution is selected by changing the ratio of the rf/dc voltages on the quadrupole rods. However, because a double-focusing magnetic-sector instrument involves focusing ion angles and ion energies, mass resolution is achieved by using two mechanical slits — one at the entrance to the mass spectrometer and another at the exit, before the detector. Varying resolution is achieved by scanning the magnetic field under different entrance- and exit-slit width conditions. Similar to optical systems, low resolution is achieved by using wide slits, whereas high resolution is achieved with narrow slits. Varying the width of both the entrance and exit slits effectively changes the operating resolution. This can be seen in Figure 4, which shows two slit width scenarios. Figure 4a shows a medium entrance slit and a wide exit slit producing relatively low resolution and a characteristic flat-topped peak. Figure 4b has the same size entrance slit, but a narrower exit slit, producing higher resolution with a characteristic triangular peak. The lowest practical resolution achievable with a double-focusing magnetic-sector instrument, using the widest entrance and exit slits, is approximately 300–400, whereas the highest practical resolution, using the narrowest entrance and exit slits, is approximately 10,000. Most commercial systems operate at fixed resolution settings — for example, low is typically 300–400; medium is typically 3000–4000, and high is typically 8000–10,000 (the choice of settings will vary depending on the instrumentation).

However, it should be emphasized that, similar to optical spectrometry, as the resolution is increased, the transmission decreases. So even though extremely high resolution is available, detection limits will be compromised under these conditions. This can be seen in Figure 5, which shows a plot of resolution against ion transmission. Figure 5 shows that a resolving power of 400 produces 100% transmission, but at a resolving power of

Table I. Resolution required to resolve some common polyatomic interferences from a selected group of isotopes.

Isotope	Matrix	Interference	Resolution	Transmission
^{39}K	H_2O	^{38}ArH	5570	6%
^{40}Ca	H_2O	^{40}Ar	199800	0%
^{44}Ca	HNO_3	$^{14}N^{14}N\ ^{16}O$	970	80%
^{56}Fe	H_2O	$^{40}Ar^{16}O$	2504	18%
^{31}P	H_2O	$^{15}N^{16}O$	1460	53%
^{34}S	H_2O	$^{16}O^{18}O$	1300	65%
^{75}As	HCl	$^{40}Ar^{35}Cl$	7725	2%
^{51}V	HCl	$^{35}Cl^{16}O$	2572	18%
^{64}Zn	H_2SO_4	$^{32}S^{16}O^{16}O$	1950	42%
^{24}Mg	Organics	$^{12}C^{12}C$	1600	50%
^{52}Cr	Organics	$^{40}Ar^{12}C$	2370	20%
^{55}Mn	HNO_3	$^{40}Ar^{15}N$	2300	20%

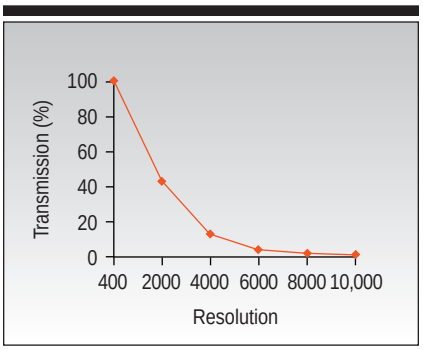

Figure 5. Ion transmission with a magnetic-sector instrument decreases as the resolution increases.

10,000, only ~2% is achievable. This dramatic loss in sensitivity could be an issue if low detection limits are required in spectrally complex samples that require the highest possible resolution; however, spectral demands of this nature are not very common. Table I shows the resolution required to resolve fairly common polyatomic interferences from a selected group of elemental isotopes, together with the achievable ion transmission.

Figure 5 is a comparison between a quadrupole instrument and a magnetic-sector instrument with one of the most common polyatomic interferences — $^{40}Ar^{16}O$ on ^{56}Fe, which requires a resolution of 2504 to separate the peaks. Figure 5a shows a spectral scan of ^{56}Fe using a quadrupole instrument. What it doesn't show is the massive polyatomic interference $^{40}Ar^{16}O$ (produced by oxygen ions from the water combining with argon ions from the plasma) completely overlapping the ^{56}Fe. It shows very clearly that these two masses are unresolvable with a quadrupole. If that same spectral scan is performed on a magnetic-sector instrument, the result is the scan shown in Figure 5b. To see the spectral scan on the same scale, it was necessary to examine a much smaller range. For this reason, a 0.100-amu window was taken, as indicated by the dotted lines.

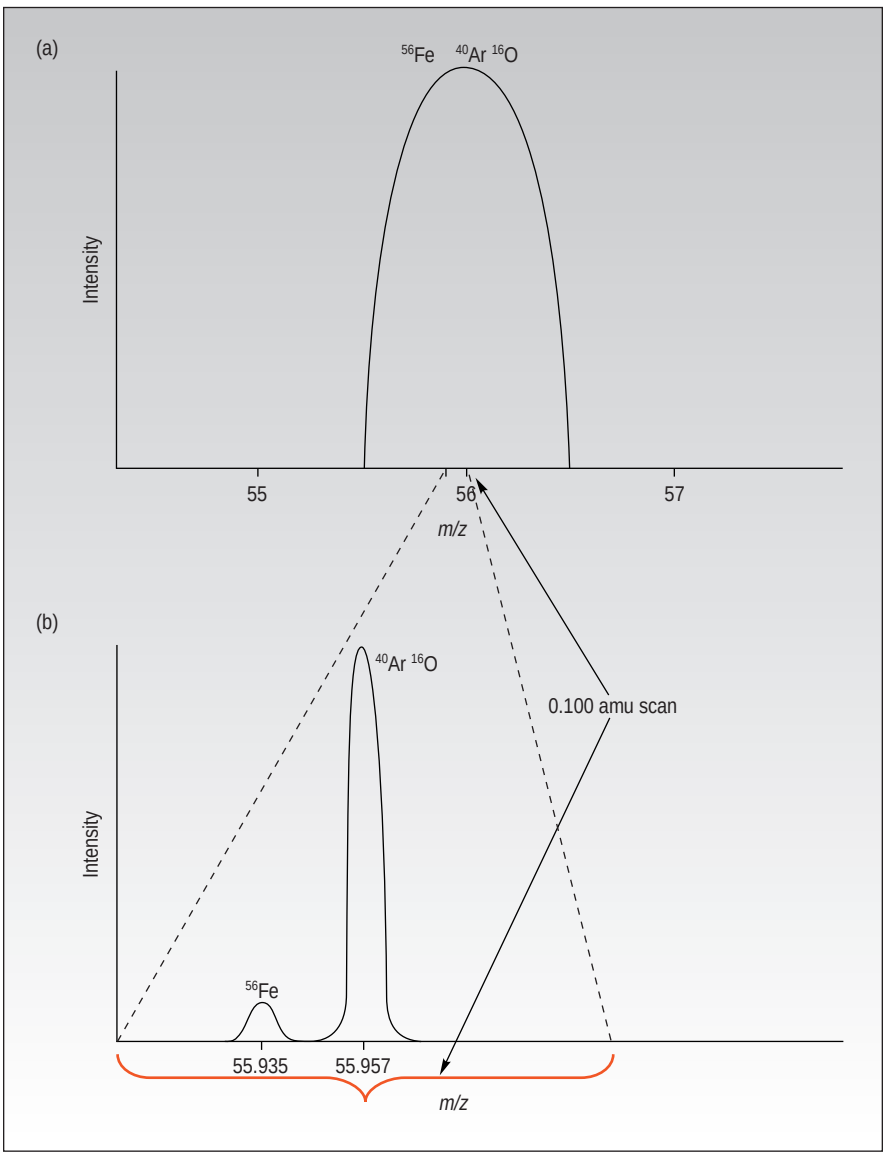

Figure 6. Comparison of resolution between (a) a quadrupole and (b) a magnetic-sector instrument for the polyatomic interference of $^{40}Ar^{16}O$ on ^{56}Fe.

OTHER BENEFITS

Besides high resolving power, another attractive feature of magnetic-sector instruments is its very high sensitivity combined with extremely low background levels. High ion transmission in low-resolution mode translates into sensitivity specifications of typically 100–200 million counts per second (mcps) per ppm, while background levels resulting from extremely low dark current noise are typically 0.1–0.2 cps. This compares with sensitivity of 10–50 mcps and background levels of ~10 cps for a quadrupole instrument. For this reason detection limits, especially for high mass elements like uranium where high resolution is generally not required, are typically an order of magnitude better than those provided by a quadrupole-based instrument.

Besides good detection capability, another of the recognized benefits of the magnetic-sector approach is its ability to quantitate with excellent precision. Measurement of the characteristically flat-topped spectral peaks translates directly into high precision data. As a result, in the low-resolution mode, relative standard deviation (RSD) values of 0.01–0.05% are fairly common, which makes magnetic-sector instruments an ideal tool for carrying out high precision isotope ratio work (7). Although precision is usually degraded as resolution is increased (because the peak shape gets worse), modern instrumentation with high speed electronics and low mass bias is still capable of precision values of <0.1% RSD in medium- or high resolution mode. (8).

The demand for ultrahigh-precision data, particularly in the field of geochemistry, has led to the development of instruments dedicated to isotope ratio

analysis. These are based on the double-focusing magnetic-sector design, but instead of using just one detector, these instruments use multiple detectors. Often referred to as multicollector systems, they offer the capability of detecting and measuring multiple ion signals at exactly the same time. As a result of this simultaneous measurement approach, they are recognized as producing the ultimate in isotope ratio precision (9).

There is no question that double-focusing magnetic-sector ICP-MS systems are no longer a novel analytical technique. They have proved themselves to be a valuable addition to the trace element toolkit, particularly for challenging applications that require good detection capability, exceptional resolving power, and very high precision. They do have their limitations, however, and perhaps should not be considered a competitor for quadrupole instruments when it comes to rapid, high-sample-throughput applications or when performing multielement determinations on fast transient peaks, using sampling accessories such as electrothermal vaporization (10) or laser ablation (11).

REFERENCES

(1) R. Thomas, *Spectroscopy* **16**(10), 44–48 (2001).

(2) N. Bradshaw, E.F.H. Hall, and N.E. Sanderson, *Journal of Analytical Atomic Spectrometry* **4**, 801–803 (1989).

(3) R. Hutton, A. Walsh, D. Milton, and J. Cantle, *ChemSA* **17**, 213–215 (1991).

(4) U. Geismann and U. Greb, *Fresnius' Journal of Analytical Chemistry* **350**, 186–193 (1994).

(5) U. Geismann and U. Greb, Poster Presentation at Second Regensburg Symposium on Elemental Mass Spectrometry, (1993).

(6) F. Adams, R. Gijbels, and R. Van Grieken, *Inorganic Mass Spectrometry* (John Wiley and Sons, New York, 1988).

(7) F. Vanhaecke, L. Moens, R. Dams, and R. Taylor, *Analytical Chemistry* **68**, 567 (1996).

(8) M. Hamester, D. Wiederin, J. Willis, W. Keri, and C.B. Douthitt, *Fresnius' Journal of Analytical Chemistry* **364**, 495–497 (1999).

(9) J. Walder, P.A. Freeman, *Journal of Analytical Atomic Spectrometry* **7**, 571 (1992).

(10) S. Beres, E. Denoyer, R. Thomas, and P. Bruckner, *Spectroscopy* **9**(1), 20–26 (1994).

(11) S. Shuttleworth and D. Kremser, *Journal of Analytical Atomic Spectrometry* **13**, 697–699 (1998).

A Beginner's Guide to ICP-MS

Part VIII — Mass Analyzers: Time-of-Flight Technology

ROBERT THOMAS

Continuing with the discussion on mass analyzers used in inductively coupled plasma–mass spectrometry (ICP-MS), let's now turn our attention to the most recent mass separation device to be commercialized — time-of-flight (TOF) technology. Although the first TOF mass spectrometer was first described in the literature in the late 1940s (1), it has taken more than 50 years to adapt it for use in an ICP-MS system. The recent growth in TOF ICP-MS sales is in response to the technology's unique ability to sample all ions generated in the plasma at exactly the same time, which is advantageous in three major areas:

- Multielement determinations of rapid transient signals generated by sampling accessories such as laser ablation and electrothermal vaporization devices
- High-precision, ratioing techniques such as internal standardization and isotope ratio analysis
- Rapid multielement measurements, especially where sample volume is limited.

TOF's simultaneous nature of sampling ions offers distinct advantages over traditional scanning (sequential) quadrupole technology for ICP-MS applications where large amounts of data need to be captured in a short amount of time. Before we go on to discuss this in greater detail, let's go through the basic principles of TOF analyzers.

BASIC PRINCIPLES OF TOF

All TOF-MS instruments are based on the same fundamental principle that the kinetic energy (E_k) of an ion is directly proportional to its mass (m) and velocity (v), represented by equation 1

$$E_k = \tfrac{1}{2}mv^2 \qquad [1]$$

Therefore, if a population of ions — all having different masses — are given the same kinetic energy by an accelerating voltage (U), the velocities of the ions will all be different, based on their masses. This principle is then used to separate ions of different mass-to-charge ratios (m/z) in the time (t) domain, over a fixed flight path distance (D) — represented by equation 2

$$m/z = 2Ut^2/D^2 \qquad [2]$$

This is shown schematically in Figure 1, with three ions of different mass-to-charge ratios being accelerated into a flight tube and arriving at the detector at different times. It can be seen that, based on their velocities, the lightest ion arrives first, followed by the medium mass ion, and finally the heaviest one. Using flight tubes of 1 m in length, even the heaviest ions typically take less than 50 μs to reach the detector. This translates into approximately 20,000 mass spectra/s — approximately 2–3 orders of magnitude faster than the sequential scanning mode of a quadrupole system.

DIFFERENT SAMPLING APPROACHES

Even though this process sounds fairly straightforward, sampling the ions in a simultaneous manner from a continuous source of ions being generated in the plasma discharge is not a trivial task. Basically two sampling approaches are used in commercial TOF mass analyzers. They are the orthogonal design (2), where the flight tube is positioned at right angles to the sampled ion beam, and the axial design (3), where the flight tube is in the same axis as the ion beam. In both designs, all ions that contribute to the mass spectrum are sampled through the interface cones, but instead of being focused into the mass filter in the conventional way, packets (groups) of ions are electrostatically injected into the flight tube at exactly the same time. With the orthogonal approach, an accelerating potential is applied at right angles to the continuous ion beam from the plasma source. The ion beam is then chopped by using a pulsed voltage supply coupled to the orthogonal accelerator to provide repetitive voltage slices at a frequency of a few kilohertz. The sliced packets of ions, which are typically long and thin in cross section (in the vertical plane), are then allowed to drift into the flight tube where the ions are temporally resolved according to their velocities. Figure 2 shows this process schematically.

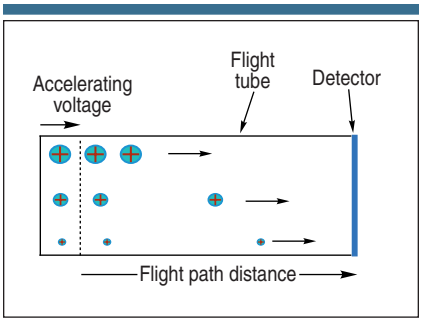

Figure 1. Principles of ion detection using TOF technology, showing separation of three masses in the time domain.

With the axial approach, an accelerating potential is applied axially (in the same axis) to the incoming ion beam as it enters the extraction region. Because the ions are in the same plane as the detector, the beam has to be modulated using an electrode grid to repel the gated packet of ions into the flight tube. This kind of modulation generates an ion packet that is long and thin in cross section (in the horizontal plane). The differ-

ent masses are then resolved in the time domain in a similar manner to the orthogonal design. The layout of an on-axis TOF system is shown schematically in Figure 3.

Figures 2 and 3 represent a rather simplistic explanation of TOF principles of operation. In practice, the many complex ion focusing components in a TOF mass analyzer ensure that a maximum number of analyte ions reach the detector and also that undesired photons, neutral species, and interferences are ejected from the ion beam. Some of these components are shown in Figure 4, which shows a more detailed view of a typical orthogonal system. This design shows that an injector plate is used to inject packets of ions at right angles from the ion beam emerging from the MS interface. These packets of ions are then directed toward a deflection–steering plate where pulsed voltages steer the ions (or throw out unwanted species) in the direction of a reflectron. The packets of ions are then deflected back 180°, where they are detected by a channel electron multiplier or discrete dynode detector. The reflectron is a type of ion mirror and functions as an energy compensation device, so that different ions of the same mass arrive at the detector at the same time. Even though the on-axis design might use slightly different components, the principles are very similar.

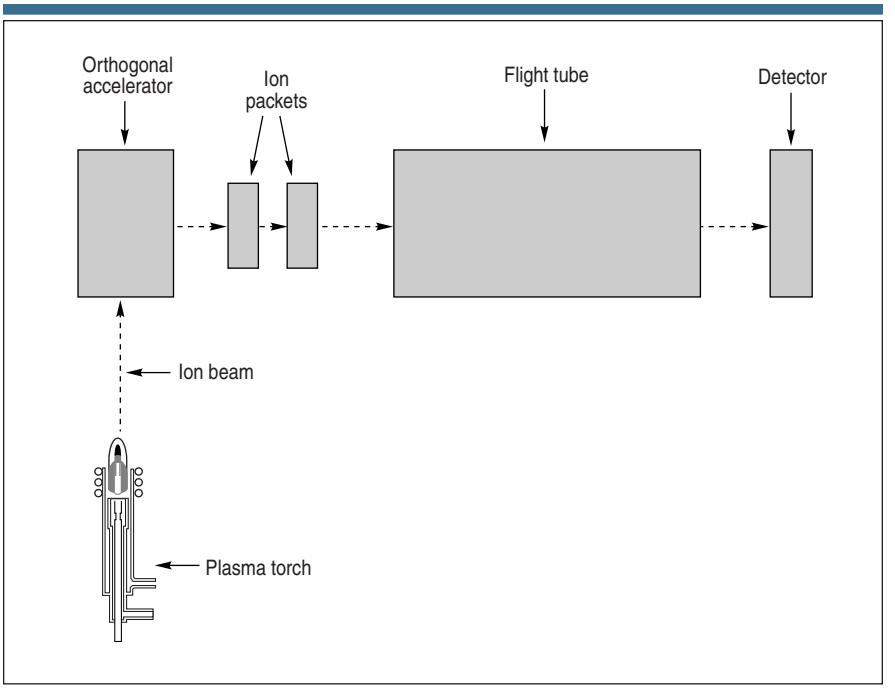

Figure 2. Schematic of an orthogonal acceleration TOF analyzer.

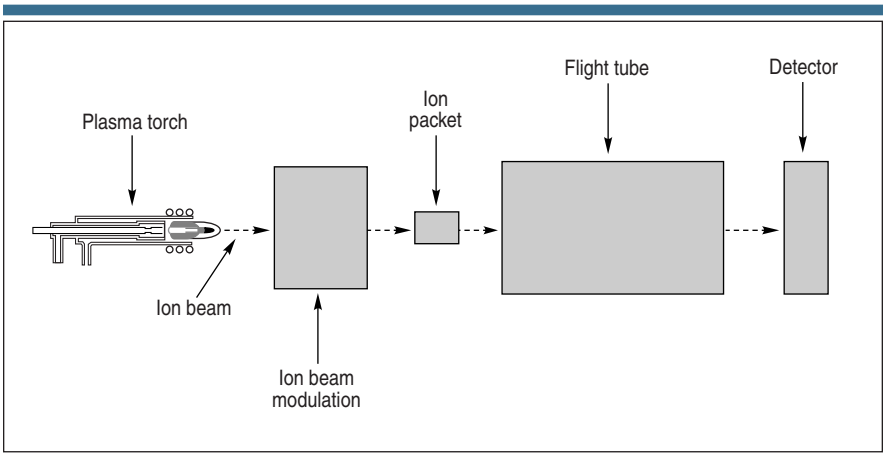

Figure 3. Schematic of an on-axis acceleration TOF analyzer.

DIFFERENCES BETWEEN ORTHOGONAL AND ON-AXIS TOF TECHNOLOGY

Although there are real benefits of using TOF over quadrupole technology for some ICP-MS applications, each type of TOF design also has subtle differences in its capabilities. (However, it is not the intent of this tutorial to make any personal judgement about the benefits or disadvantages of either design.) Let's take a look at some of these differences in greater detail (4, 5).

Sensitivity. The axial approach tends to produce higher ion transmission because the steering components are in the same plane as the ion generation system (plasma) and the detector. This means that the direction and magnitude of greatest energy dispersion is along the axis of the flight tube. In addition, when ions are extracted orthogonally, the energy dispersion can produce angular divergence of the ion beam resulting in poor transmission efficiency. However, the sensitivity of either TOF design is still generally lower than the latest commercial quadrupole instruments.

Background levels. The on-axis design tends to generate higher background levels because neutral species and photons stand a greater chance of reaching the detector. This results in background levels in the order of 20–50 counts/s — approximately 5–10 times higher than the orthogonal design. However, because the ion beam in the axial design has a smaller cross section, a smaller detector can be used, which generally has better noise characteristics. In comparison, most commercial quadrupole instruments offer background levels of 1–10 counts/s, depending on the design.

Duty cycle. Duty cycle is usually defined as the fraction (percentage) of extracted ions that actually make it into the mass analyzer. Unfortunately, with a TOF ICP-MS system that has to use pulsed ion packets from a continuous source of ions generated in the plasma, this process is not very efficient. It should be emphasized that even though the ions are sampled at the same time, detection is not simultaneous because different masses arrive at the detector at different times. The difference between the sampling mechanisms of orthogonal and axial TOF designs translates into subtle differences in their duty cycles.

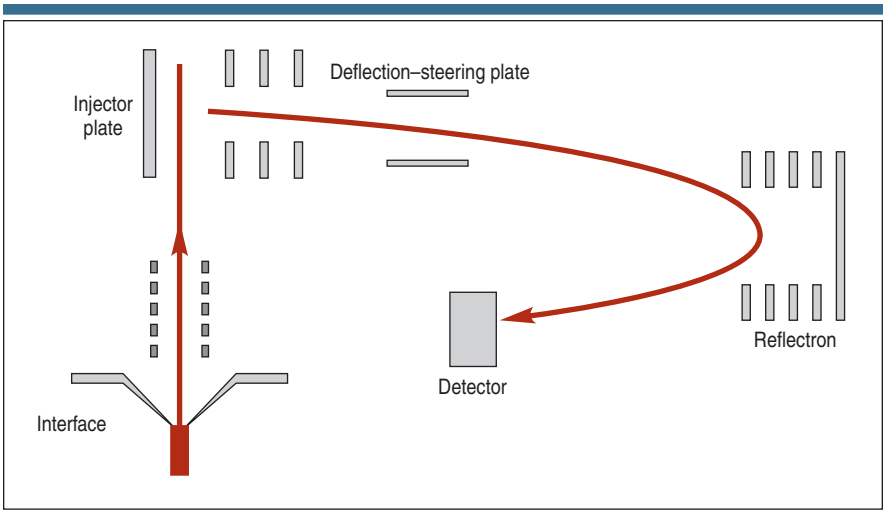

Figure 4. A more detailed view of a typical orthogonal TOF analyzer, showing some of the ion steering components.

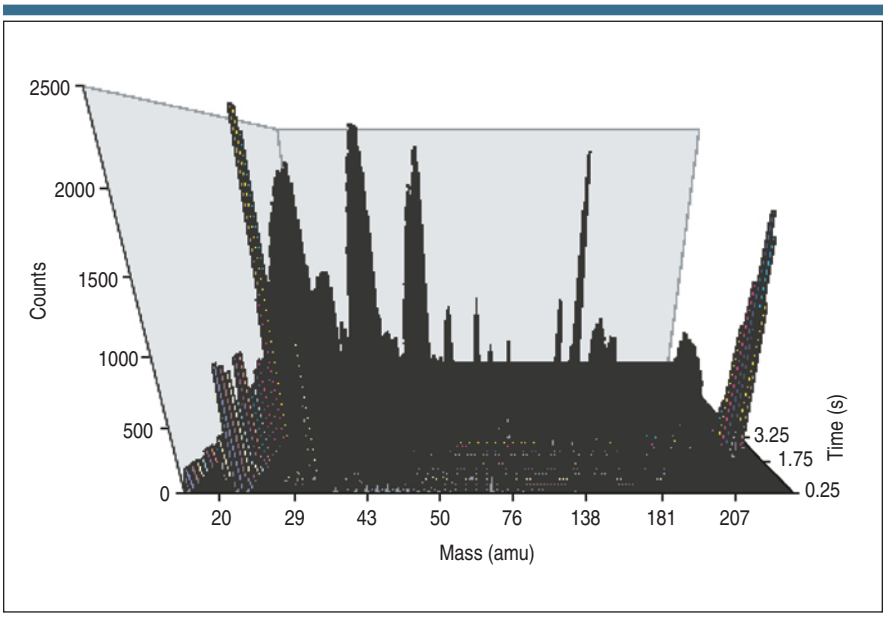

Figure 5. A full mass scan of a transient signal generated by 10 μL of a 5-ppb multielement solution using an electrothermal vaporization sampling accessory coupled to a TOF ICP-MS system (courtesy of GBC Scientific Equipment [Arlington Heights, IL]).

With the orthogonal design, duty cycle is defined by the width of the extracted ion packets, which are typically long and thin in cross section, as shown in Figure 2. In comparison, the duty cycle of the axial design is defined by the length of the extracted ion packets, which are typically wide and thin in cross section, as shown in Figure 3. Duty cycle can be improved by changing the cross-sectional area of the ion packet but, depending on the design, is generally improved at the expense of resolution. In practice, the duty cycles for both orthogonal and axial designs are in the order of 15–20%.

Resolution. The resolution of the orthogonal approach is slightly better because of its two-stage extraction/acceleration mechanism. Because a pulse of voltage pushes the ions from the extraction area into the acceleration region, the major energy dispersion lies along the axis of ion generation. For this reason, the energy spread is relatively small in the direction of extraction compared to the axial approach, resulting in better resolution. However, the resolving power of both commercial TOF ICP-MS systems is typically in the order of 500–2000 (4), depending on the mass region, which makes them inadequate to resolve many of the problematic polyatomic species encountered in ICP-MS (6). In comparison, commercial high-resolution systems based on the double-focusing magnetic-sector design offer resolving power as high as 10,000, while commercial quadrupoles typically achieve 300–400.

Mass bias. This is the degree to which ion transport efficiency varies with mass. All instruments show some degree of mass bias, which is usually compensated for by measuring the difference between the theoretical and observed ratio of two isotopes of the same element. In TOF, the velocity (energy) of the initial ion beam will affect the instrument's mass bias characteristics. In theory, mass bias should be less with the axial design because the extracted ion packets don't have any velocity in a direction perpendicular to the axis of the flight tube, which could potentially impact their transport efficiency.

BENEFITS OF TOF TECHNOLOGY FOR ICP-MS

It should be emphasized that these performance differences between the two designs are subtle and should not detract from the overall benefits of the TOF approach for ICP-MS. As mentioned earlier, a scanning device such as a quadrupole can only detect one mass at a time, which means that a compromise always exists between number of elements, detection limits, precision, and the overall measurement time. However, with the TOF approach, the ions are sampled at exactly the same moment in time, which means that multielement data can be collected with no significant deterioration in quality. The ability of a TOF system to capture a full mass spectrum, significantly faster than a quadrupole, translates into three major benefits.

RAPID TRANSIENT PEAK ANALYSIS

Probably the most exciting potential for TOF ICP-MS is in the multielement analysis of a rapid transient signal generated by sampling accessories such as laser ablation (7), electrothermal vaporization, and flow injection systems (4). Even though a scanning quadrupole can be used for this type of analysis, it struggles

Correction

In reference to Part VII of my tutorial series, "A Beginner's Guide to ICP-MS," which was published in the November 2001 issue of *Spectroscopy*, I would like to make a number of corrections. Even though the intent of the article was to give a general overview of double-focusing magnetic-sector mass analyzers for beginners, Thermo Finnigan contacted *Spectroscopy* to inform the editors and me that the column contained errors, and that it did not reflect the current performance of their instrument, the ELEMENT2. For that reason, I wish to make the following amendments to the article.

• My statement that double-focusing magnetic sector ICP-MS instruments are significantly slower than quadrupole technology does not hold true today. Recent improvements in the scan rate of the ELEMENT2 translates into speeds approaching that of quadrupole-based instruments.

• My statement that typical scan speeds for a full mass scan were 400–500 ms is reflective of older magnetic sector technology. This is not representative of the ELEMENT2, which has a scan speed in the order of 150–200 ms.

• My statement that typical sensitivity was in the order of 100–200 million cps/ppm is not reflective of the ELEMENT2, which has a specification for 115In of 1 billion cps/ppm.

• My conclusion should therefore be modified to say that if transient peak analysis is a requirement, modern double-focusing magnetic sector technology such as the ELEMENT2, with its improved scan speeds, should be considered a viable option to quadrupole technology.

I wish to apologize for any inconvenience caused by these statements.

Robert Thomas

to produce high-quality, multielement data when the transient peak lasts only a few seconds. The simultaneous nature of TOF instrumentation makes it ideally suited for this type of analysis, because the entire mass range can be collected in less than 50 μs. Figure 5 shows a full mass scan of a transient peak generated by an electrothermal vaporization sampling accessory coupled to a TOF ICP-MS system. The technique has generated a healthy signal for 10 μL of a 5-ppb multielement solution in less than 10 s. TOF technology is probably better suited than any other design of ICP-MS for this type of application.

IMPROVED PRECISION

To better understand how TOF technology can help improve precision in ICP-MS, it is important to know the major sources of instability. The most common source of noise in ICP-MS is flicker noise associated with the sample introduction process (from peristaltic pump pulsations, nebulization mechanisms, and plasma fluctuations) and shot noise derived from photons, electrons, and ions hitting the detector. Shot noise is based on counting statistics and is directly proportional to the square root of the signal. It therefore follows that as the signal intensity gets larger, the shot noise has less of an impact on the precision (% RSD) of the signal. At high ion counts the most dominant source of imprecision in ICP-MS is derived from flicker noise generated in the sample introduction area.

One of the most effective ways to reduce instability produced by flicker noise is to use a technique called internal standardization, where the analyte signal is compared and ratioed to the signal of an internal standard element (usually of similar mass and ionization characteristics) that is spiked into the sample. Even though a quadrupole-based system can do an adequate job of compensating for these signal fluctuations, it is ultimately limited by its inability to measure the internal standard at exactly the same time as the analyte isotope. So to compensate

for sample introduction– and plasma-based noise and achieve high precision, the analyte and internal standard isotopes need to be sampled and measured simultaneously. For this reason, the design of a TOF mass analyzer is perfect for true simultaneous internal standardization required for high-precision work. It follows, therefore, that TOF is also well suited for high-precision isotope ratio analysis where its simultaneous nature of measurement is capable of achieving precision values close to the theoretical limits of counting statistics. And unlike a scanning quadrupole-based system, it can measure ratios for as many isotopes or isotopic pairs as needed — all with excellent precision (8).

ANALYSIS TIME

As with a scanning ICP–optical emission spectroscopy system, the speed of a quadrupole ICP mass spectrometer is limited by its scanning rate. To determine 10 elements in duplicate with good precision and detection limits, an integration time of 3 s/mass is normally required. When overhead scanning and settling times are added for each mass and each replicate, this translates to approximately 2 min/sample. With a TOF system, the same analysis would take significantly less time because all the data are captured simultaneously. In fact, detection limit levels in a TOF instrument are typically achieved using a 10–30 s integration time, which translates into a 5–10-fold improvement in measurement time over a quadrupole instrument. The added benefit of a TOF instrument is that the speed of analysis is not impacted by the number of analytes being determined. It wouldn't matter if the suite of elements in the method was 10 or 70 — the measurement time would be approximately the same. However, one point must be stressed: A large portion of the overall analysis time is taken up with flushing an old sample out and pumping a new sample into the sample introduction system. This can be as much as 2 min/sample for real-world matrices. So when this time is taken into account, the difference between the sample throughput of a quadrupole system and a TOF ICP-MS system is not so evident.

TOF ICP-MS, with its rapid, simultaneous mode of measurement, excels at multielement applications that generate fast transient signals. It offers excellent precision, particularly for isotope-ratioing techniques, and also has the capability for high speeds of analysis. However, even though it has enormous potential, TOF was only commercialized in 1998, so it is relatively immature compared with quadrupole ICP-MS technology, which is almost 20 years old. For that reason, there is currently only a small number of TOF instruments carrying out high-throughput, routine applications.

REFERENCES

(1) A.E. Cameron and D.F. Eggers, *The Review of Scientific Instruments* **19**(9), 605 (1948).

(2) D.P. Myers, G. Li, P. Yang, and G.M. Hieftje, *J. Am. Soc. Mass Spectrom.* **5,** 1008–1016 (1994).

(3) D.P. Myers, paper presented at 12th Asilomar Conference on Mass Spectrometry, Pacific Grove, CA, Sept. 20–24, (1996).

(4) R.E. Sturgeon, J.W.H. Lam, and A. Saint, *J. Anal. At. Spectrom.* **15,** 607–616, (2000).

(5) F. Vanhaecke, L. Moens, R. Dams, L. Allen, and S. Georgitis, *Anal. Chem.* **71,** 3297 (1999).

(6) N. Bradshaw, E.F. Hall, and N.E. Sanderson, *J. Anal. At. Spectrom.* **4,** 801–803 (1989).

(7) P. Mahoney, G. Li, and G.M. Hieftje, *J. Am. Soc. Mass Spectrom.* **11,** 401–406 (1996).

(8) K.G. Heumann, S.M. Gallus, G. Radlinger, and J. Vogl, *J. Anal. At. Spectrom.* **13,** 1001 (1998).

Robert Thomas *has more than 30 years of experience in trace element analysis. He is the principal of his own freelance writing and scientific consulting company, Scientific Solutions, based in Gaithersburg, MD. He can be contacted by e-mail at thomasrj@bellatlantic.net or via his web site at www.scientificsolutions1.com.* ◆

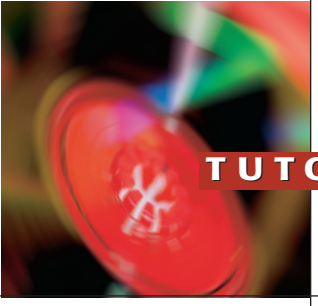

TUTORIAL

A Beginner's Guide to ICP-MS

Part IX — Mass Analyzers: Collision/Reaction Cell Technology

Robert Thomas

The detection capability of traditional quadrupole mass analyzers for some critical elements is severely compromised by the formation of polyatomic spectral interferences generated by either argon, solvent, or sample-based ionic species. Although there are ways to minimize these interferences — including correction equations, cool plasma technology, and matrix separation — they cannot be completely eliminated. However, a new approach called collision/reaction cell technology has recently been developed that virtually stops the formation of many of these harmful species before they enter the mass analyzer. Part IX of this series takes a detailed look at this innovative new technique and the exciting potential it has to offer.

A small number of elements are recognized as having poor detection limits by inductively coupled plasma mass spectrometry (ICP-MS). These elements are predominantly ones that suffer from major spectral interferences generated by ions derived from the plasma gas, matrix components, or the solvent–acid used to get the sample into solution. Examples of these interferences include:

- $^{40}Ar^{16}O$ on the determination of ^{56}Fe
- ^{38}ArH on the determination of ^{39}K
- ^{40}Ar on the determination of ^{40}Ca
- $^{40}Ar^{40}Ar$ on the determination of ^{80}Se
- $^{40}Ar^{35}Cl$ on the determination of ^{75}As
- $^{40}Ar^{12}C$ on the determination of ^{52}Cr
- $^{35}Cl^{16}O$ on the determination of ^{51}V.

The cold/cool plasma approach, which uses a lower temperature to reduce the formation of the argon-based interferences, is a very effective way to get around some of these problems (1); however, it is sometimes difficult to optimize, it is only suitable for a few of the interferences, it is susceptible to more severe matrix effects, and it can be time consuming to change back and forth between normal- and cool-plasma conditions. These limitations and the desire to improve performance led to the development of collision/reaction cells in the late 1990s. Designed originally for organic MS to generate daughter species to confirm identification of the structure of the parent molecule (2), they were used in ICP-MS to stop the appearance of many argon-based spectral interferences.

Basic Principles of Collision/Reaction Cells

With this approach, ions enter the interface in the normal manner, where they are extracted under vacuum into a collision/reaction cell that is positioned before the analyzer quadrupole. A collision/reaction gas such as hydrogen or helium is then bled into the cell, which consists of a multipole (a quadrupole, hexapole, or octapole), usually operated in the radio frequency (rf)-only mode. The rf-only field does not separate the masses like a traditional quadrupole, but instead has the effect of focusing the ions, which then collide and react with molecules of the collision/reaction gas. By a number of different ion-molecule collision and reaction mechanisms, polyatomic interfering ions like ^{40}Ar, $^{40}Ar^{16}O$, and ^{38}ArH, will either be converted to harmless noninterfering species, or the analyte will be converted to another ion which is not interfered with. This is exemplified by the reaction [1], which shows the use of hydrogen gas to reduce the ^{38}ArH polyatomic interference in the determination of ^{39}K. Hydrogen gas converts ^{38}ArH to the harmless H_3^+ ion and atomic argon, but does not react with the potassium. The ^{39}K analyte ions, free of the interference, then emerge from the collision/reaction cell, where they are directed toward the quadrupole analyzer for normal mass separation.

Robert Thomas has more than 30 years of experience in trace element analysis. He is the principal of his own freelance writing and consulting company, Scientific Solutions, based in Gaithersburg, MD. He can be contacted by e-mail at thomasrj@bellatlantic.net or via his web site at www.scientificsolutions1.com.

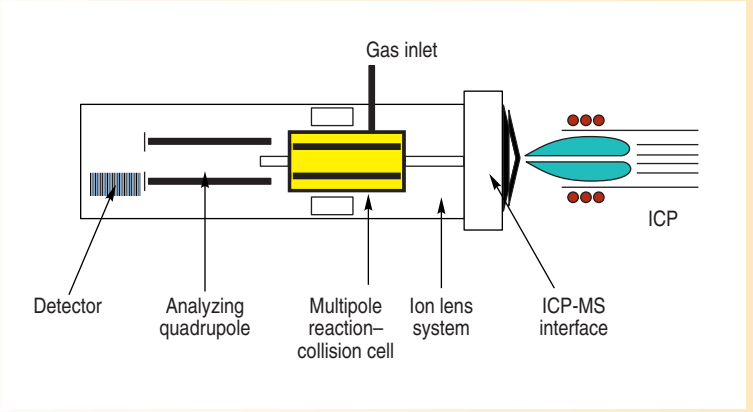

Figure 1. Layout of a typical collision/reaction cell instrument.

$^{38}ArH^+ + H_2 = H_3^+ + Ar$

$^{39}K^+ + H_2 = {}^{39}K^+ + H_2$ (no reaction) [1]

The layout of a typical collision/reaction cell instrument is shown in Figure 1.

Different Collision/Reaction Approaches

The previous example is a very simplistic explanation of how a collision/reaction cell works. In practice, complex secondary reactions and collisions take place, which generate many undesirable interfering species. If these species were not eliminated or rejected, they could potentially lead to additional spectral interferences. Basically two approaches are used to reject the products of these unwanted interactions:

- Discrimination by kinetic energy
- Discrimination by mass.

The major differences between the two approaches are in the types of multipoles used and their basic mechanism for rejection of the interferences. Let's take a closer look at how they differ.

Discrimination by Kinetic Energy

The first commercial collision cells for ICP-MS were based on hexapole technology (3), which was originally designed for the study of organic molecules using tandem MS. The more collision-induced daughter species that were generated, the better the chance of identifying the structure of the parent molecule; however, this very desirable characteristic for liquid chromatography or electrospray MS studies was a disadvantage in inorganic MS, where secondary reaction–product ions are something to be avoided. There were ways to minimize this problem, but they were still limited by the type of collision gas that could be used. Unfortunately, highly reactive gases — such as ammonia and methane, which are more efficient at interference reduction — could not be used because of the limitations of a non-scanning hexapole (in rf-only mode) to adequately control the secondary reactions. The fundamental reason is that hexapoles do not provide adequate mass discrimination capabilities to suppress the unwanted secondary reactions, which necessitates the need for kinetic energy discrimination to distinguish the collision product ions from the analyte ions. This is typically achieved by setting the collision cell bias slightly less positive than the mass filter bias. This means that the collision-product ions, which have the same energy as the cell bias, are discriminated against and rejected, while the analyte ions, which have a higher energy than the cell bias, are transmitted.

The inability to adequately control the secondary reactions meant that low reactivity gases like He, H_2, and Xe were the only option. The result was that ion-molecule collisional fragmentation (and not reactions) was thought to be the dominant mechanism of interference reduction. So even though the ion transmission characteristics of a hexapole were considered very good (with respect to the range of energies and masses transmitted), background levels were still relatively high because the interference rejection process was not very efficient. For this reason, its detection capability — particularly for some of the more difficult elements, like Fe, K, and Ca — offered little improvement over the cool plasma approach. Table I shows some typical detection limits in ppb achievable with a hexapole-based collision cell ICP-MS system (4).

Recent modifications to the hexapole design have significantly improved its

Table I. Typical detection limits (in ppb) achievable with a hexapole-based collision cell ICP-MS system (4).

Element	Isotope	Elemental Sensitivity (cps/[μg/mL])	Detection Limit (ppb)
Be	9	6.9×10^7	0.0077
Mg	24	1.3×10^8	0.028
Ca	40	2.8×10^8	0.07
V	51	1.7×10^8	0.0009
Cr	52	2.4×10^8	0.0007
Mn	55	3.4×10^8	0.0017
Fe	56	3.0×10^8	0.017
Co	59	2.7×10^8	0.0007
Ni	60	2.1×10^8	0.016
Cu	63	1.9×10^8	0.003
Zn	68	1.1×10^8	0.008
Sr	88	4.9×10^8	0.0003
Ag	107	3.5×10^8	0.0003
Cd	114	2.4×10^8	0.0004
Te	128	1.3×10^8	0.009
Ba	138	5.9×10^8	0.0002
Tl	205	4.0×10^8	0.0002
Pb	208	3.7×10^8	0.0007
Bi	209	3.4×10^8	0.0005
U	238	2.3×10^8	0.0001

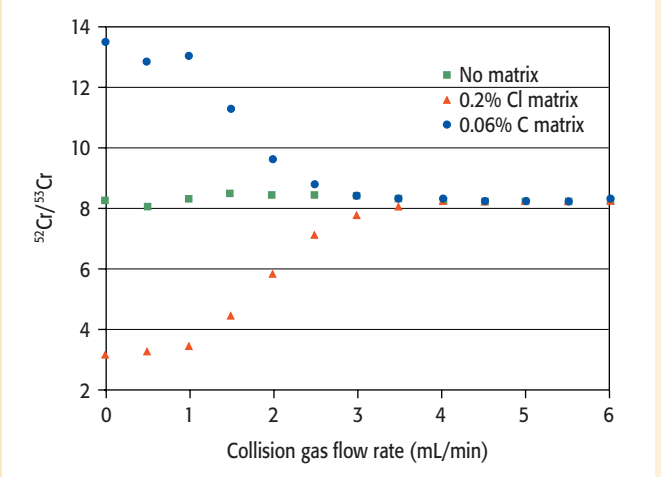

Figure 2. The use of a helium/ammonia mixture with a hexapole-based collision cell for the successful determination of $^{52}Cr/^{53}Cr$ isotopic ratios (courtesy of Thermo Elemental, Franklin, MA).

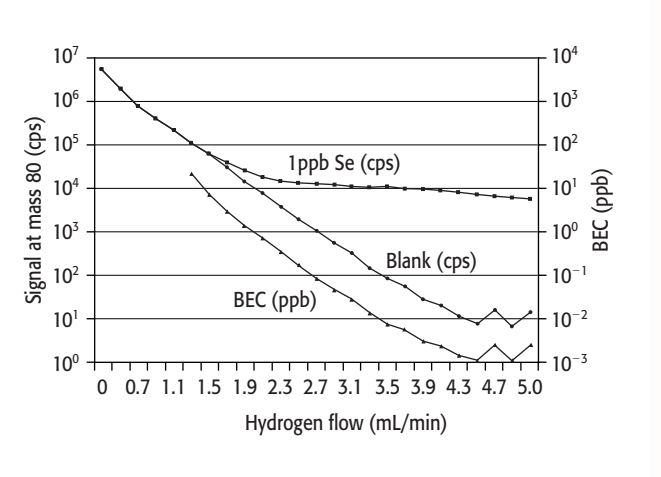

Figure 3. Background reduction of the argon dimer ($^{40}Ar_2^+$) with hydrogen gas using an octapole reaction cell (Courtesy of Agilent Technologies, Wilmington, DE).

collision/reaction characteristics. In addition to offering good transmission characteristics and kinetic energy discrimination, they now appear to offer basic mass-dependent discrimination capabilities. This means that the kinetic energy discrimination barrier can be adjusted with analytical mass, which offers the capability of using small amounts of highly reactive gases. Figure 2 shows an example of the reduction of both $^{40}Ar^{12}C$ and $^{37}Cl^{16}O$ using helium with a small amount of ammonia, in the isotopic ratio determination of $^{52}Cr/^{53}Cr$ (^{52}Cr is 83.789% and ^{53}Cr is 9.401% abundant). It can be seen that the $^{52}Cr/^{53}Cr$ ratio is virtually the same in the chloride and carbon matrices as it is with no matrix present when the optimum flow of collision/reaction gas is used (5).

Another way to discriminate by kinetic energy is to use an octapole in the collision/reaction cell instead of a hexapole. The benefit of using a higher order design is that its transmission characteristics, particularly at the low mass end, are slightly higher than lower order multipoles. Similar in design to the hexapole, collisional fragmentation and energy discrimination are the predominant mechanisms for interference reduction, which means that lower reactivity gases like hydrogen and helium are preferred. By careful design of the interface and the entrance to the cell, the collision/reaction capabilities can be improved, by reducing the number of sample/solvent/plasma-based ions entering the cell. This enables the collision gas to be more effective at reducing the interferences. An example of this is the use of H_2 as the cell gas to reduce the argon dimer ($^{40}Ar_2^+$) interference in the determination of the major isotope of selenium at mass 80 (^{80}Se). Figure 3 shows an example of a dramatic reduction in the $^{40}Ar_2^+$ background at mass 80 using an ICP-MS fitted with an octapole reaction cell. By using the optimum flow of H_2, the spectral background is reduced by about six orders of magnitude, from 10,000,000 cps to 10 cps, producing a background equivalent concentration of approximately 1 ppt for ^{80}Se (6).

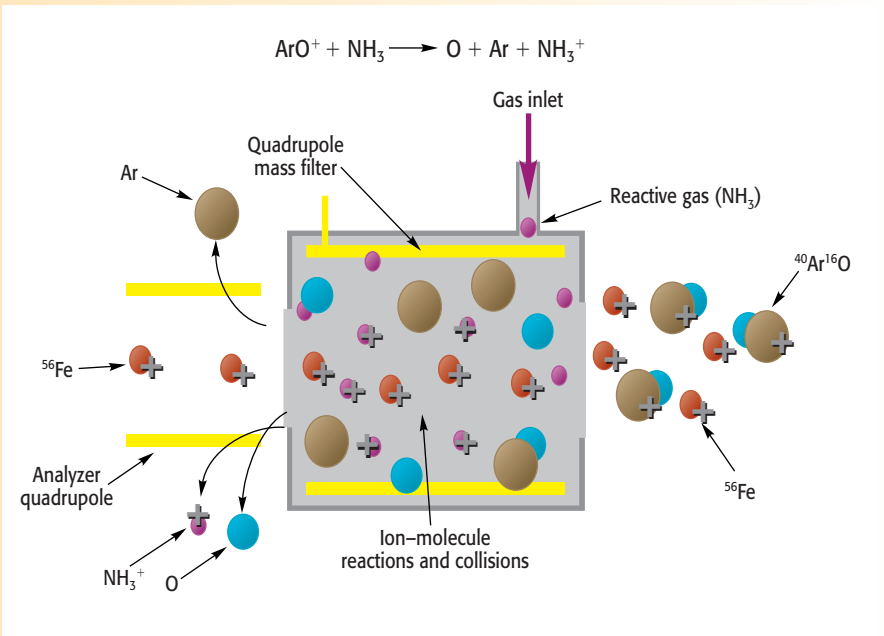

Figure 4. Elimination of the ArO interference with a dynamic reaction cell.

Discrimination by Mass

The other way to reject the products of the secondary reactions/collisions is to discriminate them by mass. Unfortunately, higher order multipoles cannot be used for efficient mass discrimination because the stability boundaries are diffuse, and sequential secondary

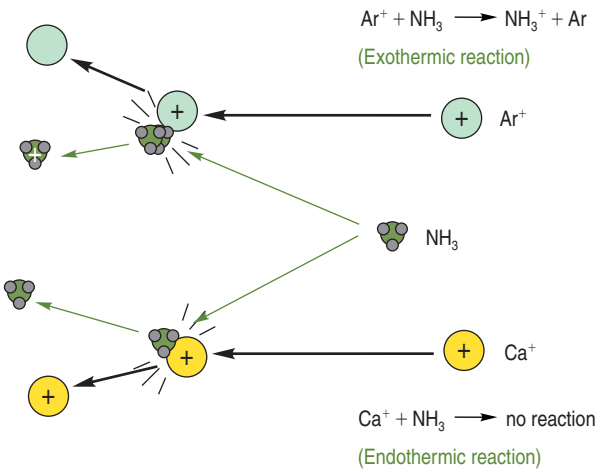

Figure 5. The reaction between NH_3 and Ar^+ is exothermic and fast, while there is no reaction between NH_3 and Ca^+ in the dynamic reaction cell.

reactions cannot be easily intercepted. The way around this problem is to use a quadrupole (instead of a hexapole or octapole) inside the reaction/collision cell, and use it as a selective bandpass filter. The benefit of this approach is that highly reactive gases can be used, which tend to be more efficient at interference reduction. One such development that uses this approach is called dynamic reaction cell technology (7, 8). Similar in appearance to the hexapole and octapole collision/reaction cells, the dynamic reaction cell is a pressurized multipole positioned before the analyzer quadrupole. However, the similarity ends there. In dynamic reaction cell technology, a quadrupole is used instead of a hexapole or octapole. A highly reactive gas, such as ammonia or methane, is bled into the cell, which is a catalyst for ion molecule chemistry to take place. By a number of different reaction mechanisms, the gaseous molecules react with the interfering ions to convert them either into an innocuous species different from the analyte mass or a harmless neutral species. The analyte mass then emerges from the dynamic reaction cell free of its interference and steered into the analyzer quadrupole for conventional mass separation. The advantages of using a quadrupole in the reaction cell is that the stability regions are much better defined than a hexapole or an octapole, so it is relatively straightforward to operate the quadrupole inside the reaction cell as a mass or bandpass filter, and not just an ion-focusing guide. Therefore, by careful optimization of the quadrupole electrical fields, unwanted reactions between the gas and the sample matrix or solvent (which could potentially lead to new interferences) are prevented. Therefore, every time an analyte and interfering ions enter the dynamic reaction cell, the bandpass of the quadrupole can be optimized for that specific problem and then changed on-the-fly for the next one. Figure 4 shows a schematic of an analyte ion ^{56}Fe and an isobaric interference $^{40}Ar^{16}O$ entering the dynamic reaction cell. The reaction gas NH_3 reacts with the ArO^+ to form atomic oxygen and argon together with a positive NH_3 ion. The quadrupole's electrical field is then set to allow the transmission of the analyte ion ^{56}Fe to the analyzer quadrupole, free of the problematic isobaric interference, $^{40}Ar^{16}O$. In addition, the NH_3^+ is prevented from reacting further to produce a new interfering ion. The advantage of this approach is that highly reactive gases can be used, which increases the number of ion–molecule reactions taking place and therefore more efficient removal of the interfering species. Of course, this also potentially generates more side reactions between the gas and the sample matrix and solvent; however, by dynamically scanning the bandpass of the quadrupole in the reaction cell, these reaction by-products are rejected before they can react to form new interfering ions.

Collision/reaction cells have given a new lease on life to quadrupole mass analyzers used in ICP-MS.

The benefit of the dynamic reaction cell is that by careful selection of the reaction gas, the user takes advantage of the different rates of reaction of the analyte and the interfering species. This process is exemplified by the elimination of $^{40}Ar^+$ by NH_3 gas in the determination of ^{40}Ca. The reaction between

Table II. Typical detection limits in ppt of an ICP-MS system fitted with a dynamic reaction cell (9).

Analyte	Detection Limit (ppt)	Analyte	Detection Limit (ppt)
Li	0.08	Co	0.07
Be	0.6	^{60}Ni	0.4
B	1.1	Zn	1
Na	0.3	As	1.2
Mg	0.6	Se*	5
Al	0.07	Sr	0.02
K*	1	Rh	0.01
^{40}Ca*	1	In	0.01
V*	0.3	Sb	0.06
Cr*	0.25	Cs	0.03
Mn*	0.09	Pb	0.03
^{56}Fe*	0.15	U	0.01

* Indicates elements determined in dynamic reaction cell mode.

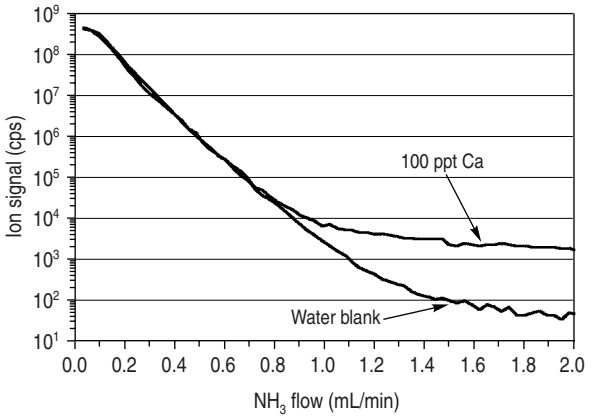

Figure 6. A reduction of eight orders of magnitude in the ^{40}Ar background signal is achievable with the dynamic reaction cell – resulting in <1 ppt detection limit for ^{40}Ca.

NH_3 gas and the $^{40}Ar^+$ interference, which is predominantly a charge exchange, occurs because the ionization potential of NH_3 (10.2 eV) is low compared with that of Ar (15.8 eV). Therefore, the reaction is exothermic and fast; however, the ionization potential of Ca (6.1 eV) is significantly less than that of NH_3, so the reaction, which is endothermic, is not allowed to proceed (8). Figure 5 shows this process in greater detail.

This highly efficient reaction mechanism translates into a dramatic reduction of the spectral background at mass 40, which is shown graphically in Figure 6. At the optimum NH_3 flow, a reduction in the ^{40}Ar background signal of about eight orders of magnitude is achieved, resulting in a detection limit of 0.5–1.0 ppt for ^{40}Ca.

Table II shows some typical detection limits in parts per trillion (ppt) of an ICP-MS system fitted with a dynamic reaction cell. The elements with an asterisk were determined using ammonia or methane as the reaction gas, while the other elements were determined in the standard mode (no reaction gas).

Collision/reaction cells have given a new lease on life to quadrupole mass analyzers used in ICP-MS. They have enhanced its performance and flexibility, and most definitely opened up the technique to more-demanding applications that were previously beyond its capabilities. However, it must be emphasized that even though differences exist between commercially available instruments, they all perform very well. The intent of this tutorial is to present the benefits of the technology to beginners and give an overview of the different approaches available. If it has created an interest, I strongly suggest that a performance evaluation is made based on your own sample matrices.

References

1. K. Sakata and K. Kawabata, *Spectrochimica Acta* **49B,** 1027 (1994).
2. B.A. Thomson, D.J. Douglas, J.J. Corr, J.W. Hager, and C.A. Joliffe, *Anal. Chem.* **67,** 1696–1704 (1995).
3. P. Turner, T. Merren, J. Speakman, and C. Haines, in *Plasma Source Mass Spectrometry: Developments and Applications*, eds. G. Holland and S. Tanner (Royal Society of Chemistry, Cambridge, UK, 1996).
4. I. Feldmann, N. Jakubowski, C. Thomas, and D. Stuewer, *Fresenius' J. Anal. Chem.* **365,** 422–428 (1999).
5. "Collision Cell Technology with Energy Discrimination," *Thermo Elemental Application Note* (Thermo Elemental, Franklin, MA, September 2001).
6. E. McCurdy and D. Potter, *Agilent Technologies ICP-MS Journal* **10,** October 2001.
7. Covered by U.S. Patent No. 6140638.
8. S.D. Tanner and V.I. Baranov, *At. Spectr.* **20**(2), 45–52, (1999).
9. U. Voellkopf, K. Klemm, and M. Pfluger, *At. Spectr.* **20**(2), 53–59, (1999). ■

TUTORIAL

A Beginner's Guide to ICP-MS

Part XI — Peak Measurement Protocol

Robert Thomas

With its multielement capability, superb detection limits, wide dynamic range, and high sample throughput, inductively coupled plasma–mass spectrometry (ICP-MS) is proving to be a compelling technique for more and more diverse application areas. However, no two application areas have the same analytical requirements. For example, environmental and clinical contract laboratories — although requiring reasonably low detection limits — do not really push the technique to its extreme detection capability. Their main requirement is usually high sample throughput because the number of samples these laboratories can analyze in a day directly impacts their revenue. On the other hand, a semiconductor fabrication plant or a supplier of high-purity chemicals to the electronics industry is interested in the lowest detection limits the technique can offer because of the contamination problems associated with manufacturing high performance electronic devices.

Robert Thomas has more than 30 years of experience in trace element analysis. He is the principal of his own freelance writing and consulting company, Scientific Solutions, based in Gaithersburg, MD. He can be contacted by e-mail at thomasrj@bellatlantic.net or via his web site at www.scientificsolutions1.com.

Modern ICP-MS must be very flexible to meet such diverse application needs and keep up with the increasing demands of its users. Nowhere is this more important than in the area of peak integration and measurement protocol. The way the analytical signal is managed in ICP-MS directly impacts its multielement capability, detection limits, dynamic range, and sample throughput — the four major strengths that attracted the trace element community to the technique almost 20 years ago. To understand signal management and its implications on data quality in greater detail, this installment of this series will discuss how measurement protocol is optimized based on the application's analytical requirements. I will discuss its impact on both continuous signals generated by traditional nebulization devices and transient signals produced by alternative sample introduction techniques such as flow injection and laser ablation.

Measurement Variables

Many variables affect the quality of the analytical signal in ICP-MS. The analytical requirements of the application will often dictate this factor, but instrumental detection and measurement parameters can have a significant impact on the quality of data in ICP-MS. Some of the variables that can affect the quality of your data, particularly when carrying out multielement analysis, include

- whether the signal is continuous or transient
- the temporal length of the sampling event
- the volume of sample available
- the number of samples being analyzed
- the number of replicates per sample
- the number of elements being determined
- the detection limits required
- the precision and accuracy expected
- the dynamic range needed
- the integration time used
- the peak quantitation routines.

Before discussing these factors in greater detail, and how they affect data quality, it is important to remember how a scanning device such as a quadrupole mass analyzer works (1). Although we will focus on quadrupole technology, the fundamental principles of measurement protocol will be very similar for all types of mass spectrometers that use a scanning approach for multielement peak quantitation.

Measurement Protocol

Figure 1 shows the principles of scanning with a quadrupole mass analyzer. In this simplified example, the analyte ion (black) and four other ions (colored) have arrived at the entrance to the four rods of the quadrupole. When a particular rf/dc voltage is applied to the rods, the positive or negative bias on the rods will electrostatically steer the analyte ion of interest down the middle of the four rods to the end, where it will emerge and be converted to an electrical pulse by the detector. The other ions of different mass-to-charge ratios will pass through the spaces between the rods and be ejected from the quadrupole. This scanning process is then repeated for another analyte at a completely different mass-to-charge ratio

until all the analytes in a multielement analysis have been measured.

The process for detecting one particular mass in a multielement run is represented in Figure 2, which shows a ^{63}Cu ion emerging from the quadrupole and being converted to an electrical pulse by the detector. As the rf/dc voltage of the quadrupole — corresponding to ^{63}Cu — is repeatedly scanned, the ions as electrical pulses are stored and counted by a multichannel analyzer. This multichannel data-acquisition system typically has 20 channels per mass and as the electrical pulses are counted in each channel, a profile of the mass is built-up over the 20 channels, corresponding to the spectral peak of ^{63}Cu. In a multielement run, repeated scans are made over the entire suite of analyte masses, as opposed to just one mass represented in this example.

The principles of multielement peak acquisition are shown in Figure 3. In this example (showing two masses), signal pulses are continually collected as the quadrupole is swept across the mass spectrum (in this case three times). After a given number sweeps, the total number of signal pulses in each channel are counted.

When it comes to quantifying an isotopic signal in ICP-MS, there are basically two approaches to consider (2). One is the multichannel ramp scanning approach, which uses a continuous smooth ramp of 1 to *n* channels (where *n* is typically 20) per mass across the peak profile. This approach is shown in Figure 4.

The peak-hopping approach is where the quadrupole power supply is driven to a discrete position on the peak (normally the peak point) and allowed to settle; a measurement is then taken for a fixed amount of time. This approach is represented in Figure 5.

The multipoint scanning approach is best for accumulating spectral and peak shape information when doing mass scans. It is normally used for doing mass calibration and resolution checks, and as a classical qualitative method development tool to find out what elements are present in the sample, as well as to assess their spectral implications

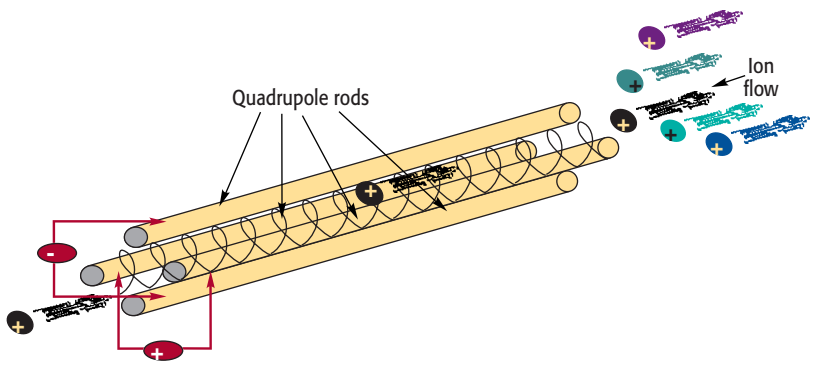

Figure 1. Principles of mass selection with a quadrupole mass filter.

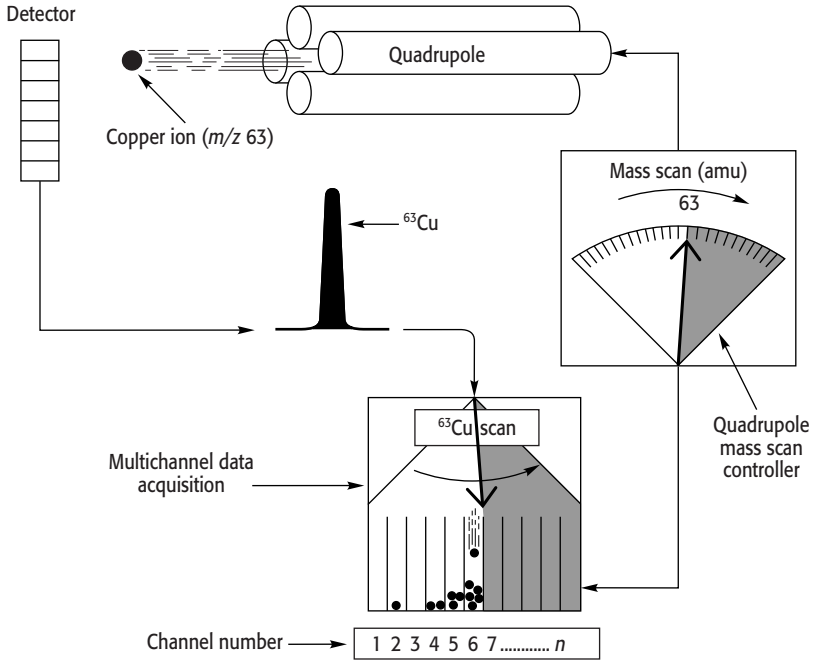

Figure 2. Detection and measurement protocol using a quadrupole mass analyzer.

on the masses of interest. Full peak profiling is not normally used for doing rapid quantitative analysis because valuable analytical time is wasted taking data on the wings and valleys of the peak, where the signal-to-noise ratio is poorest.

When the best possible detection limits are required, the peak-hopping approach is best. It is important to understand that, to get the full benefit of peak hopping, the best detection limits are achieved when single-point peak hopping at the peak maximum is chosen. However, to carry out single-point peak hopping, it is essential that the mass stability is good enough to reproducibly go to the same mass point every time. If good mass stability can be guaranteed (usually by thermostating the quadrupole power supply), measuring the signal at the peak maximum will always give the best detection limits for a given integration time. It is well documented that there is no benefit to spreading the chosen integration time over more than one measurement point per mass. If time is a major consideration in the analysis, then using multiple points is wasting valuable time on the wings and valleys of the peak, which contribute less to the analytical signal

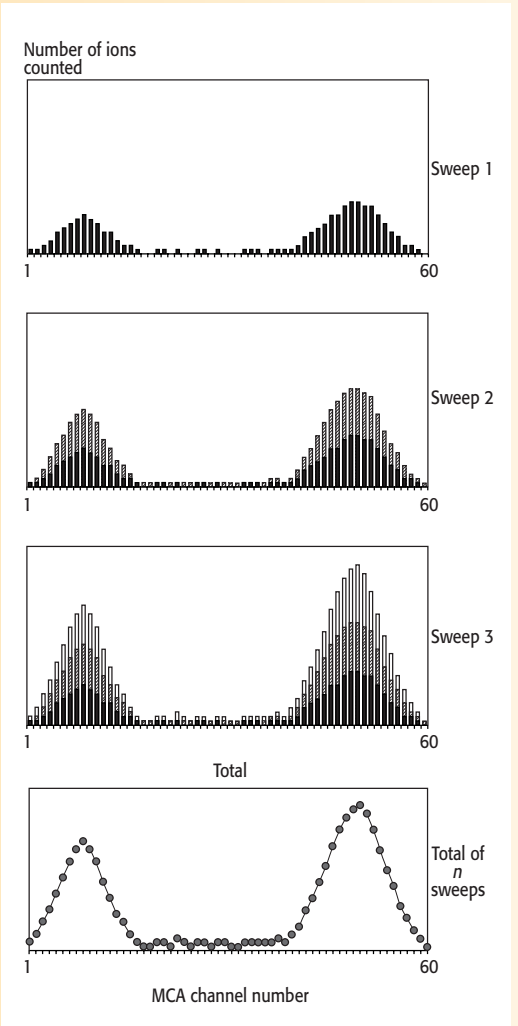

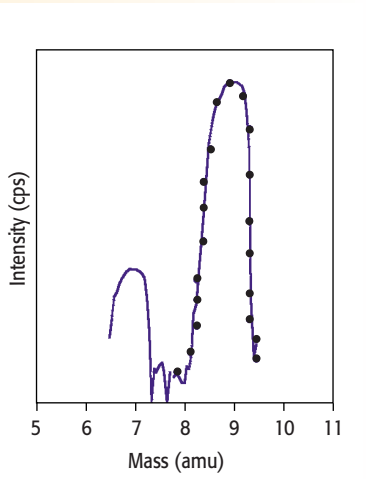

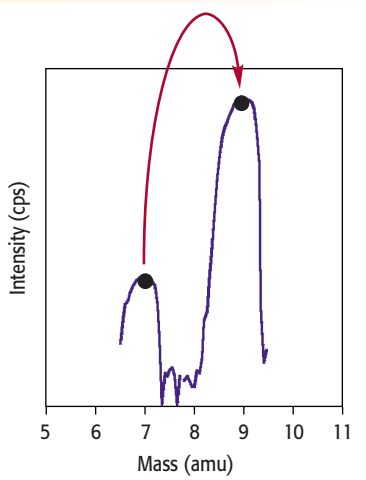

Figure 3 (above left). A profile of the peak is built up by continually sweeping the quadrupole across the mass spectrum.

Figure 4 (above right). Multichannel ramp scanning approach using 20 channels per amu.

Figure 5 (below right). Peak-hopping approach.

and more to the background noise. Figure 6 shows the degradation in signal-to-background noise ratio of 10 ppb Rh with an increase in the number of points per peak, spread over the same total integration time. Detection limit improvement for a selected group of elements using 1 point/peak, rather than 20 points/peak, is shown in Figure 7.

Optimization of Measurement Protocol

Now that the fundamentals of the quadrupole measuring electronics have been described, let us now go into more detail on the impact of optimizing the measurement protocol based on the requirement of the application. When multielement analysis is being carried out by ICP-MS, a number of decisions need to be made. First, we need to know if we are dealing with a continuous signal from a nebulizer or a transient signal from an alternative sampling accessory. If it is a transient event, how long will the signal last? Another question that needs to be addressed is, how many elements are going to be determined? With a continuous signal, this isn't such a major problem, but it could be an issue if we are dealing with a transient signal that lasts a few seconds. We also need to be aware of the level of detection capability required. This is a major consideration with a single-shot laser pulse that lasts 5–10 s. Also with a continuous signal produced by a concentric nebulizer, we might have to accept a compromise of detection limit based on the speed of analysis requirements or amount of sample available. What analytical precision is expected? If it's isotope ratio/
dilution work, how many ions do we have to count to guarantee good precision? Does increasing the integration time of the measurement help the precision? Finally, is there a time constraint on the analysis? A high-throughput laboratory might not be able to afford to use the optimum sampling time to get the ultimate in detection limit. In other words, what compromises need to be made between detection limit, precision, and sample throughput? Clearly, before the measurement protocol can be optimized, the major analytical requirements of the application need to be defined. Let's take a look at this process in greater detail.

Multielement Data Quality Objectives

Because multielement detection capability is probably the major reason why most laboratories invest in ICP-MS, it is important to understand the impact of measurement criteria on detection limits. We know that in a multielement analysis, the quadrupole's rf/dc ratio is scanned to mass regions or *driven,* which represent the elements of interest. The electronics are allowed to settle

Table I. Precision of Pb isotope ratio measurement as a function of dwell time using a total integration time of 5.5 s.

Dwell time (ms)	%RSD, $^{207}Pb/^{206}Pb$	%RSD, $^{208}Pb/^{206}Pb$
2	0.40	0.36
5	0.38	0.36
10	0.23	0.22
25	0.24	0.25
50	0.38	0.33
100	0.41	0.38

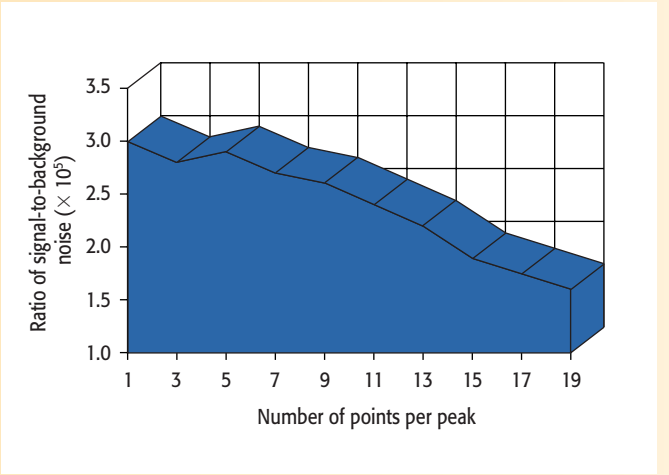

Figure 6. Signal-to-background noise ratio degrades when more than one point, spread over the same integration time, is used for peak quantitation.

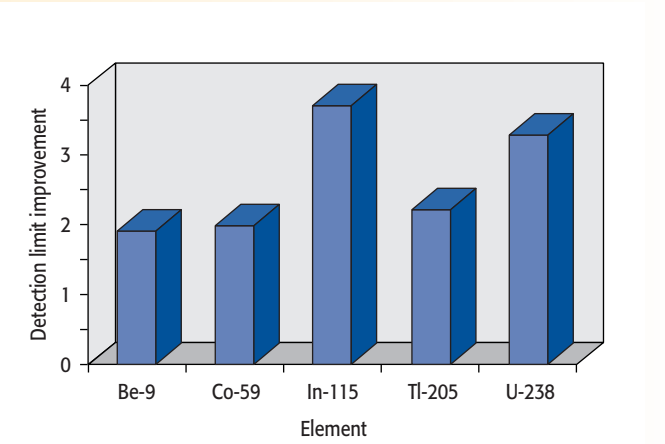

Figure 7. Detection limit improvement using 1 point/peak rather than 20 points/peak over the mass range.

and then dwell on the peak, or *sit*, and take measurements for a fixed period of time. This step is usually performed a number of times until the total integration time is fulfilled. For example, if a dwell time of 50 ms is selected for all masses and the total integration time is 1 s, then the quadrupole will carry out 20 complete sweeps per mass, per replicate. It will then repeat the same routine for as many replicates that have been built into the method. This process is illustrated very simplistically in Figure 8, which shows the scanning protocol of a multielement scan of three different masses.

In this example, the quadrupole is scanned to mass A. The electronics are allowed to settle (settling time) and left to dwell for a fixed period of time at one or multiple points on the peak (dwell time); intensity measurements are then taken (based on the dwell time). The quadrupole is then scanned to masses B and C and the measurement protocol repeated. The complete multielement measurement cycle (sweep) is repeated as many times as needed to make up the total integration per peak. It should be emphasized that this example is a generalization of the measurement routine — management of peak integration by the software will vary slightly, based on different instrumentation.

It is clear from this information that, during a multielement analysis, a significant amount of time is spent scanning and settling the quadrupole, which doesn't contribute to the quality of the analytical signal. Therefore, if the measurement routine is not optimized carefully, it can have a negative impact on data quality. The dwell time can usually be selected on an individual mass basis, but the scanning and settling times are normally fixed because they are a function of the quadrupole and detector electronics. For this reason, it is essential that the dwell time — which ultimately affects detection limit and precision — must dominate the total measurement time, compared with the scanning and settling times. It follows, therefore, that the measurement duty cycle (percentage of actual measuring time compared with total integration time) is maximized when the quadrupole and detector electronics settling times are kept to an absolute minimum. Figure 9 shows a plot of percentage of measurement efficiency against dwell time for four different quadrupole settling times — 0.2, 1.0, 3.0, and 5.0 ms for one replicate of a multielement scan of five masses, using one point per peak. In this example, the total integration time for each mass was 1 s, with the number of sweeps varying, depending on the dwell time used. For this exercise, the percentage of measurement efficiency is defined by the following calculation:

$$\frac{\text{Dwell Time} \times \#\text{Sweeps} \times \#\text{Elements} \times \#\text{Replicates}}{\left(\text{Dwell Time} \times \#\text{Sweeps} \times \#\text{Elements} \times \#\text{Replicates}\right) + \left(\text{Scanning / Settling Time} \times \#\text{Sweeps} \times \#\text{Elements} \times \#\text{Replicates}\right)} \times 100$$

So to achieve the highest measurement efficiency, the nonanalytical time must be kept to an absolute minimum. This leads to more time being spent counting ions and less time scanning and settling, which does not contribute to the quality of the analytical signal. This factor becomes critically important when a rapid transient peak is being quantified, because the available measuring time is that much shorter (3). Generally speaking, peak quantitation using multiple points per peak and long settling times should be avoided in ICP-MS because it ultimately degrades the quality of the data for a given integration time.

Figure 9 also shows that shorter dwell times translate into a lower measurement efficiency. For this reason, it is probably desirable, for normal quantitative analysis work, to carry out multiple sweeps with longer dwell times (typically 50 ms) to get the best detection limits. So if an integration time of 1 s is used for each element, this would translate into 20 sweeps of 50 ms dwell time per mass. Although 1 s is long enough to achieve reasonably good detection limits, longer integration times generally have to be used to reach the

lowest possible detection limits. Figure 10 shows detection limit improvement as a function of integration time for ^{238}U. As would be expected, there is a fairly predictable improvement in the detection limit as the integration time is increased because more ions are being counted without an increase in the background noise. However, this only holds true up to the point where the pulse-counting detection system becomes saturated and no more ions can be counted. In the case of ^{238}U, this occurs around 25 s, because there is no obvious improvement in detection limit at a higher integration time. So from these data, we can say that there appears to be no real benefit in using an integration time longer than 7 s. When deciding the length of the integration time in ICP-MS, you have to weigh the detection limit improvement against the time taken to achieve that improvement. Is it worth spending 25 s measuring each mass to get a 0.02 ppt detection limit if 0.03 ppt can be achieved using a 7-s integration time? Alternatively, is it worth measuring for 7 s when 1 s will only degrade the performance by a factor of 3? It really depends on your data quality objectives.

For applications such as isotope dilution/ratio studies, high precision is also a very important data quality objective (4). However, to understand what is realistically achievable, we must be aware of the practical limitations of measuring a signal and counting ions in ICP-MS. Counting statistics tells us that the standard deviation of the ion signal is proportional to the square root of the signal. It follows, therefore, that the relative standard deviation (RSD), or precision, should improve with an increase in the number (N) of ions counted as shown by the following equation:

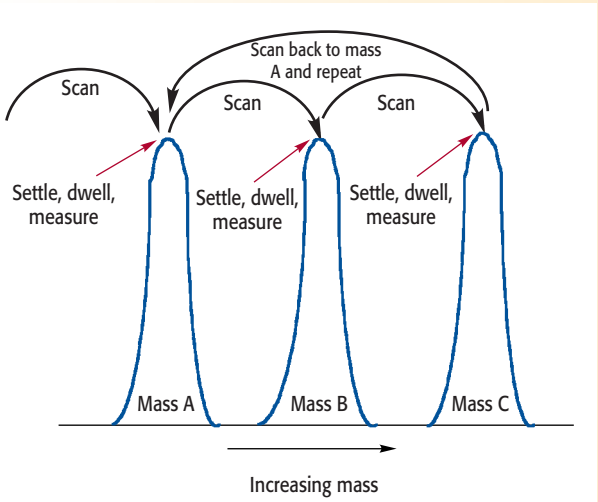

Figure 8 (left). Multielement scanning and measurement protocol of a quadrupole.

Figure 9 (below). Percent of measurement efficiency as a function of dwell time with varying scanning/settling times.

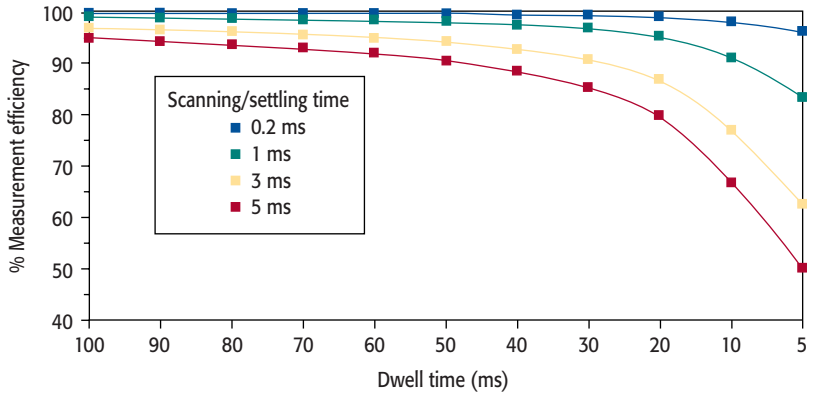

$$\%RSD = \frac{\sqrt{N}}{N} = 100$$

In practice this holds up very well, as shown in Figure 11. In this plot of standard deviation as a function of signal intensity for ^{208}Pb, the dots represent the theoretical relationship as predicted by counting statistics. It can be seen that the measured standard deviation (bars) follows theory very well up to about 100,000 cps. At that point, additional sources of noise (for example, sample introduction pulsations or plasma fluctuations) dominate the signal, which leads to poorer standard deviation values.

So based on counting statistics, it is logical to assume that the more ions that are counted, the better the precision will be. To put this in perspective, it means that at least 1 million ions need to be counted to achieve an RSD of 0.1%. In practice, of course, these kinds of precision values are very difficult to achieve with a scanning quadru-

Table II. Impact of integration time on the overall analysis time for Pb isotope ratios.

Dwell time (ms)	Number of sweeps	Integration time (s)/mass	%RSD, $^{207}Pb/^{206}Pb$	%RSD, $^{207}Pb/^{206}Pb$	Analysis time for 9 reps
25	220	5.5	0.24	0.25	2 min 29 s
25	500	12.5	0.21	0.19	6 min 12 s
25	700	17.5	0.20	0.17	8 min 29 s

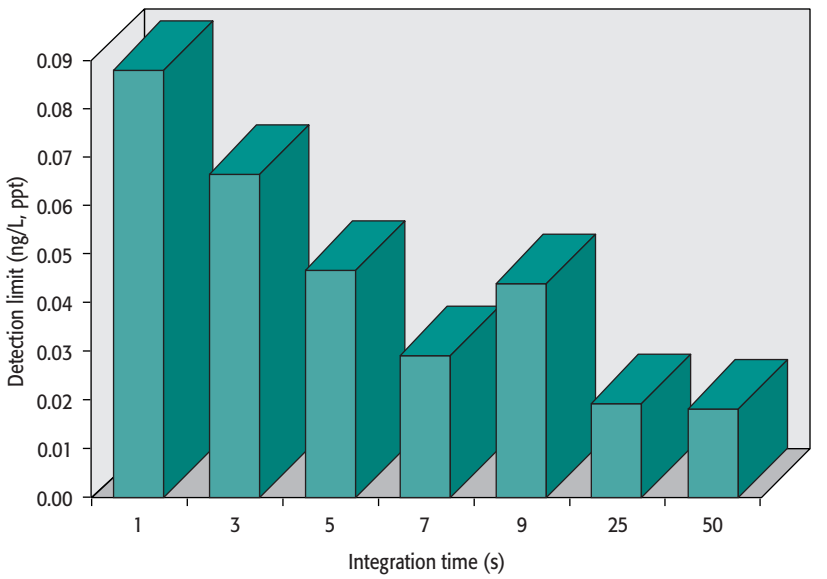

Figure 10. Plot of detection limit against integration time for ^{238}U.

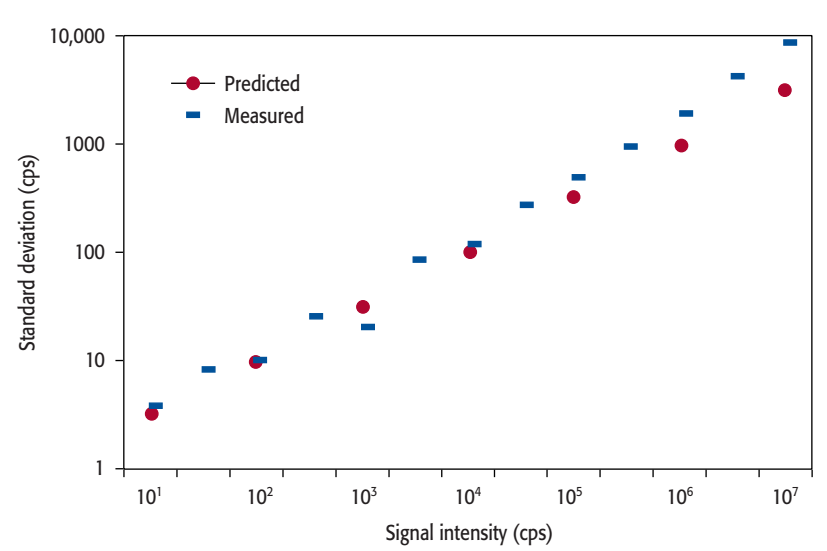

Figure 11. Comparison of measured standard deviation of a ^{208}Pb signal against that predicted by counting statistics.

pole system because of the additional sources of noise. If this information is combined with our knowledge of how the quadrupole is scanned, we begin to understand what is required to get the best precision. This is confirmed by the spectral scan in Figure 12, which shows the predicted precision at all 20 channels of a 5 ppb ^{208}Pb peak (2).

Therefore, the best precision is obtained at the channels where the signal is highest, which as we can see are the ones at or near the center of the peak. For this reason, if good precision is a fundamental requirement of your data quality objectives, it is best to use single-point peak hopping with integration times in the order of 5–10 s. On the other hand, if high-precision isotope ratio or isotope dilution work is being done — in which analysts would like to achieve precision values approaching counting statistics — then much longer measuring times are required. That is why integration times of 5–10 min are commonly used for determining isotope ratios with a quadrupole ICP-MS system (5, 6). For this type of analysis, when two or more isotopes are being measured and ratioed to each other, it follows that the more simultaneous the measurement, the better the precision becomes. Therefore, the ability to make the measurement as simultaneous as possible is considered more desirable than any other aspect of the measurement. This is supported by the fact that the best isotope ratio precision data are obtained with time-of-flight or multicollector, magnetic sector ICP-MS systems, which are both considered simultaneous in nature. So the best way to approximate simultaneous measurement with a rapid scanning device, such as a quadrupole, is to use shorter dwell and scanning/settling times, resulting in more sweeps for a given integration time. Table I shows precision of Pb isotope ratios at different dwell times carried out by researchers at the Geological Survey of Israel (7). The data are based on nine replicates of a NIST SRM-981 (75 ppb Pb) solution, using 5.5 s of integration time per isotope.

From these data, the researchers concluded that a dwell time of 10 or 25 ms offered the best isotope ratio precision measurement (quadrupole settling time was fixed at 0.2 ms). They also found that they could achieve slightly better precision by using a 17.5-s integration time (700 sweeps at a 25-ms dwell time), but felt the marginal improvement in precision for nine replicates was not worth spending the approximately 3.5-times-longer analysis time, as shown in Table II.

This work shows the benefit of optimizing the dwell time, settling time, and the number of sweeps to get the best isotope ratio precision data. The researchers were also very fortunate to be dealing with relatively healthy signals for the three Pb isotopes, ^{206}Pb, ^{207}Pb, and ^{208}Pb (24.1%, 22.1%, and 52.4% abundance, respectively). If the isotopic signals were dramatically different like in ^{235}U to ^{238}U (0.72 % and 99.2745% abundance, respectively), then the ability to optimize the measurement proto-

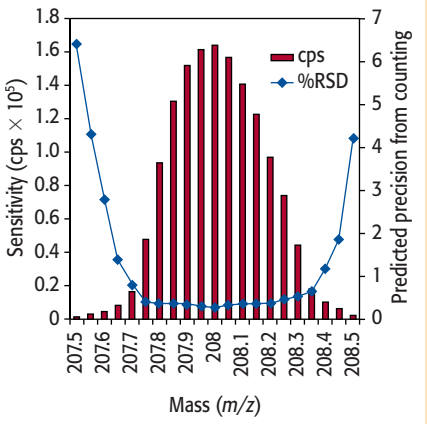

Figure 12. Comparison of % RSD with signal intensity across the mass profile of a ^{208}Pb peak.

col for individual isotopes becomes of even greater importance to guarantee precise data.

It is clear that the analytical demands put on ICP-MS are probably higher than any other trace element technique because it is continually being asked to solve a wide variety of application problems. However, by optimizing the measurement protocol to fit the analytical requirement, ICP-MS has shown that it has the capability to carry out rapid trace element analysis, with superb detection limits and good precision on both continuous and transient signals, and still meet the most stringent data quality objectives.

References

1. R. Thomas, *Spectroscopy* **16**(10), 44–48 (2001).
2. E.R. Denoyer, *At. Spectroscopy* **13**(3), 93–98 (1992).
3. E.R. Denoyer and Q.H. Lu, *At. Spectroscopy* **14**(6), 162–169 (1993).
4. T. Catterick, H. Handley, and S. Merson, *At. Spectroscopy* **16**(10), 229–234 (1995).
5. T.A. Hinners, E.M. Heithmar, T.M. Spittler, and J.M. Henshaw, *Anal. Chem.* **59**, 2658–2662 (1987).
6. M. Janghorbani, B.T.G. Ting, and N.E. Lynch, *Microchemica Acta* **3**, 315–328, (1989).
7. L. Halicz, Y. Erel, and A. Veron, *At. Spectroscopy* **17**(5), 186–189 (1996). ■

"Conference Preview" continued from page 27

applications and provides everything necessary for a typical x-ray detector, incorporating one DXP spectrometer channel, preamplifier power, and detector HV bias in one compact chassis. Its input is compatible with a wide range of common detectors, including pulsed optical reset, transistor reset, and RC feedback preamplifiers. The Saturn offers complete computer control over all amplifier and spectrometer functions including gain, filter peaking time, and pileup inspection criteria. Its DXP digital filters significantly increase throughput compared to typical analog systems.

The new X-Beam x-ray source from **X-Ray Optical Systems** (Albany, NY) delivers an intense, micrometer-sized focal spot. Designed for OEM use in micro-XRF instruments, the compact unit uses polycapillary focusing optics and 50 W of power to generate an extremely high flux-density gain, the company reports. Increased spatial resolution and beam stability are also promised. An integrated cooling system eliminates the need for a separate cooling unit.

Attendees can see many of these products, along with others not mentioned, at the 2002 Denver X-ray Conference — sponsored by the International Centre for Diffraction Data — at Antlers Adam's Mark Hotel (formerly Antlers Doubletree Hotel), Colorado Springs, Colorado, July 29–August 2, 2002. For more information, contact Denise Flaherty, DXC Conference Coordinator, 12 Campus Boulevard, Newtown Square, PA 19073-3273, (610) 325-9814, fax: (610) 325-9823, e-mail: flaherty@icdd.com, web site: www.dxcicdd.com. ■

TUTORIAL

A Beginner's Guide to ICP-MS

Part XII – A Review of Interferences

Robert Thomas

We have previously covered the major instrumental components of an ICP mass spectrometer; now let's turn our attention to the technique's most common interferences and what methods are used to compensate for them. Although interferences are reasonably well understood in inductively coupled plasma–mass spectrometry (ICP-MS), it can often be difficult and time-consuming to compensate for them, particularly in complex sample matrices. Having prior knowledge of the interferences associated with a particular set of samples will often dictate the sample preparation steps and the instrumental methodology used to analyze them.

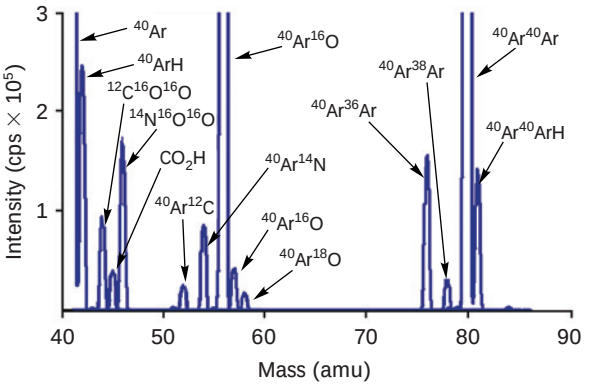

Figure 1. Mass spectrum of deionized water from mass 40 to mass 85.

Robert Thomas has more than 30 years of experience in trace element analysis. He is the principal of his own freelance writing and consulting company, Scientific Solutions, based in Gaithersburg, MD. He can be contacted by e-mail at thomasrj@bellatlantic.net or via his web site at www.scientificsolutions1.com.

Interferences in ICP-MS are generally classified into three major groups — spectral, matrix, and physical. Each of them has the potential to be problematic in its own right, but modern instrumentation and good software, combined with optimized analytical methodologies, has minimized their negative impact on trace element determinations by ICP-MS. Let us take a look at these interferences in greater detail and describe the different approaches used to compensate for them.

Spectral Interferences

Spectral overlaps are probably the most serious types of interferences seen in ICP-MS. The most common type is known as a polyatomic or molecular spectral interference, which is produced by the combination of two or more atomic ions. They are caused by a variety of factors, but are usually associated with either the plasma and nebulizer gas used, matrix components in the solvent and sample, other analyte elements, or entrained oxygen or nitrogen from the surrounding air. For example, in the argon plasma, spectral overlaps caused by argon ions and combinations of argon ions with other species are very common. The most abundant isotope of argon is at mass 40, which dramatically interferes with the most abundant isotope of calcium at mass 40, whereas the combination of argon and oxygen in an aqueous sample generates the $^{40}Ar^{16}O$ interference, which has a significant impact on the major isotope of Fe at mass 56. The complexity of these kinds of spectral problems can be seen in Figure 1, which shows a mass spectrum of deionized water from mass 40 to mass 90.

Additionally, argon can also form polyatomic interferences with elements found in the acids used to dissolve the sample. For example in a hydrochloric acid medium, ^{40}Ar combines with the most abundant chlorine isotope at 35 amu to form $^{40}Ar^{35}Cl$, which interferes with the only isotope of arsenic at mass 75, while in an organic solvent ma-

Relative Abundance of the Natural Isotopes

Isotope	%	%	%	Isotope	%	%	%	Isotope	%	%	%	Isotope	%	%	%
1	H 99.985			61			Ni 1.140	121			Sb 57.36	181	Ta 99.988		
2	H 0.015			62			Ni 3.634	122	Sn 4.63	Te 2.603		182		W 26.3	
3		He 0.000137		63	Cu 69.17			123		Te 0.908	Sb 42.64	183		W 14.3	
4		He 99.999863		64		Zn 48.6	Ni 0.926	124	Sn 5.79	Te 4.816	Xe 0.10	184	Os 0.02	W 30.67	
5				65	Cu 30.83			125		Te 7.139		185			Re 37.40
6			Li 7.5	66		Zn 27.9		126		Te 18.95	Xe 0.09	186	Os 1.58	W 28.6	
7			Li 92.5	67		Zn 4.1		127	I 100			187	Os 1.6		Re 62.60
8				68		Zn 18.8		128		Te 31.69	Xe 1.91	188	Os 13.3		
9	Be 100			69			Ga 60.108	129			Xe 26.4	189	Os 16.1		
10		B 19.9		70	Ge 21.23	Zn 0.6		130	Ba 0.106	Te 33.80	Xe 4.1	190	Os 26.4		Pt 0.01
11		B 80.1		71			Ga 39.892	131			Xe 21.2	191		Ir 37.3	
12			C 98.90	72	Ge 27.66			132	Ba 0.101		Xe 26.9	192	Os 41.0		Pt 0.79
13			C 1.10	73	Ge 7.73			133		Ce 100		193		Ir 62.7	
14	N 99.643			74	Ge 35.94	Se 0.89		134	Ba 2.417		Xe 10.4	194			Pt 32.9
15	N 0.366			75			As 100	135	Ba 6.592			195			Pt 33.8
16		O 99.762		76	Ge 7.44	Se 9.36		136	Ba 7.854	Ce 0.19	Xe 8.9	196	Hg 0.15		Pt 25.3
17		O 0.038		77		Se 7.63		137	Ba 11.23			197		Au 100	
18		O 0.200		78	Kr 0.35	Se 23.78		138	Ba 71.70	Ce 0.25	La 0.0902	198	Hg 9.97		Pt 7.2
19			F 100	79			Br 50.69	139			La 99.9098	199	Hg 16.87		
20	Ne 90.48			80	Kr 2.25	Se 49.61		140		Ce 88.48		200	Hg 23.10		
21	Ne 0.27			81			Br 49.31	141			Pr 100	201	Hg 13.18		
22	Ne 9.25			82	Kr 11.6	Se 8.73		142	Nd 27.13	Ce 11.08		202	Hg 29.86		
23		Na 100		83	Kr 11.5			143	Nd 12.18			203			Tl 29.524
24			Mg 78.99	84	Kr 57.0	Sr 0.56		144	Nd 23.80	Sm 3.1		204	Hg 6.87	Pb 1.4	
25			Mg 10.00	85			Rb 72.165	145	Nd 8.30			205			Tl 70.476
26			Mg 11.01	86	Kr 17.3	Sr 9.86		146	Nd 17.19			206		Pb 24.1	
27	Al 100			87		Sr 7.00	Rb 27.835	147		Sm 15.0		207		Pb 22.1	
28		Si 92.23		88		Sr 82.58		148	Nd 5.76	Sm 11.3		208		Pb 52.4	
29		Si 4.67		89			Y 100	149		Sm 13.8		209	Bi 100		
30		Si 3.10		90	Zr 51.45			150	Nd 5.64	Sm 7.4		210			
31			P 100	91	Zr 11.22			151			Eu 47.8	211			
32	S 95.02			92	Zr 17.15	Mo 14.84		152	Gd 0.20	Sm 26.7		212			
33	S 0.75			93			Nb 100	153			Eu 52.2	213			
34	S 4.21			94	Zr 17.38	Mo 9.25		154	Gd 2.18	Sm 22.7		214			
35		Cl 75.77		95		Mo 15.92		155	Gd 14.80			215			
36	S 0.02		Ar 0.337	96	Zr 2.80	Mo 16.68	Ru 5.52	156	Gd 20.47	Dy 0.06		216			
37		Cl 24.23		97		Mo 9.55		157	Gd 15.65			217			
38			Ar 0.063	98		Mo 24.13	Ru 1.88	158	Gd 24.84	Dy 0.10		218			
39	K 93.2581			99			Ru 12.7	159			Tb 100	219			
40	K 0.0117	Ca 96.941	Ar 99.600	100		Mo 9.63	Ru 12.6	160	Gd 21.86	Dy 2.34		220			
41	K 6.7302			101			Ru 17.0	161		Dy 18.9		221			
42		Ca 0.647		102	Pd 1.02		Ru 31.6	162	Er 0.14	Dy 25.5		222			
43		Ca 0.135		103		Rh 100		163		Dy 24.9		223			
44		Ca 2.086		104	Pd 11.14		Ru 18.7	164	Er 1.61	Dy 28.2		224			
45			Sc 100	105	Pd 22.33			165			Ho 100	225			
46	Ti 8.0	Ca 0.004		106	Pd 27.33	Cd 1.25		166	Er 33.6			226			
47	Ti 7.3			107			Ag 51.839	167	Er 22.95			227			
48	Ti 73.8	Ca 0.187		108	Pd 26.46	Cd 0.89		168	Er 26.8	Yb 0.13		228			
49	Ti 5.5			109			Ag 48.161	169			Tm 100	229			
50	Ti 5.4	V 0.250	Cr 4.345	110	Pd 11.72	Cd 12.49		170	Er 14.9	Yb 3.05		230			
51		V 99.750		111		Cd 12.80		171		Yb 14.3		231	Pa 100		
52			Cr 83.789	112	Sn 0.97	Cd 24.13		172		Yb 21.9		232	Th 100		
53			Cr 9.501	113		Cd 12.22	In 4.3	173		Yb 16.12		233			
54	Fe 5.8		Cr 2.365	114	Sn 0.65	Cd 28.73		174		Yb 31.8	Hf 0.162	234	U 0.0055		
55		Mn 100		115	Sn 0.34		In 95.7	175	Lu 97.41			235	U 0.7200		
56	Fe 91.72			116	Sn 14.53	Cd 7.49		176	Lu 2.59	Yb 12.7	Hf 5.206	236			
57	Fe 2.2			117	Sn 7.68			177			Hf 18.606	237			
58	Fe 0.28		Ni 68.077	118	Sn 24.23			178			Hf 27.297	238	U 99.2745		
59		Co 100		119	Sn 8.59			179			Hf 13.629				
60			Ni 26.223	120	Sn 32.59	Te 0.096		180	Ta 0.012	W 0.13	Hf 35.100				

Figure 2. Relative isotopic abundances of the naturally occurring elements, showing all the potential isobaric interferences.

trix, argon and carbon combine to form $^{40}Ar^{12}C$, which interferes with ^{52}Cr, the most abundant isotope of chromium. Sometimes, matrix or solvent species need no help from argon ions and combine to form spectral interferences of their own. A good example is in a sample that contains sulfuric acid. The dominant sulfur isotope ^{32}S combines with two oxygen ions to form a $^{32}S^{16}O^{16}O$ molecular ion, which interferes with the major isotope of Zn at mass 64. In the analysis of samples containing high concentrations of sodium, such as seawater, the most abundant isotope of Cu at mass 63 cannot be used because of interference from the $^{40}Ar^{23}Na$ molecular ion. There are many more examples of these kinds of polyatomic and molecular interferences (1). Table I represents some of the most common ones seen in ICP-MS.

Oxides, Hydroxides, Hydrides, and Doubly Charged Species

Another type of spectral interference is produced by elements in the sample combining with H, ^{16}O, or ^{16}OH (either from water or air) to form molecular hydride (H), oxide (^{16}O), and hydroxide (^{16}OH) ions, which occur at 1, 16, and 17 mass units higher than its mass (2). These interferences are typically produced in the cooler zones of the plasma, immediately before the interface region. They are usually more serious when rare earth or refractory-type elements are present in the sample, because many of them readily form molecular species (particularly oxides), which create spectral overlap problems on other elements in the same group. Associated with oxide-based spectral overlaps are doubly charged spectral interferences. These are species that are formed when an ion is generated with a double positive charge, as opposed to a normal single charge, and produces a peak at half its mass. Like the formation of oxides, the level of doubly charged species is related to the ionization conditions in the plasma and can usually be minimized by careful optimization of the nebulizer gas flow, rf power, and sampling position within the plasma. It can also be impacted by the severity of the secondary discharge present at the interface (3), which was described in greater detail in Part IV of the series (4). Table II shows a selected group of elements, that readily form oxides, hydroxides, hydrides, and doubly charged species, together with the analytes that are affected by them.

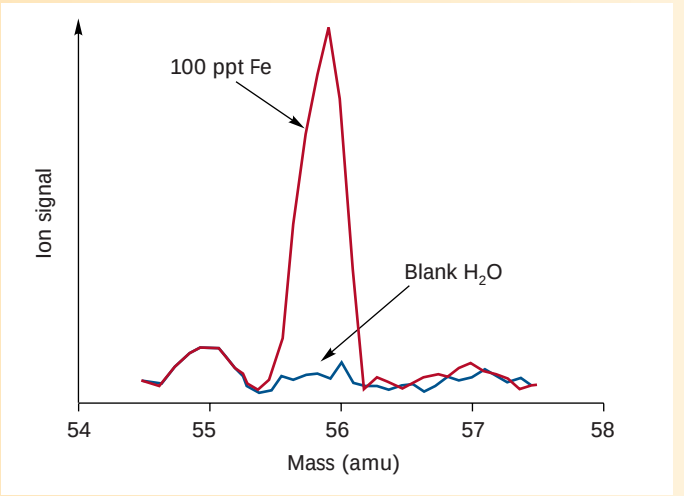

Figure 3. Spectral scan of 100 ppt ^{56}Fe and deionized water using cool plasma conditions.

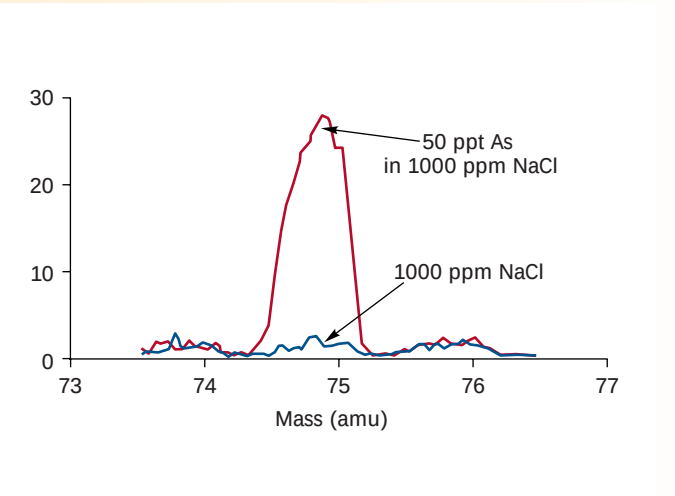

Figure 4. Reduction of the $^{40}Ar^{35}Cl$ interference makes it possible to determine low ppt levels of monoisotopic ^{75}As in a high chloride matrix using dynamic reaction cell technology.

Table I. Some common plasma, matrix, and solvent-related polyatomic spectral interferences seen in ICP-MS.

Element/ Isotope	Matrix/ solvent	Interference
^{39}K	H_2O	^{38}ArH
^{40}Ca	H_2O	^{40}Ar
^{56}Fe	H_2O	$^{40}Ar^{16}O$
^{80}Se	H_2O	$^{40}Ar^{40}Ar$
^{51}V	HCl	$^{35}Cl^{16}O$
^{75}As	HCl	$^{40}Ar^{35}Ci$
^{28}Si	HNO_3	$^{14}N^{14}N$
^{44}Ca	HNO_3	$^{14}N^{14}N^{16}O$
^{55}Mn	HNO_3	$^{40}Ar^{15}N$
^{48}Ti	H_2SO_4	$^{32}S^{16}O$
^{52}Cr	H_2SO_4	$^{34}S^{18}O$
^{64}Zn	H_2SO_4	$^{32}S^{16}O^{16}O$
^{63}Cu	H_3PO_4	$^{31}P^{16}O^{16}O$
^{24}Mg	Organics	$^{12}C^{12}C$
^{52}Cr	Organics	$^{40}Ar^{12}C$
^{65}Cu	Minerals	$^{48}Ca^{16}OH$
^{64}Zn	Minerals	$^{48}Ca^{16}O$
^{63}Cu	Seawater	$^{40}Ar^{23}Na$

Isobaric Interferences

The final classification of spectral interferences is called "isobaric overlaps," produced mainly by different isotopes of other elements in the sample that create spectral interferences at the same mass as the analyte. For example, vanadium has two isotopes at 50 and 51 amu. However, mass 50 is the only practical isotope to use in the presence of a chloride matrix, because of the large contribution from the $^{16}O^{35}Cl$ interference at mass 51. Unfortunately mass 50 amu, which is only 0.25% abundant, also coincides with isotopes of titanium and chromium, which are 5.4% and 4.3% abundant, respectively. This makes the determination of vanadium in the presence of titanium and chromium very difficult unless mathematical corrections are made. Figure 2 — the relative abundance of the naturally occurring isotopes — shows all the naturally occuring isobaric spectral overlaps possible in ICP-MS (5).

Ways to Compensate for Spectral Interferences

Let us look at the different approaches used to compensate for spectral interferences. One of the very first ways used to get around severe matrix-derived spectral interferences was to remove the matrix somehow. In the early days, this involved precipitating the matrix with a complexing agent and then filtering off the precipitate. However, this has been more recently carried out by automated matrix removal and analyte preconcentration techniques using chromatography-type equipment. In fact, this method is preferred for carrying out trace metal determinations in seawater because of the matrix and spectral problems associated with such high concentrations of sodium and magnesium chloride (6).

Mathematical Correction Equations

Another method that has been successfully used to compensate for isobaric interferences and some less severe polyatomic overlaps (when no alternative isotopes are available for quantitation) is to use mathematical interference correction equations. Similar to interelement corrections (IECs) in ICP–optical emission spectroscopy, this method works on the principle of measuring the intensity of the interfering isotope or interfering species at another mass, which ideally is free of any interferences. A correction is then applied by knowing the ratio of the intensity of the interfering species at the analyte mass to its intensity at the alternate mass.

Let's take a look at a real-world example of this type of correction. The most sensitive isotope for cadmium is at mass 114. However, there is also a minor isotope of tin at mass 114. This means that if there is any tin in the sample, quantitation using ^{114}Cd can only be carried out if a correction is made for ^{114}Sn. Fortunately Sn has a total of 10 isotopes, which means that at least one of them will probably be free of a spectral interference. Therefore, by measuring the intensity of Sn at one of its most abundant isotopes (typically ^{118}Sn) and ratioing it to ^{114}Sn, a correction is made in the method software in the following manner:

Table II. Some elements that readily form oxides, hydroxides, or hydrides and doubly charged species in the plasma and the analyte affected by the potential interference.

Oxide/hydroxide/ hydride doubly charged species	Analyte
$^{40}Ca^{16}O$	^{56}Fe
$^{48}Ti^{16}O$	^{64}Zn
$^{98}Mo^{16}O$	^{114}Cd
$^{138}Ba^{16}O$	^{154}Sm, ^{154}Gd
$^{139}La^{16}O$	^{155}Gd
$^{140}Ce^{16}O$	^{156}Gd, ^{156}Dy
$^{40}Ca^{16}OH$	^{57}Fe
$^{31}P^{18}O^{16}OH$	^{66}Zn
^{79}BrH	^{80}Se
$^{31}P^{16}O_2H$	^{64}Zn
$^{138}Ba^{2+}$	^{69}Ga
$^{139}La^{2+}$	^{69}Ga
$^{140}Ce^{2+}$	^{70}Ge, ^{70}Zn

Total counts at mass 114 = $^{114}Cd + ^{114}Sn - (0.0268)*(^{118}Sn)$.

Therefore ^{114}Cd = total counts at mass 114 − ^{114}Sn

To find out the contribution from ^{114}Sn, it is measured at the interference-free isotope of ^{118}Sn and a correction of the ratio of $^{114}Sn/^{118}Sn$ is applied:

Which means ^{114}Cd = counts at mass 114 = $(^{114}Sn/^{118}Sn) \times (^{118}Sn)$

Now the ratio $(^{114}Sn/^{118}Sn)$ is the ratio of the natural abundances of these two isotopes (0.65%/24.23%) and is always constant

Therefore ^{114}Cd = mass 114 − (0.65%/24.23%) × (^{118}Sn)

or ^{114}Cd = mass 114 − (0.0268) × (^{118}Sn)

An interference correction for ^{114}Cd would then be entered in the software as:

This is a relatively simple example, but explains the basic principles of the process. In practice, especially in spectrally complex samples, corrections often have to be made to the isotope being used for the correction — these corrections are in addition to the analyte mass, which makes the mathematical equation far more complex.

This approach can also be used for some less severe polyatomic-type spectral interferences. For example, in the determination of V at mass 51 in diluted brine (typically 1000 ppm NaCl), there is a substantial spectral interference from $^{35}Cl^{16}O$ at mass 51. By measuring the intensity of the $^{37}Cl^{16}O$ at mass 53, which is free of any interference, a correction can be applied in a similar way to the previous example.

Cool/Cold Plasma Technology

If the intensity of the interference is large, and analyte intensity is extremely

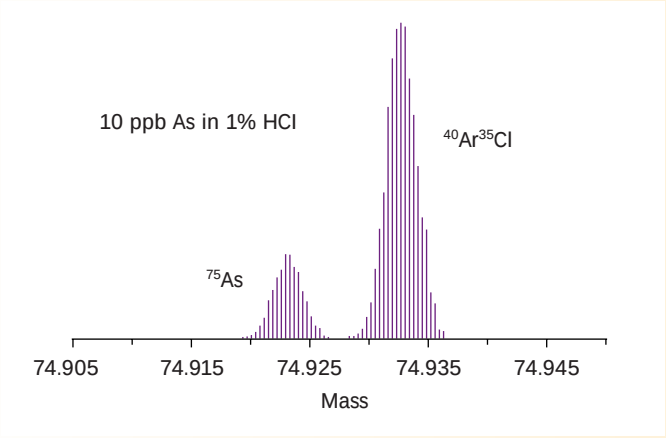

Figure 5 (above). Separation of ^{75}As from $^{40}Ar^{35}Cl$ using the high resolving power (10,000) of a double-focusing magnetic sector instrument (Courtesy of Thermo Finnigan).

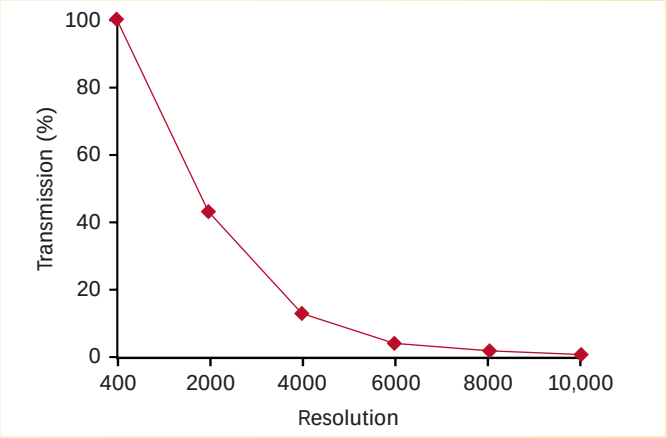

Figure 6 (upper right). The transmission characteristics of a magnetic sector ICP mass spectrometer decreases as the resolving power increases.

low, mathematical equations are not ideally suited as a correction method. For that reason, alternative approaches have to be considered to compensate for the interference. One such approach, which has helped to reduce some of the severe polyatomic overlaps, is to use cold/cool plasma conditions. This technology, which was reported in the literature in the late 1980s, uses a low-temperature plasma to minimize the formation of certain argon-based polyatomic species (7).

Under normal plasma conditions (typically 1000–1400 W rf power and 0.8–1.0 L/min of nebulizer gas flow), argon ions combine with matrix and solvent components to generate problematic spectral interferences such as ^{38}ArH, ^{40}Ar, and $^{40}Ar^{16}O$, which impact

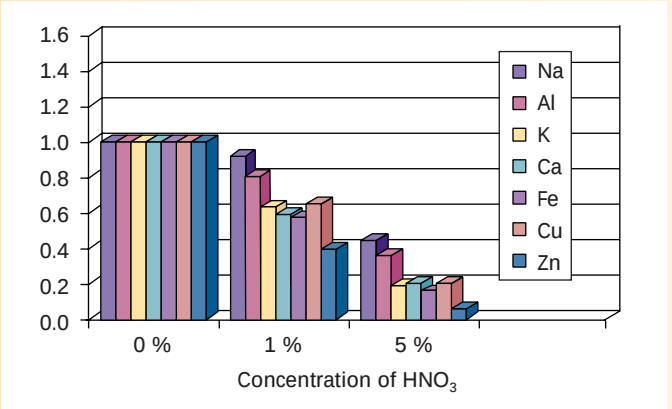

Figure 7. Matrix suppression caused by increasing concentrations of HNO_3, using cool plasma conditions (rf power: 800 W, nebulizer gas: 1.5 L/min).

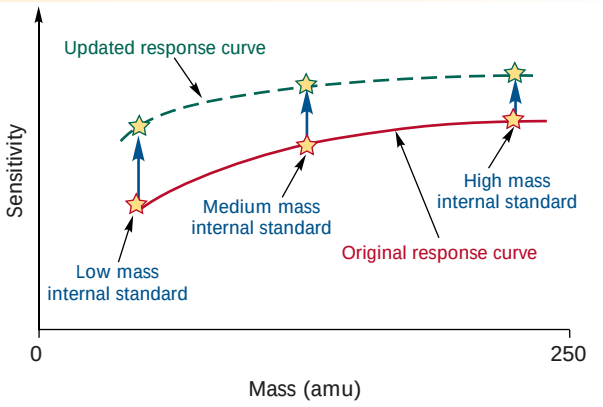

Figure 8. The analyte response curve is updated across the full mass range, based on the intensities of low, medium, and high mass internal standards.

the detection limits of a small number of elements including K, Ca, and Fe. By using cool plasma conditions (500–800 W rf power and 1.5–1.8 L/min nebulizer gas flow), the ionization conditions in the plasma are changed so that many of these interferences are dramatically reduced. The result is that detection limits for this group of elements are significantly enhanced (8).

An example of this improvement is seen in Figure 3, which shows a spectral scan of 100 ppt of ^{56}Fe (its most sensitive isotope) using cool plasma conditions. It can be clearly seen that there is virtually no contribution from $^{40}Ar^{16}O$, as indicated by the extremely low background for deionized water, resulting in single-figure parts-per-trillion (ppt) detection limits for iron. Under normal plasma conditions, the $^{40}Ar^{16}O$ intensity is so large that it would completely overlap the ^{56}Fe peak.

Cool plasma conditions are limited to a small group of elements in simple aqueous solutions that are prone to argon-based spectral interferences. It offers very little benefit for the majority of the other elements, because its ionization temperature is significantly lower than a normal plasma. In addition, it is often impractical for the analysis of complex samples, because of severe signal suppression caused by the matrix.

Collision/Reaction Cells

These limitations have led to the development of collision and reaction cells, which use ion–molecule collisions and reactions to cleanse the ion beam of harmful polyatomic and molecular interferences before they enter the mass analyzer. Collision/reaction cells are showing enormous potential to eliminate spectral interferences and make available isotopes that were previously unavailable for quantitation. For example, Figure 4 shows a spectral scan of 50 ppt As in 1000 ppm NaCl, together with 1000 ppm NaCl at mass 75, using a dynamic reaction cell with hydrogen/argon mixture as the reaction gas. It can be seen that there is insignificant contribution from the $^{40}Ar^{35}Cl$ interference, as indicated by the NaCl baseline. The capability of this type of reaction cell to virtually eliminate the $^{40}Ar^{35}Cl$ interference now makes it possible to determine low ppt levels of mono-isotopic ^{75}As in a high chloride matrix — previously not achievable by conventional interference correction methods (9). For a complete review of the benefits of collision/reaction cells for ICP-MS, refer to part 9 of this series (10).

High Resolution Mass Analyzers

The best and probably most efficient way to remove spectral overlaps is to resolve them away using a high resolution mass spectrometer (11). During the past 10 years this approach, particularly with double-focusing magnetic sector mass analyzers, has proved to be invaluable for separating many of the problematic polyatomic and molecular interferences seen in ICP-MS, without the need to use cool plasma conditions or collision/reaction cells. Figure 5 shows 10 ppb of ^{75}As resolved from the $^{40}Ar^{35}Cl$ interference in a 1% hydrochloric acid matrix, using normal, hot plasma conditions and a resolution setting of 10,000.

However, even though their resolving capability is far more powerful than quadrupole-based instruments, there is a sacrifice in sensitivity if extremely high resolution is used, as shown in Figure 6. This can often translate into a degradation in detection capability for some elements, compared to other spectral interference correction approaches. You will find an overview of the benefits of magnetic sector technology for ICP-MS in part VII of this series (12).

Matrix Interferences

Let's now take a look at the other class of interference in ICP-MS — suppression of the signal by the matrix itself. There are basically two types of matrix-induced interferences. The first and simplest to overcome is often called a sample transport effect and is a physical suppression of the analyte signal, brought on by the matrix components. It is caused by the sample's impact on droplet formation in the nebulizer or droplet-size selection in the spray chamber. In the case of organic matrices, it is usually caused by a difference in sample viscosities of the solvents being aspirated. In some matrices, signal suppression is caused not so much

by sample transport effects, but by its impact on the ionization temperature of the plasma discharge. This is exemplified when different concentrations of acids are aspirated into a cool plasma. The ionization conditions in the plasma are so fragile that higher concentrations of acid result in severe suppression of the analyte signal. Figure 7 shows the sensitivity for a selected group of elements in varying concentrations of nitric acid in a cool plasma (13).

Internal Standardization

The classic way to compensate for a physical interference is to use internal standardization. With this method of correction, a small group of elements (usually at the parts-per-billion level) are spiked into the samples, calibration standards, and blank to correct for any variations in the response of the elements caused by the matrix. As the intensity of the internal standards change, the element responses are updated every time a sample is analyzed. The following criteria are typically used for selecting the internal standards:

- They are not present in the sample
- The sample matrix or analyte elements do not spectrally interfere with them
- They do not spectrally interfere with the analyte masses
- They should not be elements that are considered environmental contaminants
- They are usually grouped with analyte elements of a similar mass range. For example, a low mass internal standard is grouped with the low mass analyte elements and so on up the mass range
- They should be of a similar ionization potential to the groups of analyte elements so they behave in a similar manner in the plasma
- Some of the common ones reported to be good candidates include ^{9}Be, ^{45}Sc, ^{59}Co, ^{74}Ge, ^{89}Y, ^{103}Rh, ^{115}In, ^{169}Tm, ^{175}Lu, ^{187}Re, and ^{232}Th.

A simplified representation of internal standardization is seen in Figure 8, which shows updating the analyte response curve across the full mass range, based on the intensities of low, medium, and high mass internal standards. It should also be noted that internal standardization is also used to compensate for long-term signal drift produced by matrix components slowly blocking the sampler and skimmer cone orifices. Even though total dissolved solids are kept below <0.2% in ICP-MS, this can still produce instability of the analyte signal over time with some sample matrices.

Space-Charge Interferences

Many of the early researchers reported that the magnitude of signal suppression in ICP-MS increased with decreasing atomic mass of the analyte ion (14). More recently it has been suggested that the major cause of this kind of suppression is the result of poor transmission of ions through the ion optics due to matrix-induced space charge effects (15). This has the effect of defocusing the ion beam, which leads to poor sensitivity and detection limits, especially when trace levels of low mass elements are being determined in the presence of large concentrations of high mass matrices. Unless any compensation is made, the high-mass matrix element will dominate the ion beam, pushing the lighter elements out of the way. Figure 9 shows the classic space charge effects of a uranium (major isotope ^{238}U) matrix on the determination of ^{7}Li, ^{9}Be, ^{24}Mg, ^{55}Mn, ^{85}Rb, ^{115}In, ^{133}Cs, ^{205}Tl, and ^{208}Pb. The suppression of low mass elements such as Li and Be is significantly higher than with high mass elements such as Tl and Pb in the presence of 1000 ppm uranium.

There are a number of ways to compensate for space charge matrix suppression in ICP-MS. Internal standardization has been used, but unfortunately doesn't address the fundamental cause of the problem. The most common approach used to alleviate or at least reduce space charge effects is to apply voltages to the individual ion lens components. This is achieved in a number of ways but, irrespective of the design of the ion focusing system, its main function is to reduce matrix-based suppression effects by steering as many of the analyte ions through to the mass analyzer while rejecting the maximum number of matrix ions. Space charge effects and different designs of ion optics were described in greater detail in part V of this series (16).

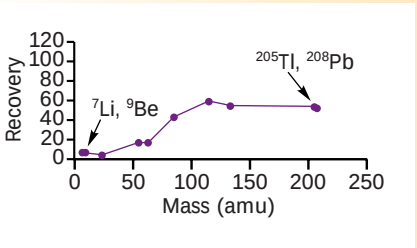

Figure 9. Space charge matrix suppression caused by 1000 ppm uranium is significantly higher on low mass elements Li and Be than it is with the high mass elements Tl and Pb.

References

1. G. Horlick and S.N. Tan, *Appl. Spectrosc.* **40,** 4 (1986).
2. G. Horlick and S.N. Tan, *Appl. Spectrosc.* **40,** 4 (1986).
3. D.J. Douglas and J.B. French, *Spectrochim. Acta* **41B**(3), 197 (1986).
4. R. Thomas, *Spectroscopy* **16**(7), 26–34, (2001).
5. "Isotopic Composition of the Elements," *Pure Applied Chemistry* **63**(7), 991–1002, (IUPAC, 1991).
6. S.N. Willie, Y. Iida, and J.W. McLaren, *Atom. Spectrosc.* **19**(3), 67 (1998).
7. S.J. Jiang, R.S. Houk, and M.A. Stevens, *Anal. Chem.* **60,** 1217 (1988).
8. S.D. Tanner, M. Paul, S.A. Beres, and E.R. Denoyer, *Atom. Spectrosc.* **16**(1), 16 (1995).
9. K.R. Neubauer and R.E. Wolf, "Determination of Arsenic in Chloride Matrices," *PerkinElmer Instruments Application Note* (PerkinElmer Instruments, Shelton, CT, 2000).
10. R. Thomas, *Spectroscopy* **17**(2), 42–48, (2002).
11. R. Hutton, A. Walsh, D. Milton, and J. Cantle, *ChemSA* **17,** 213–215 (1992).
12. R. Thomas, *Spectroscopy* **16**(11), 22–27, (2001).
13. J.M. Collard, K. Kawabata, Y. Kishi, and R. Thomas, *Micro,* January, 2002.
14. J.A. Olivares and R.S Houk, *Anal. Chem.* **58,** 20 (1986).
15. S.D. Tanner, D.J. Douglas, and J.B. French, *Appl. Spectrosc.* **48,** 1373, (1994).
16. R. Thomas, *Spectroscopy* **16**(9), 38–46, (2001). ■

Table I. Precision of Pb isotope ratio measurement as a function of dwell time using a total integration time of 5.5 s.

Dwell time (ms)	%RSD, $^{207}Pb/^{206}Pb$	%RSD, $^{208}Pb/^{206}Pb$
2	0.40	0.36
5	0.38	0.36
10	0.23	0.22
25	0.24	0.25
50	0.38	0.33
100	0.41	0.38

TUTORIAL

Beginner's Guide to ICP-MS

Part XIV: Sampling Accessories, Part II

Robert Thomas

(AUTHOR: The reference to Part 1 has been added, and the following references renumbered. Please check to make sure all callouts are updated.))

Sampling accessories are considered critical to enhance the practical capabilities of inductively coupled plasma–mass spectrometry (ICP-MS); since their development more than 10 years ago, they have proved to be invaluable for difficult, real-world applications. In the first part of the tutorial on sampling accessories (1), we looked at laser ablation and flow injection techniques. In this second installment, we will focus on three other important sampling approaches: electrothermal vaporization, desolvation systems, and chromatographic separation devices.

Robert Thomas has more than 30 years of experience in trace element analysis. He is the principal of his own freelance writing and consulting company, Scientific Solutions, based in Gaithersburg, MD. He can be contacted by e-mail at thomasrj@bellatlantic.net or via his web site at www.scientificsolutions1.com.

Electrothermal atomization (ETA) for use with atomic absorption (AA) has proven to be a very sensitive technique for trace element analysis during the previous three decades; however, the possibility of using the atomization/heating device for electrothermal vaporization (ETV) sample introduction into an ICP mass spectrometer was identified in the late 1980s (2). The ETV sampling process relies on the basic principle that a carbon furnace or metal filament can be used to thermally separate the analytes from the matrix components and then sweep them into the ICP mass spectrometer for analysis. This is achieved by injecting a small amount of the sample (usually 20–50 µL via an autosampler) into a graphite tube or onto a metal filament. After the sample is introduced, drying, charring, and vaporization are achieved by slowly heating the graphite tube/metal filament. The sample material is vaporized into a flowing stream of carrier gas, which passes through the furnace or over the filament during the heating cycle. The analyte vapor recondenses in the carrier gas and is then swept into the plasma for ionization.

One of the attractive characteristics of ETV for ICP-MS is that the vaporization and ionization steps are carried out separately, which allows for the optimization of each process. This is particularly true when a heated graphite tube is used as the vaporization device, because the analyst typically has more control of the heating process and, as a result, can modify the sample by means of a very precise thermal program before it is introduced to the ICP for ionization. By boiling off and sweeping the solvent and volatile matrix components out of the graphite tube, spectral interferences arising from the sample matrix can be reduced or eliminated. The ETV sampling process consists of six discrete stages: sample introduction, drying, charring (matrix removal), vaporization, condensation, and transport. Once the sample has been introduced, the graphite tube is slowly heated to drive off the solvent. Opposed gas flows, entering from each end of the graphite tube, then purge the sample cell by forcing the evolving vapors out the dosing hole. As the temperature increases, volatile matrix components are vented during the charring steps. Just before vaporization, the gas flows within the sample cell are changed. The central channel (nebulizer) gas then enters from one end of the furnace, passes through the tube, and exits out the other end. The sample-dosing hole is then automatically closed, usually by means of a graphite tip, to ensure no analyte vapors escape. After this gas flow pattern has been established, the temperature of the graphite tube is ramped up very quickly, vaporizing the residual components of the sample. The vaporized analytes either recondense in the rapidly moving gas stream or remain in the vapor phase. These particulates and vapors are then transported to the ICP in the carrier gas where they are ionized by the ICP for analysis in the mass spectrometer.

Another benefit of decoupling the sampling and ionization processes is the opportunity for chemical modification of the sample. The graphite furnace itself can serve as a high-temperature reaction vessel where the chemical nature of compounds within it can be altered. In a manner similar to

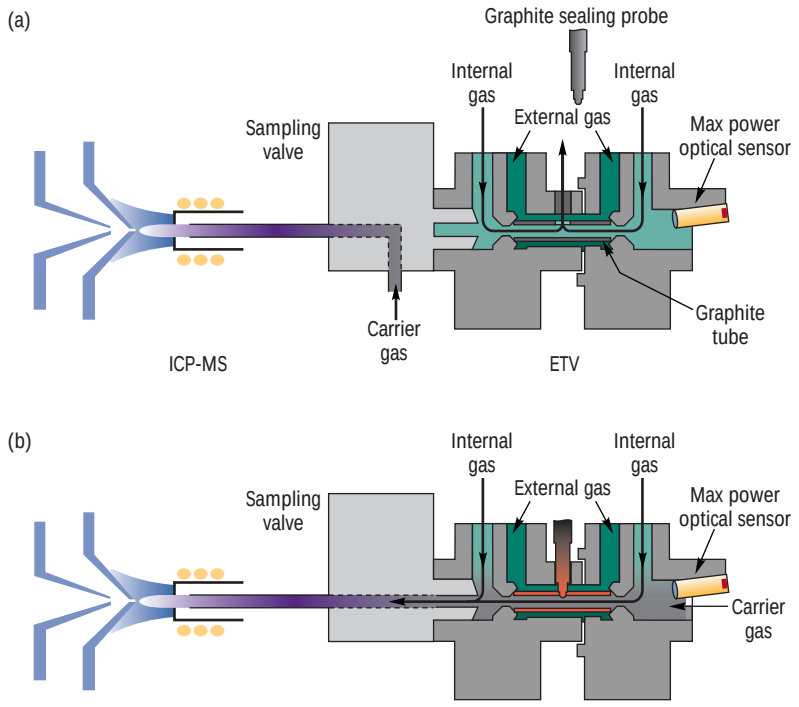

Figure 1. A graphite furnace ETV sampling device for ICP-MS, showing the two distinct steps of (a) sample pretreatment and (b) vaporization into the plasma. **((AUTHOR: Correct for a and b ?))**

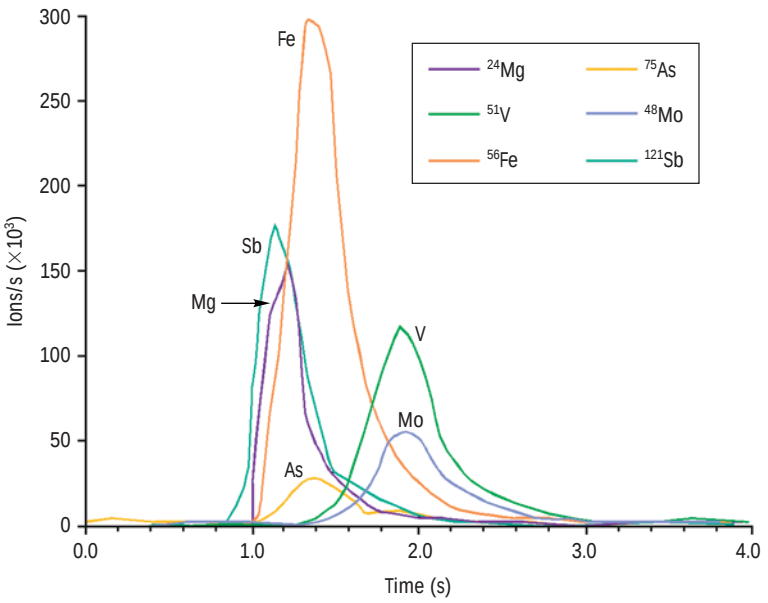

Figure 2. A temporal display of 50 pg of magnesium, antimony, arsenic, iron, vanadium, and molybdenum in 37% hydrochloric acid by ETV-ICP-MS.

that used in AA, chemical modifiers can change the volatility of species to enhance matrix removal and increase elemental sensitivity (3). An alternate gas such as oxygen may also be introduced into the sample cell to aid in the charring of the carbon in organic matrices such as biological or petrochemical samples. Here the organically bound carbon reacts with the oxygen gas to produce carbon dioxide, which is then vented from the system. A typical ETV sampling device, showing the two major steps of sample pretreatment (drying and ashing) and vaporization into the plasma, is shown schematically in Figure 1.

During the past 15 years, ETV sampling for ICP-MS has mainly been used for the analysis of complex matrices including geological materials (4), biological fluids (5), seawater (6), and coal slurries (7), which have proven difficult or impossible by conventional nebulization. By removal of the matrix components, the potential for severe spectral and matrix-induced interferences is dramatically reduced. Even though ETV-ICP-MS was initially applied to the analysis of very small sample volumes, the advent of low-flow nebulizers has mainly precluded its use for this type of work.

An example of the benefit of ETV sampling is in the analysis of samples containing high concentrations of mineral acids such as hydrochloric, nitric, and sulfuric acids. Besides physically suppressing analyte signals, these acids generate massive polyatomic spectral overlaps that interfere with many analytes, including arsenic, vanadium, iorn, potassium, silicon, zinc, and titanium. By carefully removing the matrix components with the ETV device, the determination of these elements becomes relatively straightforward. Figure 2 shows a spectral display in the time domain for 50 pg spikes of a selected group of elements in concentrated hydrochloric acid (37% w/w) using a graphite furnace-based ETV-ICP-MS (8). It can be seen in particular that good sensitivity is obtained for ^{39}K, ^{51}V, ^{56}Fe, and ^{75}As, which would have been virtually impossible by direct aspiration because of spectral overlaps from ^{39}ArH, ^{35}Cl^{16}O, ^{40}Ar^{16}O, and ^{40}Ar^{35}Cl, respectively. The removal of the chloride and water from the matrix translates

Table I. Detection limits for potassium, vanadium, iron, and arsenic in 37% hydrochloric acid by ETV-ICP-MS.

Element	DL (ppt)
^{39}K	170
^{51}V	50
^{56}Fe	20
^{75}As	40

into parts-per-trillion detection limits directly in 37% hydrochloric acid, as shown in Table I.

Figure 2 also shows that the elements are vaporized off the graphite tube in the order of their boiling points. In other words, magnesium, which is the most volatile, is driven off first, while vanadium and molybdenum, which are the most refractory, come off last. However, even though they emerge at different times, the complete transient event lasts <3 s. This physical time limitation, imposed by the duration of the transient signal, makes it imperative that all isotopes of interest be measured under the highest signal-to-noise conditions throughout the entire event. The rapid nature of the transient also limits the usefulness of ETV sampling for routine multielement analysis because realistically only a small number of elements can be quantified with good accuracy and precision in <3 s. In addition, the development of low flow nebulizers, desolvation devices, and collision cell technology has meant that rapid multielement analysis can now be carried out on difficult samples without the need for ETV sample introduction.

Desolvation Devices

Desolvation devices are mainly used in ICP-MS to reduce the amount of solvent entering the plasma. With organic samples, desolvation is absolutely critical because most volatile solvents would extinguish the plasma if they weren't removed or at least significantly reduced. However, desolvation of all types of samples can be very useful because it reduces the severity of the solvent-induced spectral interferences like oxides, hydroxides, and argon/solvent-based polyatomics that are common in ICP-MS. The most common desolvation systems used today include:

- Water-cooled spray chambers
- Peltier-cooled spray chambers
- Ultrasonic nebulizers (USN) with water/Peltier coolers
- Ultrasonic nebulizers (USN) with membrane desolvation
- Microconcentric nebulizers (MCN) with membrane desolvation.

Water- and/or Peltier- (thermo electric) cooled spray chambers are standard on a number of commercial instruments. They are usually used with conventional or low flow pneumatic nebulizers to reduce the amount of solvent entering the plasma. This has the effect of minimizing solvent-based spectral interferences formed in the plasma, and can also help to reduce the effects of a nebulizer-flow–induced secondary discharge at the interface of the plasma with the sampler cone. With some organic samples, it has proved to be very beneficial to cool the spray chamber to −10 to −20 °C (with an ethylene glycol mix) in addition to adding a small amount of oxygen into the nebulizer gas flow. This has the effect of reducing the amount of organic solvent entering the interface, which is beneficial in eliminating the build-up of carbon deposits on the sampler cone orifice and also minimizing the problematic carbon-based spectral interferences (9).

Ultrasonic nebulization was first developed in the late 1980s for use with ICP–optical emission spectroscopy (OES) (10). Its major benefit was that it offered an approximately 10–20× improvement in detection limits because of its more efficient aerosol generation. However, this was not such an obvious benefit for ICP-MS because more matrix was entering the system compared with a conventional nebulizer, increasing the potential for signal drift, matrix suppression, and spectral interferences. This was not such a major problem for simple aqueous samples, but was problematic for real-world matrices. The elements that showed the most improvement were the ones that benefited from lower solvent-based spectral interferences. Unfortunately, many of the other elements exhibited higher background levels and, as a result, showed no significant improvement in detection limit. In addition, because of the increased amount of matrix entering the mass spectrometer, it usually necessitated the need for larger dilutions of the sample, which again negated the benefit of using an USN with ICP-MS. This limitation led to the development of an ultrasonic nebulizer fitted with a membrane desolvator — in addition to the conventional desolvation system. This design virtually removed all the solvent from the sample, which dramatically improved detection limits for a large number of the problematic elements and also lowered oxide levels by at least an order of magnitude (11).

The principle of aerosol generation using an ultrasonic nebulizer is based on a sample being pumped onto a quartz plate of a piezo-electric transducer. Electrical energy of 1–2 MHz frequency is coupled to the transducer, which causes it to vibrate at high frequency. These vibrations disperse the sample into a fine droplet aerosol, which is carried in a stream of argon. With a conventional ultrasonic nebulizer, the aerosol is passed through a heating tube and a cooling chamber, where most of the sample solvent is removed as a condensate before it enters the plasma. If a membrane desolvation system is fitted to the ultrasonic nebulizer, it is positioned after the cooling unit. The sample aerosol enters the

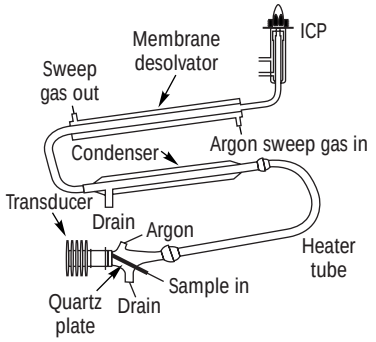

Figure 3. Schematic of an ultrasonic nebulizer fitted with a membrane desolvation system.

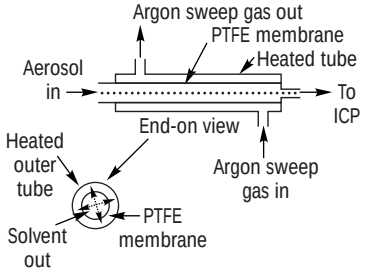

Figure 4. Principles of membrane desolvation.

membrane desolvator, where the remaining solvent vapor passes through the walls of a tubular microporus PTFE membrane. A flow of argon gas removes the volatile vapor from the exterior of the membrane, while the analyte aerosol remains inside the tube and is carried into the plasma for ionization. Figure 3 shows a schematic of an ultrasonic nebulizer, and Figure 4 shows the principles of membrane desolvation.

For ICP-MS, the system is best operated with both desolvation stages working, although for less demanding ICP-OES analysis, the membrane stage can be by-passed if required. The power of

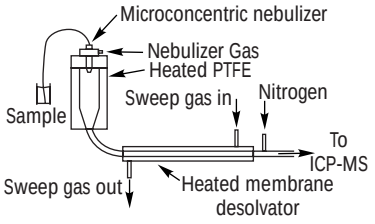

Figure 5. Schematic of a microconcentric nebulizer fitted with a membrane desolvation system.

the system when coupled to an ICP mass spectrometer can be seen in Table II, which compares the sensitivity (counts per second [cps]) and signal-to-background of a membrane desolvation USN with a conventional crossflow nebulizer for three classic solvent-based polyatomic interferences, $^{12}C^{16}O_2$ on ^{44}Ca, $^{40}Ar^{16}O$ on ^{56}Fe, and $^{40}Ar^{16}OH$ on ^{57}Fe, using a quadrupole ICP-MS system. The sensitivity for the analyte isotopes are all background subtracted.

It can be seen that for all three analyte isotopes, the net signal to background ratio is significantly better with the membrane ultrasonic nebulizer than with the crossflow design, which is a direct impact of the reduction of the solvent-related spectral background levels. Even though this approach works equally well and sometimes better when analyzing organic samples, it does not work for analytes that are bound to an organic molecule. The high volatility of certain types of organometallic species means that they stand a very good chance of passing through the microporus teflon membrane and never making it into the ICP-MS. For this reason, caution must be used when using a membrane desolvation system for the analysis of organic samples.

A variation of the membrane desolvation system is with a microconcentric nebulizer in place of the ultrasonic nebulizer. A schematic of this design is shown in Figure 5.

The benefit of this approach is not only the reduction in solvent-related spectral interferences with the membrane desolvation system, but also advantage can be taken of the microconcentric nebulizer's ability to aspirate very low sample volumes (typically 20–100 µL). This can be particularly useful when sample volume is limited like in vapor phase decomposition (VPD) analysis of silicon wafers. The problem with this kind of demanding work is that there is typically only 500 µL of sample available, which makes it extremely difficult using a traditional low-flow nebulizer because it requires the use of both cool and normal plasma conditions to carry out a complete multielement analysis. By using an MCN with a membrane desolvation system, the full suite of elements — including the notoriously difficult iron, potassium, and calcium — can be determined on 500 µL of sample using one set of normal plasma conditions (12).

Low flow nebulizers were described in greater detail in Part II of this series. The most common ones used in ICP-MS are based on the microconcentric design, which operate at 20–100µL/min. Besides being ideal for small sample volumes, the major benefit is that less matrix is entering the mass spec-

Table II. Comparison of sensitivity and signal/background ratios for three isotopes.

Isotope/ interference	Mass (amu)	Crossflow nebulizer (cps)	Net signal/ BG	Membrane Desolvation USN (cps)	Net signal/ BG
^{44}Ca (25 ppb)		2300		20,800	
$^{12}C^{16}O_2$	44	7640	0.3	1730	12
^{56}Fe (10 ppb)		95,400		262,000	
$^{40}Ar^{16}O$	56	868,000	0.1	8200	32
^{57}Fe (10 ppb)		2590		6400	
$^{40}Ar^{16}OH$	57	5300	0.5	200	

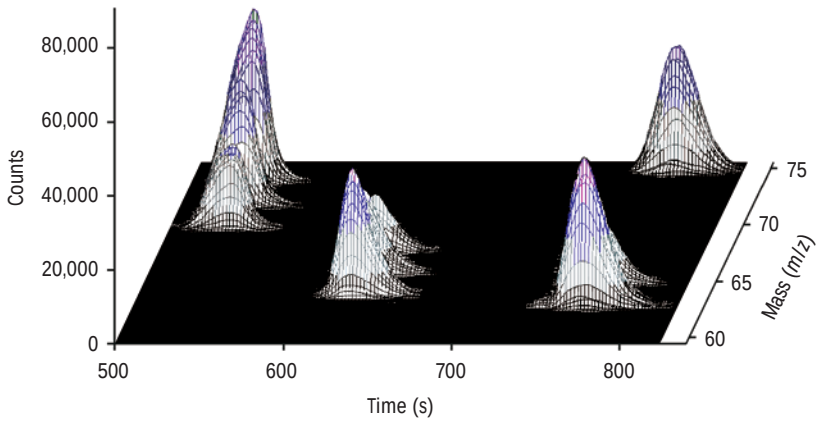

Figure 6. A typical chromatogram generated by a liquid chromatograph coupled to an ICP mass spectrometer, showing a temporal display of intensity against mass.

Table III. Some elemental species that have been studied by researchers using chromatographic separation devices coupled to ICP-MS.

Redox systems	Alkylated forms	Biomolecules
Se(IV)/Se(VI)	Methyl — Hg, Ge, Sn, Pb, As, Sb,Se, Te, Zn, Cd, Cr	Organo — As, Se, Cd
As(III)/As(V)	Ethyl — Pb, Hg	Metallo-porphyrines
Sn(II)/Sn(IV)	Butyl — Sn	Metallo-proteins
Cr(III)/Cr(VI)	Phenyl — Sn	Metallo-drugs
Fe(II)/Fe(III)	Cyclohexyl — Sn	Metallo-enzymes

trometer, which means that there is less chance of sample-induced long-term drift. In addition, most low-flow nebulizers use chemically inert plastic capillaries, which makes them well suited for the analysis of highly corrosive chemicals. This kind of flexibility has made low-flow nebulizers very popular, particularly in the semiconductor industry where it is essential to analyze high-purity acids using sample introduction systems free of sources of contamination (13).

Chromatographic Separation Devices

ICP-MS has gained popularity of the years, based mainly on its ability to rapidly quantitate ultratrace metal contamination levels. However, in its basic design, ICP-MS cannot reveal anything about the metal's oxidation state, alkylated form or how it is bound to a biomolecule. The desire to understand in what form or species an element exists led researchers to investigate the combination of chromatographic separation devices with ICP-MS. The ICP mass spectrometer becomes a very sensitive detector for trace element speciation studies when coupled with a chromatographic technique like high performance liquid chromatography (HPLC), ion chromatography (IC), gas chromatography (GC), and capillary electrophoresis (CE). In these hybrid techniques, element species are separated based on their chromatographic retention/mobility times and then eluted/passed into the ICP mass spectrometer for detection (14). The intensity of the eluted peaks are then displayed for each isotopic mass of interest in the time domain as shown in Figure 6, which shows a typical chromatogram for a selected group of masses between 60 and 75 amu.

There is no question that the extremely low detection capability of ICP-MS has allowed researchers in the environmental, biomedical, geochemical, and nutritional fields to gain a much better insight into the impact of different elemental species on us and our environment — something that would not have been possible 10–15 years ago. The majority of trace element speciation studies being carried out today, can be broken down into three major categories:

- Those involving redox systems, where the oxidation state of a metal can change. For example, hexavalent chromium, Cr(VI), is a powerful oxidant and extremely toxic, but in soils and water systems, it reacts with organic matter to form trivalent chromium, Cr(III), which is the more common form of the element and is an essential micronutrient for plants and animals (15)
- Another important class is alkylated forms of the metal. Very often the natural form of an element can be toxic, while its alkylated form is relatively harmless — or vice versa. A good example of this is the element arsenic. Inorganic forms of the element like As(III) and As(V) are toxic, whereas many of its alkylated forms, such as monomethylarsonic acid (MMA) and dimethylarsonic acid (DMA), are relatively innocuous (16)
- An area being investigated more and more is biomolecules. For example, in animal studies, activity and mobility of an innocuous arsenic-based growth promoter is determined by studying its metabolic impact and excretion characteristics. Measurement of the biochemical form of arsenic is crucial to know its growth potential (17).

Table III represents a small cross section of speciation work that has been carried out by chromatography techniques coupled to ICP-MS in these three major categories.

As mentioned previously, there is a large body of application work in the public domain that has investigated the use of different chromatographic separation devices, such as LC (18, 19), IC (20), GC (21, 22), and CE (23, 24) with ICP-MS. The area that is probably get-

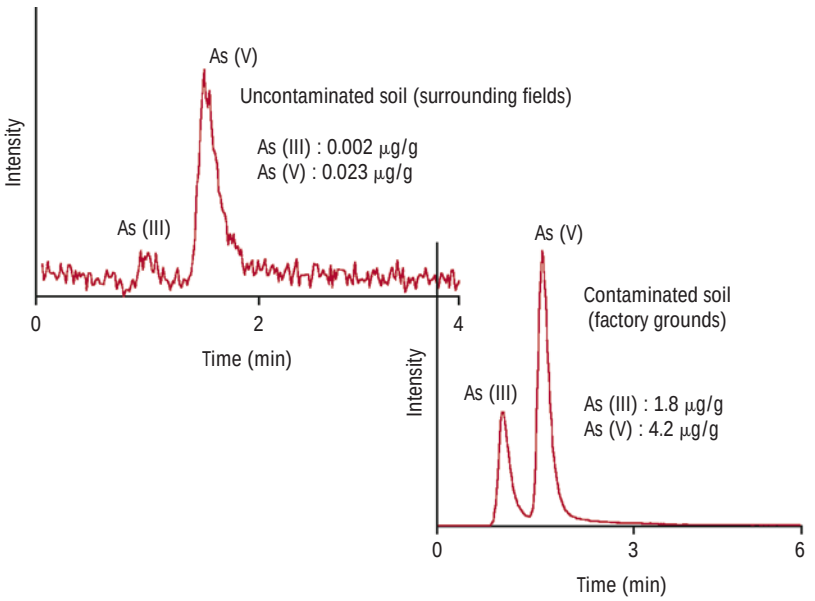

Figure 7. HPLC-ICP-MS chromatogram showing comparison of As(III) and As(V) levels in two different soil samples in and around an industrial site.

ting the most attention is the coupling of HPLC with ICP-MS. By using either adsorption, ion-exchange, gel permeation, or normal- or reversed-phase chromatography configurations, valuable elemental speciation information can be derived from a sample. Let's take a look at one of these applications — the determination of different forms of inorganic arsenic in soil, using ion-exchange HPLC coupled to ICP-MS, to get a better understanding of how the technique works.

Arsenic toxicity depends directly on the chemical form of the arsenic. In its inorganic form, arsenic is highly toxic, while many of its organic forms are relatively harmless. Inorganic species of arsenic that are of toxological interest are the trivalent form (As[III]), such as arsenious acid, H_3AsO_3 and its arsenite salts; the pentavalent form (As[V]), such as arsenic acid, H_3AsO_5, and its arsenate salts; and arsine (AsH_3), a poisonous, unstable gas used in the manufacture of semiconductor devices. Arsenic is introduced into the environment and ecosystems from natural sources by volcanic activity and the weathering of minerals, and also from anthropogenic sources, such as ore smelting, coal burning, industrial discharge, and pesticide use. The ratio of natural arsenic to anthropogenic arsenic is approximately 60:40.

A recent study investigated a potential arsenic contamination of the soil in and around an industrial site in Europe. Soil in a field near the factory in question was sampled, as well as soil inside the factory grounds. The soil was dried, weighed, extracted with water, and filtered. This careful, gentle extraction procedure was used to avoid disturbing the distribution of arsenic species originally present in the sample — an important consideration in speciation studies. A 10-mL sample was injected onto an amine-based, anion-exchange resin, where the different oxidation states of arsenic in soil were chromatographically extracted from the matrix and separated using a standard LC pump. The matrix components passed straight through the column, whereas the arsenic species were retained and then isocratically eluted into the nebulizer of the ICP mass spectrometer using 5 mM ammonium malonate. The arsenic species were then detected and quantified by running the instrument in the single-ion monitoring mode, set at mass 75 — the only isotope for arsenic. Figure 7 shows that both As(III) and As(V) have been eluted off the column in less than three minutes using this HPLC-ICP-MS set-up. The chromatogram also shows that both species are approximately three orders of magnitude lower in the soil sample from the surrounding field, compared to the soil sample inside the factory grounds. Although the arsenic does not exceed average global soil levels, it is a clear indication that the factory is a source of arsenic contamination.

It is worth mentioning that for some reversed-phase HPLC separations, gradient elution of the analyte species with mixtures of organic solvents like methanol might have to be used. If this is a requirement, consideration must be given to the fact that large amounts of organic solvent will extinguish the plasma (25), so introduction of the eluent into the ICP mass spectrometer cannot be carried out using a conventional nebulization. For this reason, special sample introduction systems like refrigerated spray chambers (26) or desolvation systems (27) have to be used, in addition to small amounts of oxygen in the sample aerosol flow to stop the build-up of carbon deposits on the sampler cone. Other approaches, such as direct injection nebulization (DIN) (28), have been used to introduce the sample eluent into the ICP-MS, but unfortunately have not gained widespread acceptance because of usability issues. DIN was very popular when first developed in the early 1990s because of its ability to handle small sample volumes and its low memory characteristics. However, it has been replaced by other sampling techniques and, as a result, appears to have limited commercial viability.

References

1. *Spectroscopy* **17**(11), 26–33 (2002).
2. C.J. Park, J.C. Van Loon, P. Arrowsmith, and J.B. French, *Anal. Chem.* **59,** 2191–2196 (1987).

3. R.D. Ediger and S.A. Beres, *Spectrochimica Acta* **47B,** 907 (1992).
4. C.J. Park and G.E.M. Hall, *J. Anal. At. Spectrom.* **2,** 473-480 (1987).
5. C.J. Park and J.C. Van Loon, *Trace Elements in Medicine* **7**, 103 (1990).
6. G. Chapple and J.P. Byrne, *J. Anal. At. Spectrom.* **11,** 549–553, (1996).
7. U. Voellkopf, M. Paul, and E.R. Denoyer, *Fresenius' J. Anal. Chem.* **342,** 917–923 (1992).
8. S.A. Beres, E.R. Denoyer, R. Thomas, and P. Bruckner, *Spectroscopy* **(9)**1, 20–26 (1994).
9. F. McElroy, A. Mennito, E. Debrah, and R. Thomas, *Spectroscopy* **13**(2), 42–53 (1998).
10. K.W. Olson, W.J. Haas Jr., and V.A. Fassel, *Anal. Chem.* **49,** 4, 632–637, (1977).
11. J. Kunze, S. Koelling, M. Reich, and M.A. Wimmer, *Atom. Spectrosc.* **19,** 5 (1998).
12. G. Settembre and E. Debrah, **Micro** (June, 1998).
13. R.A. Aleksejczyk and D. Gibilisco, **Micro** (September, 1997).
14. R. Lobinski, I.R. Pereiro, H. Chassaigne, A. Wasik, and J. Szpunar, *J. Anal. Atom. Spectrom.* **13,** 860–867 (1998).
15. A.G. Cox and C.W. McLeod, *Mikrochimica Acta* **109,** 161–164, (1992).
16. S. Branch, L. Ebdon, and P. O'Neill, *J. Anal. Atom. Spectrom.* **9,** 33–37 (1994).
17. J.R. Dean, L. Ebdon, M.E. Foulkes, H.M. Crews, and R.C. Massey, *J. Anal. Atom. Spectrom.* **9,** 615–618 (1994).
18. N.P. Vela and J.A. Caruso, *J. Anal. Atom. Spectrom.* **8,** 787 (1993).
19. S. Caroli, F. La Torre, F. Petrucci, and N. Violante, *Environ: Science and Pollution Research* **(1)**4, 205–208 (1994).
20. J.I. Garcia-Alonso, A. Sanz-Medel, and L. Ebdon, *Analytica Chimica Acta* **283,** 261–271 (1993).
21. A.W. Kim, M.E. Foulkes, L. Ebdon, S.J. Hill, R.L. Patience, A.G. Barwise, and S.J. Rowland, *J. Anal. Atom. Spectrom.* **7,** 1147–1149 (1992).
22. H. Hintelmann, R.D. Evans, and J.Y. Villeneuve, *J. Anal. Atom. Spectrom.* **10,** 619–624 (1995).
23. J.W. Olesik, K.K. Thaxton, J.A. Kinzer, and E.J. Grunwald, paper given at the Winter Conference on Plasma Spectrochemistry, T8, **((AUTHOR: What does T8 mean? What is the title of the paper? Conference sponsor, and city of headquarters? Location of conference that year?))** (1998).
24. J. Miller-Ihli, paper given at the Winter Conference on Plasma Spectrochemistry, T10, **((AUTHOR: What does T10 mean? What is the title of the paper?))** (1998).
25. J. Szpunar, H. Chassaigne, O.F.X. Donard, J. Bettmer, and R. Lobinski, *Applications of ICP-MS,* ed. G. Holland and S. Tanner, Royal Society of Chemistry, **((AUTHOR: Location of headquarters?))** (1997).
26. A. Al-Rashdan, D. Heitkemper, and J.A. Caruso, *J. Chromatogr. Sciences* **29,** 98 (1996).
27. H. Ding, L.K. Olson, and J.A. Caruso, *Spectrochimica Acta, Part B,* **51,** 1801 (1996).
28. S.C.K. Shum, R. Nedderden, and R.S. Houk, *Analyst,* **117,** 577 (1992). ■